Organization of the OXPHOS System in Plant and Yeast Mitochondria

Von der Naturwissenschaftlichen Fakultät
der Gottfried Wilhelm Leibniz Universität Hannover
zur Erlangung des Grades Doktorin der Naturwissenschaften
Dr. rer. nat.

genehmigte Dissertation
von
Dipl.-Ing. (agr.) Stephanie Sunderhaus
geboren am 9. Februar 1979 in Mettingen

Referent:	Prof. Dr. Peterhänsel
Korreferenten:	Prof. Dr. H.-P. Braun
	Prof. Dr. U. K. Schmitz
Tag der Promotion:	17.11.2008

Zusammenfassung

Eine Basismethode zur Untersuchung des OXPHOS Systems von Pflanzen und Hefe ist die Blau-native Polyacrylamid Gelelektrophorese (BN-PAGE). Diese Methode vereint die schonende Solubilisierung der OXPHOS Komplexe mittels nicht-ionischer Detergenzien mit der Implementation negativer Ladung in die Proteinkomplexe durch den Farbstoff Coomassie Blau (Kapitel 4). Mit dieser Methode konnte die Existenz supramolekularer Strukturen sowie spezifischer Untereinheiten der pflanzlichen OXPHOS Komplexe in den letzten Jahren erfolgreich nachgewiesen werden (Kapitel 2, 5). In Kombination mit „*single particle*“ Elektronenmikroskopie (EM) konnte vor kurzem gezeigt werden, dass der NADH Dehydrogenase Komplex aus *Arabidopsis thaliana* an der zur Matrix exponierten Seite eine Extradomäne aufweist. Diese Dissertation präsentiert eindeutige Anhaltspunkte dafür, dass es sich dabei um mitochondriale γ-Carboanhydrasen handelt. Diese sind essentiell für die Aktivität und Assemblierung des Komplexes und mutmaßlich an einem Mechanismus beteiligt, der mitochondriales CO_2 aus der Photorespiration recycelt und den Chloroplasten zur Photosynthese zur Verfügung stellt (Kapitel 2). Untersuchungen von Mitochondrien aus *Polytomella* und *Saccharomoyces cerevisiae* mittels BN-PAGE und „*single particle*“ EM ergaben neue Erkenntnisse hinsichtlich der Dimerisierung des ATP-Synthase Komplexes. ATP-Synthase Dimere sind über ihre F_0-Teile miteinander verbunden und bilden in *Polytomella* einen Winkel von 70° aus, wohingegen Dimere aus *S. cerevisiae* Winkel von 90° und 35° ausbilden. Ultradünnschnitte kombiniert mit Negativfärbung ganzer Mitochondrien aus beiden Organismen konnten zeigen, dass es sich bei diesen Dimeren um Grundbausteine von ATP-Synthase Oligomerketten handelt, die maßgeblich an der Krümmung der inneren Mitochondrienmembran beteiligt sind (Kapitel 3). Weiterhin konnte die Existenz eines äußerst stabilen $I+III_2$, sowie weniger stabiler $I+III_2+IV$ und III+IV Superkomplexe aus *Arum maculatum* gezeigt werden. *A. maculatum* ist eine europäische Landpflanze, die als Bestäubungsstrategie Thermogenese betreibt. Dazu wird ein Enzym genutzt, dass eine Besonderheit vieler pflanzlicher OXPHOS Systeme darstellt: die Alternative Oxidase (AOX). AOX erzeugt zu einem physiologisch genau definierten Zeitpunkt kontrolliert Wärme, ohne dabei zur Synthese von ATP beizutragen. Es konnte gezeigt werden, dass trotz erheblicher „alternativer“ Verbrennung von Substraten die OXPHOS Komplexe in hoher Abundanz vorliegen, sehr aktiv sind und äußerst stabile Superkomplexe bilden (Kapitel 6).

Schlagwörter: OXPHOS System, BN-PAGE, γ-Carboanhydrasen, dimere ATP-Synthase , Alternative Oxidase, Superkomplexe

Abstract

A basic method used in the investigation of the OXPHOS system of plants and yeast is the blue-native polyacrylamide gel electrophoresis (BN-PAGE). This method combines the gentle solubilization of OXPHOS complexes using non-ionic detergents and the implementation of negative charge into protein complexes by the dye coomassie blue (Chapter 4). During the course of the past years, the existence of a supramolecular structure as well as the occurrence of plant specific subunits of OXPHOS complexes could be demonstrated (Chapter 2 and 5). Very recently, BN-PAGE in combination with single particle electron microscopy (EM) revealed the existence of a plant-specific extra domain at the matrix exposed side of *Arabidopsis thaliana* mitochondrial NADH dehydrogenase. In this thesis, evidence is presented, which demonstrates that this extra domain contains mitochondrial γ- type carbonic anhydrases. These enzymes are essential for the activity as well as the assembly of the complex. It is speculated that they are involved in a mechanism which allows recycling of CO_2 released in mitochondria for photosynthesis in chloroplasts (Chapter 2). Investigations of *Polytomella* and *Saccharomyces cerevisiae* mitochondria using BN-PAGE and single particle EM led to new insights into the dimerization of the ATP synthase complex. Analyses of EM pictures showed that ATP synthase dimers from *Polytomella* are associated with each other via their F_0 parts and that they form an angle of 70°, whereas ATP synthase dimers from S. *cerevisiae* form angles of 90° and 35°. Ultrathin sectioning together with negative stain of whole mitochondria from both organisms confirmed that the dimers are the building blocks of oligomers, which are involved in the curvature of the inner mitochondrial membrane (Chapter 3). Furthermore, the existence of a very stable I+III_2 as well as the less stable I+III_2+IV and III_2+IV supercomplexes from *Arum maculatum* could be demonstrated. *A. maculatum* is a European land plant, which uses thermogenesis as a pollination strategy. Prerequisite is an enzyme, which is characteristic for the OXPHOS system of several plant species: the Alternative Oxidase (AOX). AOX is utilized to produce heat at a particular period in spring without contributing to the generation of ATP. Despite high rates of "alternative" respiration, the OXPHOS complexes I – V are of high abundance, very active and form stable supercomplexes (Chapter 6).

Key words: OXPHOS system, BN-PAGE, γ-carbonic anhydrases, dimeric ATP synthase, Alternative Oxidase, supercomplexes

CONTENTS

Abbreviations		1
Chapter 1	General Introduction	2
Chapter 2	Carbonic anhydrase subunits form a matrix exposed domain attached to the membrane arm of mitochondrial complex I in plants. *J. Biol. Chem. 2006, 281, 6482 – 6488.*	27
Chapter 3	Characterization of Dimeric ATP Synthase and Cristae Membrane Ultrastructure from *Saccharomyces* and *Polytomella* Mitochondria. *FEBS Lett. 2006, 580, 3427 – 3432.*	35
Chapter 4	Two-dimensional Blue Native/Blue Native Polyacrylamide Gel Electrophoresis for the Characterization of Mitochondrial Protein Complexes and Supercomplexes. *Meth. Mol. Biol. 2007, 372, 315 – 324.*	42
Chapter 5	The Higher Level of Organization of the Oxidative Phosphorylation System: Mitochondrial Supercomplexes. *J. Bioenerg. Biomembr. 2008 40, 419 – 924.*	57
Chapter 6	Supramolecular Structure of the OXPHOS System in Highly Thermogenic Tissue of *Arum maculatum.* *to be submitted*	63
Chapter 7	Supplementary Discussion and Outlook	81
Publications		90
Curriculum vitae		91
Danksagung		93

ABBREVIATIONS

1D	one dimensional
2D	two dimensional
AOX	alternative oxidase
ADP	adenosine diphosphate
ATP	adenosine triphosphate
BN	blue native
C_i	inorganic carbon
CA	carbonic anhydrase
γCA	gamma-type carbonic anhydrase
γCAL	gamma-type carbonic anhydrase like
CAM	carbonic anhydrase from *Methanosarcina thermophila*
CCM	CO_2 concentrating mechanism
EM	electron microscopy
ETC	electron transfer chain
F_0	F_0 part of the complex V
$FADH_2$	flavin adenine dinucleotide
FMN	flavin mononucleotide
IMM	inner mitochondrial membrane
IMS	inter membrane space
kDa	kilo Dalton
MPP	mitochondrial processing protease
NADH	nicotine amid dinucleotid
NADPH	nicotine amid dinucleotid phosphate
OMM	outer mitochondrial membrane
OXPHOS	oxidative phosphorylation system
PAGE	polyacrylamide gel electrophoresis
RubisCO	ribulose 1,5-bisphosphate Carboxylase/Oxygenase
SA	salicylic acid
SDS	sodium dodecylsulphate
SHAM	salicylhydroxamic acid
UQ	ubiquinone
UQH_2	ubiquinol

Chapter 1

GENERAL INTRODUCTION

GENERAL INTRODUCTION

1. The Respiratory Chain of Mitochondria and the Oxidative Phosphorylation System 4

2. Membrane Structure: “Fluid State Model” versus “Solid State Model” 6

3. Special Functions of the OXPHOS System in Plants 10

3.1. Alternative Oxidase and Thermogenesis in *Arum maculatum* 11

3.2. Carbonic Anhydrase Subunits of Respiratory Complex I in *Arabidopsis thaliana* 14

4. Experimental Strategies to Investigate the OXPHOS System 17

5. Objective of the Thesis 18

6. References 19

1. The Respiratory Chain of Mitochondria and the Oxidative Phosphorylation System

Mitochondria are double-membrane bound organelles with a size of 1 – 3 µm and an abundance of 1 – 1000 per cell. According to the endosymbiontic hypothesis, the ancestor of mitochondria was an aerobe prokaryote, taken up by the eukaryotic cell via endocystosis (Sagan 1967 and references therein). The closest living relatives of this prokaryote alive today are the α-proteobacteria (reviewed in Gray et al. 2001). In most cells, mitochondria are the compartments which produce the main part of ATP. Additionally, mitochondria are involved in numerous metabolic processes including the biosynthesis of amino acids, vitamin cofactors, fatty acids and iron-sulphur clusters (reviewed in Logan 2006). Mitochondria possess their own small genome, but the majority of mitochondrial proteins are nuclear encoded, synthesized in the cytosol and post-transcriptionally imported into the organelle via the outer and inner mitochondrial membrane (OMM, IMM). These two membranes enclose the inter membrane space (IMS) whereby the IMM encloses the mitochondrial matrix (Fig. 1).

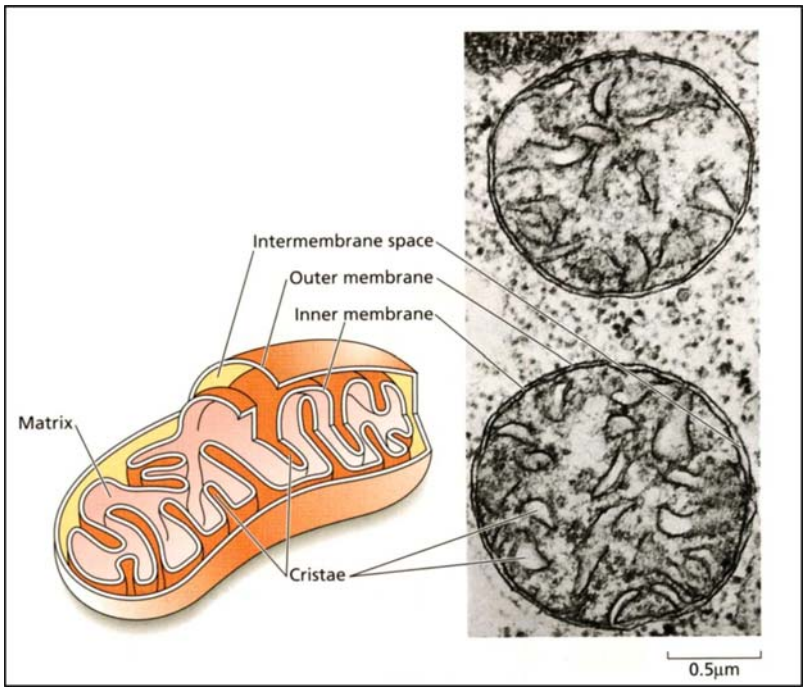

Figure 1. Structural organization of the mitochondrion. The OMM is permeable to molecules of 10kDa or less. The highly invaginated IMM contains all components of the OXPHOS system and serves as a permeability barrier for the organelle (from Taiz Zeiger (Ed) Plant Physiology, Sinauer Associates, 4th Edition, p. 263).

The IMM is heavily folded and contains all the enzymes of the oxidative phosphorylation system, namely the NADH-dehydrogenase (complex I), the succinate dehydrogenase (complex II), the cytochrome c reductase (complex III), the cytochrome c oxidase (complex IV) and the ATP synthase (complex V). Presence of these five protein complexes forms the basis for aerobic respiration – the controlled oxidation of reduced organic substrates to CO_2 and H_2O. This process releases a large amount of energy, which is used to form ATP molecules.

Aerobic respiration is a multi-step process (Fig. 2). In a first step, complex I oxidizes NADH and transfers electrons to ubiquinone (UQ), which in turn is oxidized at complex III. The passage of electrons through complex I is accompanied by H^+ translocation from the mitochondrial matrix across the IMM into the IMS. In a parallel step, electrons from $FADH_2$, which is oxidized by complex II, are also transferred to UQ. No protons are translocated at this complex.

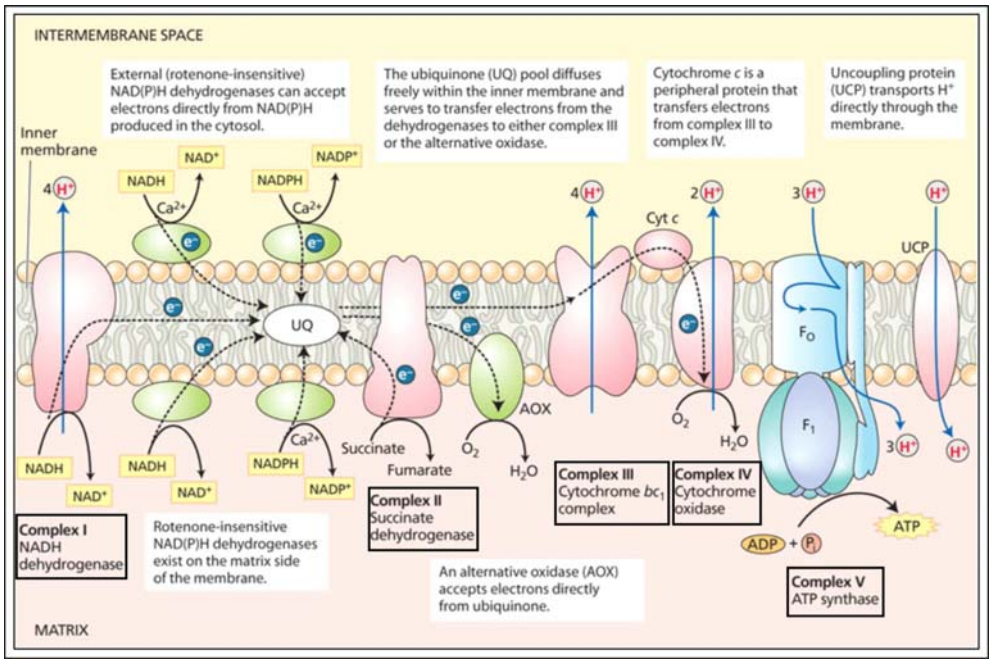

Figure 2. Organization of the respiratory chain of higher plants in planar arrangement. Additionally to the five OXPHOS complexes, plants possess two external and two internal NAD(P)H dehydrogenases and one alternative oxidase at the matrix exposed side of the IMM (blue). Modified from Møller and Rassmusson (2006) In: Taiz Zeiger (Ed) Plant Physiology, Sinauer Associates.

At complex III, which has two binding sites for ubiquinol (UQH_2), the two electrons from UQH_2 take different pathways: one electron is transferred to mobile cytochrome c via a Rieske iron-sulphur center and further transferred to complex IV. The other electron is transferred

back to UQ. This mechanism is called Q-cycle. Reduction as well as oxidation of UQ/UQH_2 is accompanied by the uptake of protons from the mitochondrial matrix and release of protons into the IMS. In a final step, Complex IV accepts electrons from reduced cytochrome c and donates them to the final electron acceptor, molecular oxygen. The redox reactions at complexes I, III and IV serve to create a proton gradient across the IMM. This gradient has an electrochemical nature. The main part of the return flow of protons into the matrix arises via complex V, which uses the energy of the proton gradient for the phosphorylation of ADP.

2. Membrane Structure: "Fluid State Model" versus "Solid State Model"

Cells require membranes for their existence. The plasma membrane forms the outer border of the cell, whereas other membranes enclose organelles and also form internal compartments. The principle function of all these membranes is to serve as a barrier to the free diffusion of molecules. All membranes consist of lipid bilayers with integrated as well as associated proteins. The general model of membranes is the "fluid mosaic model" of Singer and Nicholson (Singer and Nicholson 1972) (Fig. 3).

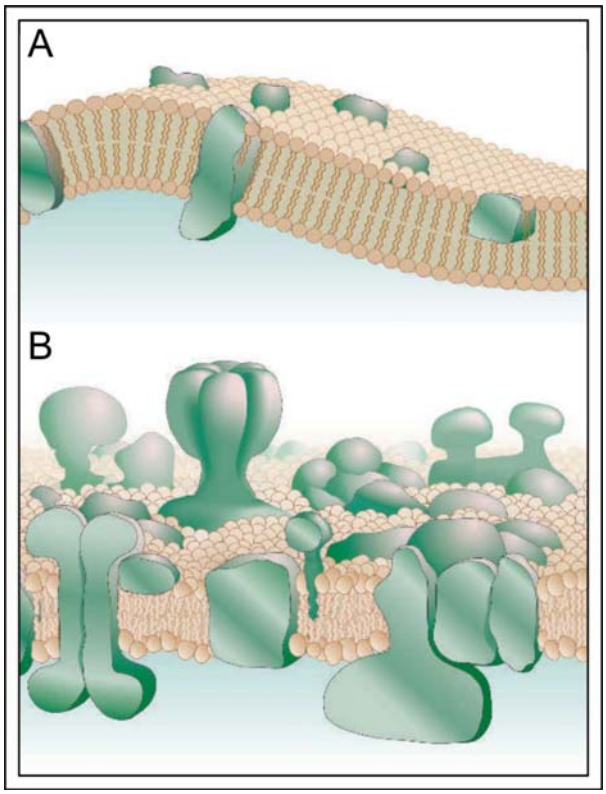

Figure 3. General models for the membrane structure. A. The "fluid mosaic model" according to Singer and Nicholson; B. General model based on the new data pertaining to membrane protein structures and functions (from Engelman 2005).

This model introduced the idea that proteins of a membrane are dispersed and at a comparatively low concentration. The lipids are seen as a "sea" in which mainly monomeric proteins float unimpeded. (Fig. 3A) Today, this model is much more advanced and sophisticated. Biological membranes are more complex than first thought when the "fluid mosaic model" was proposed in 1972. Membranes are a mixture of several different types of lipids and protein components. There is, however, some fluidity between these membrane compartments, but the model has to be seen much more mosaic than fluid where non-randomness is the rule (Fig. 3B).

Several mechanisms influencing membrane composition and structure are ascertained. First of all there are the lipids. Membrane lipids are essential for biological functions ranging from membrane trafficking to signal transduction. Also, the biophysical properties of the lipid bilayer have a significant effect on the properties of membrane proteins (reviewed in Lee 2004). Each membrane in a plant cell has a characteristic and distinct complement of lipid types. The asymmetrical distribution of different lipids between the two leaflets of a membrane bilayer can generate membrane curvature. More or larger phospholipids, for example, in the outer leaflet increase the surface area relative to that of the inner leaflet. However, membrane curvature is not solely based upon lipid composition. The attachment of membranes to the cytoskeleton or to each other is an additional way of curving membranes. In many higher eukaryotes, membranes and organelles bind to the cytoskeleton or to each other. By tethering the membrane to components of the cytoskeleton, such as microtubules, organellar shape can further be defined. In addition, tethering membranes to each other can shape membranes, e.g. via the generation of dimers of integral membrane proteins that are present in opposing membranes. Tethering membranes to each other and to the cytoskeleton, shapes for example, the nuclear envelope. Maintaining tubules, cristae and other shapes with high curvature requires proteins. Proteins can occupy a large area in the inner or outer leaflet of a bilayer, thereby acting as a wedge in the membrane. Integral membrane proteins with their transmembrane domains inserted into the bilayer can dimerize to form protein scaffolds (Engelman 2005, McMahon and Gallop 2005, Voeltz and Prinz 2007).

Mitochondria are, in addition to chloroplasts, a type of exception in the cell because they are bounded by a double membrane. The OMM contains only a small percentage of the total mitochondrial mass and relatively few enzymes. The IMM contains 80 – 95% of the total membrane-bound proteins and more than 90% of the total mitochondrial lipid, including the characteristic lipid cardiolipin. Cardiolipin is a bi-lipid, which is exclusively observed in

bacterial and mitochondrial membranes and thought to interact with protein complexes and protein supercomplexes of the OXPHOS system (reviewed in Schlame 2008). Furthermore, the IMM is heavily folded into a so-called cristae structure which forms tubules or ribbons that extend deeply into the mitochondrial matrix (Figure 1). These structures greatly increase the surface of the IMM. This is significant because the IMM is the locus where respiration and ATP generation take place.

Currently there is considerable debate on the structural organization of the OXPHOS system in mitochondria. Two oppositional models for the arrangement of the OXPHOS complexes were published: the "solid-state model" (Chance 1955) and the "fluid state model" (reviewed in Hackenbrock et al. 1986). The latter proposes, that the respiratory protein complexes are randomly distributed in the plane of the membrane, where they freely diffuse laterally. UQ and cytochrome c are considered to be mobile electron carriers, whose diffusion rates are faster than those of the respiratory complexes. Consequently, electron transfer would either be reaction limited or diffusion limited. In contrast, according to the "solid state model", the components of the respiratory chain form aggregates ranging from small clusters of a few complexes to very large mega complexes. These aggregates may be either permanent or transient (reviewed in Lenaz and Genova 2007).

Early evidence supporting the "solid state model" was based on findings that individual OXPHOS complexes could be co-purified (Fowler and Hatefi 1961, Hatefi et al. 1961, Fowler and Richardson 1961, Hatefi et al. 1962). Furthermore, reconstitution experiments using isolated OXPHOS complexes revealed maximal enzyme activities at defined ratios of the complexes. Over the course of several years, additional experimental results partially approved as well as partially disapproved the "solid state model". Inhibition of the activity of the $I+III_2$ supercomplex by Antimycin A was found to be reestablished by the addition of free complex III, which questioned the occurrence of stable supercomplex structures. In addition, dilution of the IMM with exogenous phospholipids was found to reduce the electron transfer rates of the respiratory chain, which further challenged the "solid state model". These and other findings led to the broad acceptance of the "fluid state model", which is also termed "random collision model" because electron transport of the respiratory chain is believed to take place on the basis of random collision between individual OXPHOS complexes and the mobile electron carriers cytochrome c and ubiquinone (reviewed in Hackenbrock et al. 1986).

However, over the course of the past few years, newly published results strongly support the "solid state model": defined associations of respiratory complexes can be observed upon gentle solubilization of the IMM using non-ionic detergents and gentle separation techniques like blue native polyacrylamide gel electrophoresis (BN-PAGE) or gel filtration (Schägger and Pfeiffer 2000, Cruciat et al. 2000). Based on these data, Schägger and co-workers suggested a new "Respirasome model". Respirasomes consist of complex I, dimeric complex III and one to four copies of complex IV ($I+III_2+IV_{1-4}$). Within Respirasomes, electron transport is based on direct substrate channeling between the complexes and not on their random collision (Schägger and Pfeiffer 2000, Schägger 2001b, Schägger and Pfeiffer 2001). Recently, single particle electron microscopy and flux control experiments approved the "solid state model". Eubel et al. reported a very stable $I+III_2$ supercomplex in the mitochondria of *Arabidopsis thaliana* of which Dudkina et al. published single particle EM pictures (Eubel et al. 2003, Dudkina et al. 2005a). Recently, EM pictures of the very stable $I+III_2$ supercomplex were also reported for bovine heart mitochondria (Dudkina et al. 2008). Results on the supramolecular structure of the OXPHOS complexes in plants are summarized in Chapter 5 of this thesis.

Additional evidence regarding defined interactions of protein complexes within the IMM also comes from investigations concerning the ATP synthase complex. In the late 1980s Allen et al. published evidence that the ATP synthase of *Paramecium* forms dimers on tubular cristae (Allen et al. 1989). They furthermore proposed that an ATP synthase dimer might offer the potential to form a rigid arc, which leads to the bending of the IMM. The oligomerization of dimers might then form the typical tubular structures (Allen 1995). Recently, Paumard et al. were able to show that the ATP synthase subunits *e* and *g* from the yeast *Saccharomyces cerevisiae* are essential for the biogenesis of the mitochondrial cristae. Mutant strains, which are devoid of either subunit *e* or *g*, show that the IMM does not form the typical cristae structure but rather displays onion like structures (Paumard et al. 2002). Furthermore Dudkina et al. (Dudkina et al. 2005b, Dudkina et al. 2006) could show by single particle electron microscopy in combination with ultrathin sectioning and negative stain of whole mitochondria from *Saccharomyces cerevisiae* and *Polytomella* that the ATP synthase complex indeed forms dimers (Fig. 4).

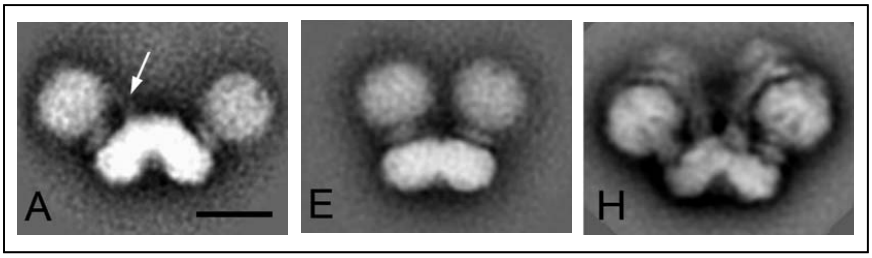

Figure 4. Projection maps of purified ATP synthase dimers from *S. cerevisiae* and *Polytomella*.
A+B. Complete ATP synthase dimers from *S. cerevisiae* with an angle of ~90° (A) and ~35° (B); H. Complete ATP synthase dimer from *Polytomella* (from Dudkina et al. 2005b and Dudkina et al. 2006).

These dimers are the building blocks of oligomers. The dimer formation is based on specific interaction between the F_0 parts. The angle between the two F_0 parts is about 70° in *Polytomella*, whereas in yeast, two dimer types occur. One type has an angle of about 90° and a second type of about 35°. Chapter 3 of this thesis will give new insight into the dimerization of ATP synthase of *Polytomella* and *Saccharomyces cerevisiae.*

3. Special Functions of the OXPHOS System in Plants

The OXPHOS system of plants differs in many respects from its counterparts in other organisms. A first remarkable fact is that the plant mitochondrial genome encodes for more subunits of respiratory protein complexes than those of other heterotrophic organisms. Furthermore, the plant mitochondrial OXPHOS system is branched at several sites (Figure 2). It possesses different alternative oxidoreductases, which do not contribute to proton translocation across the IMM, thus not taking part in energy conservation. Complex I is bypassed by at least four different rotenone-insensitive alternative NAD(P)H dehydrogenases, which are located in the IMM and are able to either oxidize cytosolic or mitochondrial NADH or NADPH (Møller 2001). Additionally there is an alternative oxidase (AOX) which bypasses the complexes III and IV (Siedow 1982). It is insensitive to inhibitors like Antimycin or cyanide but sensitive to salicylhydroxamic acid (SHAM). A further specialty of plants is the fact that some respiratory protein complexes contain additional subunits, which introduce side functions into the respiratory chain. These side functions are not involved in electron transfer. One example for these side activities are the two core subunits of complex III, which show mitochondrial processing protease (MPP) activity (Braun et al. 1992). A second one is the L-galactono-1,4-lactone dehydrogenase, the final enzyme of the ascorbate synthesis pathway,

which is associated with a subunit of complex I (Millar et al. 2003). Very recently it could be shown, that a group of five structurally related proteins, which have sequence similarity to a gamma-type carbonic anhydrase (γCA) from archae bacteria, also forms part of complex I (Parisi et al. 2004, Perales et al. 2004, Perales et al. 2005, Sunderhaus et al. 2006).

3.1. Alternative Oxidase and Thermogenesis in *Arum maculatum*

Some flowers of a group of monocotyledonous plants, mostly from the family Araceae, are able to regulate their flower temperature during blooming by increasing the rate of heat production in order to remain warmer than their surroundings. This process, called thermogenesis, is not common to the kingdom of plants. *Arum maculatum* is a typical European example for a plant using thermogenesis for pollination (Fig. 5). Plants of this family deceit insects by volatilization of odoriferous compounds similar to that of feces or urine emitted by the appendix. This simulates the natural insect laying sites. Insects are attracted and trapped in the floral chamber of the protogynous inflorescence. Fertile male and female flowers are enclosed in this floral chamber at the base of the spathe, which is closed at the top by fibrous sterile male flowers to bar insects from escaping. Simultaneously to the maturity of the female flowers, insects are allured and fall into the chamber (Gibernau et al. 2004).

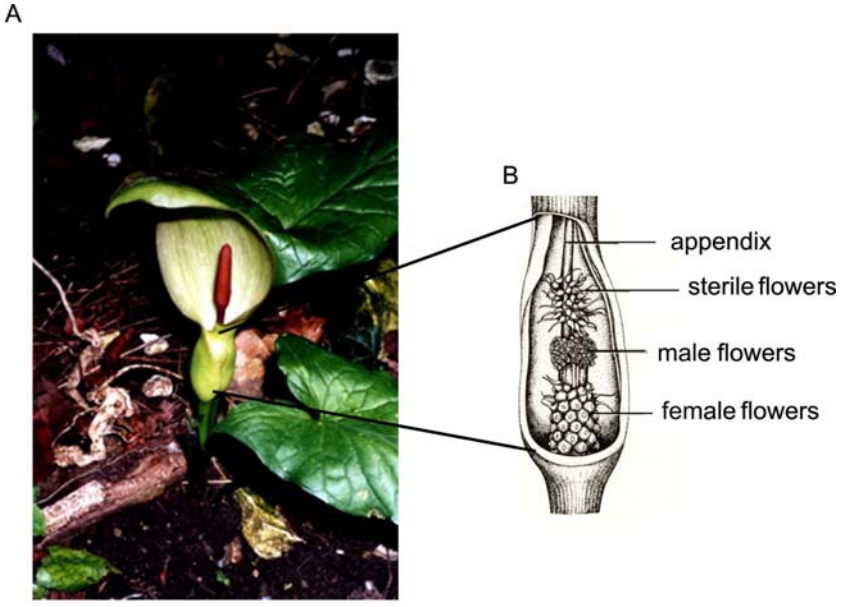

Figure 5. Structural features of Arum maculatum. (A) *Arum maculatum* plant in its natural surrounding. The unfolded spathe reveals the appendix, which constitutes the thermogenic organ (from Wagner at al. 2008). (B) Schematic view of a longitudinal section of the floral chamber of *Arum maculatum* (modified from Schopfer P and Brennicke A (Ed): Pflanzenphysiologie, Springer Verlag).

During their period of habitation in the floral chamber, insects may deposit pollen from other *Arum* plants on the receptive female stigma. This phase mostly ends the next day when the pollen matures. During this time the fibrous sterile male flowers begin wilting, whereby the trapped flies are draped with pollen while escaping from the floral chamber. Thermogenesis seems to play different roles during this pollination process: a first heating event appears to be responsible for the unfolding of the spathe, a second for the release of the odors of the appendix and a third one for the maturation of pollen (Albre et al. 2003). In some species, heating often continues throughout the entire period of insect habitation. It is assumed that this may be related to the fact that insects require an elevated body temperature for activity. A warming floral environment may therefore be a significant energy reward for pollinators, enabling them to reduce the energy cost of their pollinating activity (Seymour et al. 2003). It is well established that the inflorescences of plants from Aracaceae and several other families (further information in Seymour 2001) generate the heat used for thermogenesis via the mitochondrial OXPHOS system, namely via the cyanide resistant AOX. This lowers the efficency of respiration exceedingly since redox energy is released as heat.

Unfortunately, little is known about AOX structure, regulation and function (reviewed in Vanlerberghe and McIntosh 1997, Juszczuk and Rychter 2003). Its occurrence in the IMM along with its unusually poor stability of activity in the presence of detergents makes it difficult to study (Berthold and Stenmark 2003). Nowadays it is commonly accepted that AOX belongs to the di-iron carboxylate protein family and exists as a 32 kDa homodimeric interfacially bound protein on the matrix side of the IMM (Andersson and Nordlund 1999, Albury et al. 2002, Berthold et al. 2002). Activity of the AOX protein is regulated via two major mechanisms: on the one hand at the level of UQ concentration and on the other hand at the level of the oxidation state of the enzyme itself and the abundance of substrates like pyruvate (Millar et al. 1993, Affourtit et al. 2002, Juszczuk and Rychter 2003). In an oxidized form AOX is present as a dimer consisting of two monomers covalently linked by a disulfide bond (Umbach and Siedow 1993, Siedow and Umbach 2000). Reductive conditions yield a non-covalently linked homodimeric protein (Fig. 6). No evidence exists that supports a direct correlation between the abundance of AOX protein and its activity in respiration, which suggests that partitioning of electrons from the UQ pool is determined by posttranslational mechanisms.

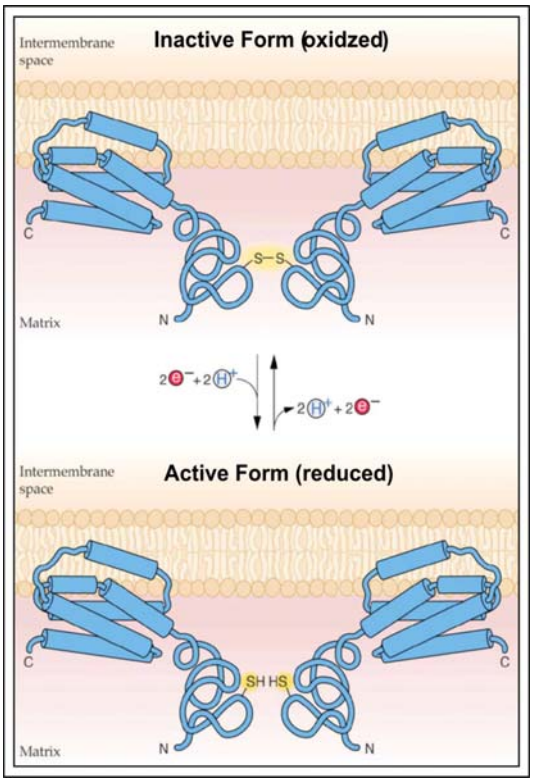

Figure 6. The structure and regulatory features of the Alternative Oxidase in plant mitochondria. Modified from Møller and Rassmusson (2006) In: Taiz Zeiger (Ed) Plant Physiology, Sinauer Associates.

AOX in higher plants is exclusively encoded in the nuclear genome by two gene subfamilies: AOX1 and AOX2. Expression of the AOX genes in thermogenic and pre-thermogenic tissues seems to be induced by salicylic acid (SA), whereas the role of SA in posttranslational regulation is still a matter of debate (Raskin et al. 1987, Rhoads and McIntosh 1992, Considine et al. 2002 and references therein, Grant et al. 2008).

In addition to its comparatively well characterized and confirmed thermogenic function, AOX is also supposed to be involved in several different cell processes. Especially in non-thermogenic plants like *Arabidopsis thaliana,* it is postulated that AOX acts as a marker for stress due to the fact that AOX1 genes are induced by stress induced cell signaling compounds such as H_2O_2 and NO (Arnold-Schmitt et al. 2006). It is reported that AOX expression increases during high and low temperatures, water stress, phosphate deficiency, SA treatment, herbicides and inhibitors of the cytochrome pathway (Grant et al. 2008 and references therein). Chapter 6 will give new insights into the organization of the OXPHOS system of *Arum maculatum* mitochondria in a context with thermogenesis.

3.2. Carbonic Anhydrase Subunits of Respiratory Complex I in *Arabidopsis thaliana*

Complex I is the first enzyme of the respiratory chain of plant mitochondria, but the name is more commonly used as a generic name for a family of NADH-quinone oxidoreductases, which include bacterial enzymes as well as Na^+-translocating enzymes found in certain organisms. It is also the largest and to date the least understood mitochondrial respiratory complex and therefore considered as a "black box" (Matsuno-Yagi and Yagi 2001). The basic function of complex I, as well as its analog complexes in other organisms, is the translocation of protons across the IMM and respectively across the plasma membrane in bacteria. For this function, its minimal form is composed of 14 subunits as described for prokaryotes (reviewed in Brandt 2006). Complex I has an L-shaped structure (Fig. 5) as revealed by EM analyses for *Escherichia coli* (A), bovine heart (B), *Yarrowia lipolytika* (C) and *Arabidopsis thaliana* (D).

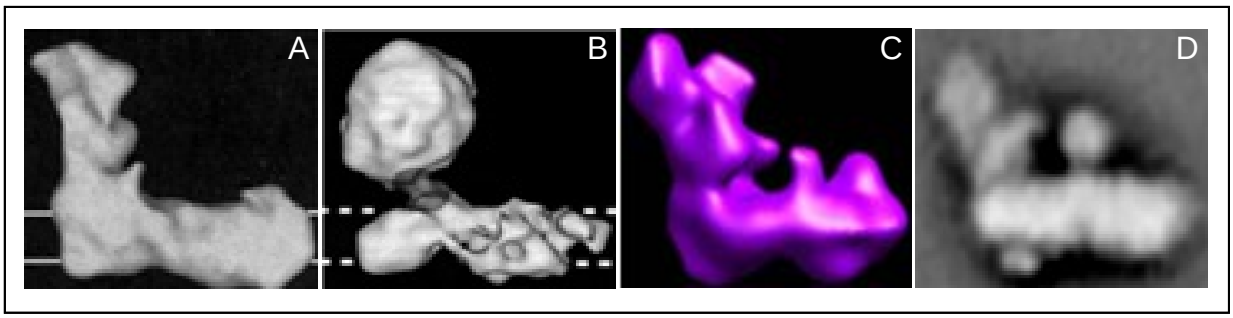

Figure 5. Structure of complex I. Complex I consists of 2 major segments. The peripheral segment protrudes into the mitochondrial matrix (or bacterial cytosol). The other is the membrane segment. The peripheral segment is a "catalytic" domain and is composed of 7 (bacteria) to 12 (mitochondria) subunits. The membrane segment consists mainly of hydrophobic subunits including, in the case of mitochondrial enzyme, all mitochondrial DNA-encoded subunits. A: *Escherichia coli* NDH-1 complex (Guenebaut et al. 1998) B: bovine heart complex I (Grigorieff 1998) C: *Yarrowia lipolytika* complex I (Rademacher et al. 2006), D: *Arabidopsis thaliana* complex I (Dudkina et al. 2005a).

Complex I is frequently described as a cluster, consisting of three different modules: the N Module, the Q Module and the P Module. The N Module, the NADH dehydrogenase module, is the input module that transfers electrons from NADH via FMN onto a chain of iron-sulphur clusters. The Q Module, the electron output module, accepts electrons from the iron sulphur clusters and transfers them via three more iron-sulphur clusters onto ubiquinone. The subunits assigned to the N and Q Module are part of the peripheral arm of complex I, which protrudes into the mitochondrial matrix. These two modules transfer electrons from NADH to UQ. Proton pumping therefore must take place in the third module, the P Module, which is

membrane embedded. The P Module, the proton translocating module, comprises at least seven membrane embedded subunits and transfers protons from the matrix over the IMM into the IMS (Brandt 2006).

In addition to the 14 basic subunits from bacteria, which provide for the basic functions – NADH oxidation, electron transport and proton pumping – complex I of mitochondria from higher eukaryotes, e.g. *Arabidopsis thaliana,* contains up to 32 additional subunits resulting in an overall mass of app. 1000 kDa. The function of these "accessory" subunits is largely unknown. In plants, complex I includes amongst others, five structurally related proteins, which exhibit sequence similarity to a bacterial gamma type carbonic anhydrase (γCA) (Parisi et al. 2004, Perales et al. 200, Perales et al. 2005, Sunderhaus et al. 2006).

Carbonic anhydrases (CA) are zinc containing metallo-enzymes that catalyze the very rapid interconversion of CO_2 and HCO_3^-. Under distinct conditions, the uncatalyzed reaction is frequently slow. The first CA enzyme was found in 1933 in human erythrocytes (Meldrum and Roughton 1933). In plants, CAs are involved in e.g. processes during photosynthesis, respiration and participate in the transport of inorganic carbon (C_i) to photosynthesizing cells. CAs are encoded by at least three distinct, interestingly evolutionary unrelated gene families and are designated as α, β and γ (Hewett-Emmett and Tashian 1996). The α-class is by far the best characterized, with 11 isoenzymes identified. α -CAs have been found in animals, plants, eubacteria and viruses. The β-class CAs are not as widely distributed as the α-type, but have been isolated from plants, algae, eubacteria, archaebacteria and *Saccharomyces cerevisiae.* They have not been found in vertebrates. The third class, the γ-class CAs, were recently discovered in *Methanosarcina thermophila* (reviewed in Moroney et al. 2001 and Tripp et al. 2001). Even more recently, δ-class carbonic anhydrase were reported in archetypal diatoms and marine phytoplankton (in McGinn and Morel 2008).

During the past few years, systematic plant mitochondrial proteome analyses led to the identification of unknown proteins, homologues to 29/30 kDa subunits of complex I. These were termed, "similar to unknown protein from *Rickettsia prowazekii*" (Kruft et al. 2001). Later, these proteins could be identified in forming part of plant mitochondrial complex I in *Arabidopsis*, *Oryza* and *Chlamydomonas* (Heazlewood et al. 2003, Cardol et al. 2004, Perales et al. 2004, Sunderhaus et al. 2006). *Arabidopsis* complex I was shown to include five structurally related subunits of this type. Sequence comparisons including more than one

hundred homologous sequences of plants displayed highest conservation of these proteins to the γCA of *Methanosarcina thermophila* (CAM). Accordingly, it was proposed that the novel complex I subunits represent a protein family showing characteristics of γCA. The *Arabidopsis* γCA family is represented by five members. Three of them contain nearly all functionally important amino acids: γCA1 (At1g19580), γCA2 (At1g47260) and γCA3 (At5g66510). The two other members are more divergent proteins: γCAL1 (CAL = carbonic anhydrase like, At5g63510), γCAL2 (At3g48680) (reviewed in Braun and Zabaleta 2007). Their suborganellar localization was studied by two dimensional blue native/sodium dodecylsulphate polyacrylamide gel electrophoresis (2D BN/SDS-PAGE) in combination with immuno blotting using a polyclonal antibody directed against γCA2, which recognizes all γCA and γCAL proteins, as well as protease protection experiments. If results of the above mentioned experiments are compared with single particle EM pictures of *Arabidopsis* complex I, which shows a spherical extra domain at the matrix exposed side of the complex (Fig. 7), it becomes more and more obvious that the γCA subunits form this plant specific extra domain (Sunderhaus et al. 2006, Braun and Zabaleta 2007).

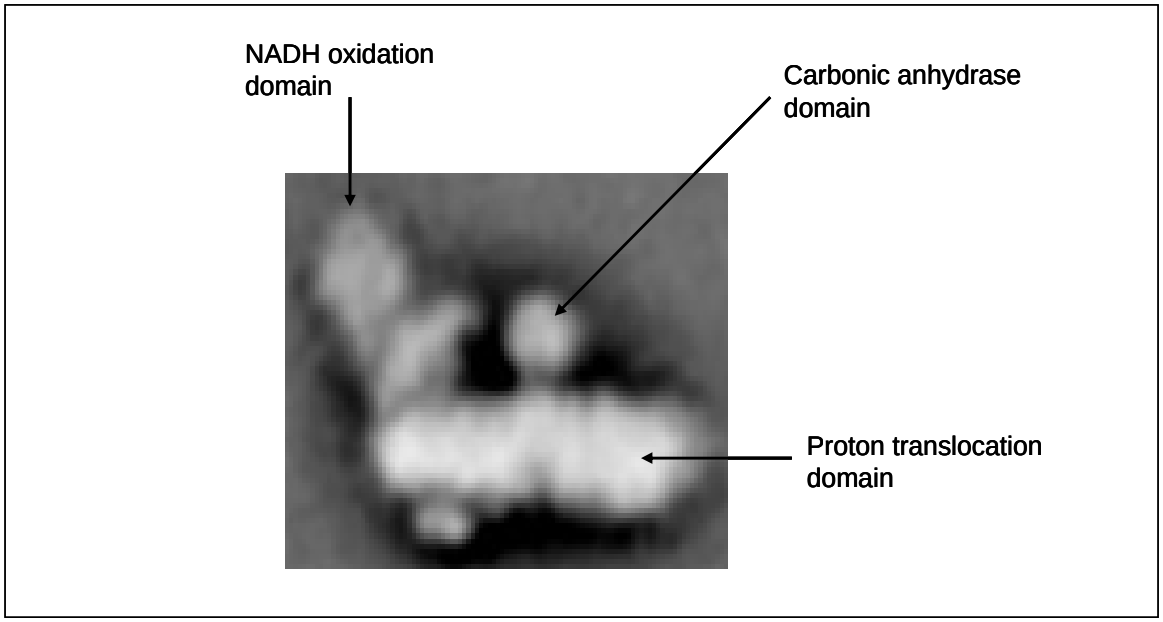

Figure 7. Domain structure of plant mitochondrial complex I. Structural characterization of Arabidopsis mitochondrial complex I by single particle EM indicates a plant specific spherical extra domain of about 60 A in diameter. This domain is attached to the membrane arm of complex I and contains γCAs (Sunderhaus et al. 2006).

However, the physiological role of γCAs in plant mitochondria still remains uncertain. In human mitochondria, CAs have been shown to provide HCO_3^-, which is required for glyconeogenesis and ureagenesis (Fujikawa-Adachi et al. 1999). Additionally, CAs could be

involved in the regulation of the intramitochondrial calcium level, thus contributing to the stability of the intracellular calcium concentration (Ghandur et al. 2000). It is also supposed that CA probably evolved as an enzyme of trans-membrane facilitated CO_2 transport and took on a secondary metabolic role later in metazoan evolution (Henry 1996). None of these functions however seem to be likely to occur in plant mitochondria. Currently, the function of carbonic anhydrases in plant mitochondrial complex I can only be speculated upon. The extra domain could be involved in proton translocation as well as photorespiration. Novel functional insights into structure and function of the mitochondrial CAs of plants are given in Chapter 2.

4. Experimental Strategies to Investigate the OXPHOS System

The most important method for the investigations on the respiratory chain presented in this thesis is blue native polyacrylamide gel electrophoresis (BN-PAGE). BN-PAGE was originally developed for the separation of membrane protein complexes from bacteria and mitochondria from mammals (Schägger and von Jagow 1991, Schägger 2001a, Wittig et al. 2006). The two basic compounds of this method are: 1. non-ionic detergents and 2. negatively charged coomassie dye. The non-ionic detergent of choice for mitochondrial solubilization depends significantly on the stability of the protein complex of interest. The most common detergent for BN-PAGE is dodecyl-β-D-maltoside (DDM). For the investigation presented in this thesis, the detergent of choice is digitonin, which showed to be extremely gentle, especially for the solubilization of mitochondrial complex I from *Arabidopsis thaliana*, the $I+III_2$ supercomplex from *Arum maculatum* and the dimeric ATP synthase complex from *Polytomella* and *Saccharomyces cerevisiae*.

In a first step, membrane protein complexes are gently resolved in a digitonin buffer. Following solubilization, the anionic dye Coomassie blue is added to the protein mixture. This dye is sufficiently soluble in water but also binds excellently to membrane proteins because of its hydrophobic properties. By binding a large number of dye molecules, a negative charge is introduced into the native proteins and protein complexes without denaturing them. Every protein, including the basic ones are now negatively charged and migrate to the anode during gel electrophoresis. The advantage is, that native proteins are no longer separated according to their charge but according to their size. In order to provide a good resolution capacity over a broad range, acrylamide gels used for BN-PAGE are almost always gradient gels. Individual

proteins stop when they approach their size-dependent specific pore-size limit. A second significant advantage is the fact that due to their overall negative charge, hydrophobic membrane proteins do not aggregate during sample preparation and electrophoresis. BN-PAGE is often the starting point for several different techniques dedicated to further investigation of the supramolecular structure of the OXPHOS system and the subunit composition of single proteins and protein complexes, such as *in-gel* enzyme activity stainings, SDS-PAGE, native immuno blotting, electroelution, isoelectric focusing (IEF) or a second BN-PAGE (2D BN/BN-PAGE) (Werhahn and Braun 2002, Zerbetto et al. 1997, Eubel et al. 2005, Wittig et al. 2006). Chapter 4 will describe the latter application in more detail.

5. Objective of the Thesis

This PhD thesis describes systematic investigations related to the structure of the respiratory chain. Initially, a general overview of the structure of the OXPHOS system and an overview of recent progress in this field is given (Chapter 1). One of the main questions of the current thesis was to investigate in which manner the OXPHOS system is organized. The results obtained in plants as well as in yeast demonstrate that the OXPHOS system is organized on higher molecular levels, thereby significantly affecting the membrane structure of the inner mitochondrial membrane (Chapter 3, 5). A second aim was to gain deeper insights into the structure of the NADH dehydrogenase complex. Results obtained in thesis (Chapter 2) support the hypothesized occurrence of a CO_2 recycling mechanism, which provides mitochondrial CO_2 for carbon fixation of chloroplasts during photosynthesis. Finally, the supramolecular organization of the OXPHOS system is investigated in a conjunction with alternative pathways for respiration, namely the cyanide resistant pathway via the Alternative Oxidase. It is shown that formation of supercomplexes does not restrict access of Alternative Oxidase to its substrate ubiquinol (Chapter 6). New methods for the characterization of large membrane bound protein complexes are presented (Chapter 4).

6. References

Affourtit C, Albury MS, Crichton PG, Moore AL (2002) Exploring the molecular nature of alternative oxidase regulation and catalysis. FEBS Lett. 510, 121 – 126.

Albre J, Quilichini A, Gibernau M (2003) Pollination ecology of *Arum italicum* (Araceae). Botanical Journal of the Linnean Society 141, 205 – 214.

Albury MS, Affourtit C, Crichton PG, Moore AL (2002) Structure of plant alternative oxidase. J Biol. Chem. 277, 1190 – 1194.

Allen RD, Schroeder CC, Fok AK (1989) An investigation of mitochondrial inner membranes by rapid-freeze deep-etch techniques. J. Cell Biol. 108, 2233 – 2240.

Allen RD (1995) Membrane tubulation and proton pumps. Protoplasma 189, 1-8.

Andersson ME, Nordlund P (1999) A revised model of the active side of alternative oxidase. FEBS Lett. 449, 17 – 22.

Arnold-Schmitt B, Costa JH, de Melo DF (2006) AOX – a functional marker for efficient cell reprogramming under stress? Trends Plant Sci. 11, 281 – 287.

Berthold DA, Voevodskaya N, Stenmark P, Gräslund A, Nordlund P (2002) EPR studies of the mitochondrial alternative oxidase. J. Biol. Chem. 277, 43608 – 43614.

Berthold DA, Stenmark P (2003) Membrane-bound diiron carboxylate proteins. Annu. Rev. Plant Biol. 54, 497 – 517.

Brandt U (2006) Energy converting NADH:quinone oxdioreductase (complex I). Annu. Rev. Biochem. 75, 69 – 92.

Braun HP, Emmermann M, Kruft V, Schmitz UK (1992) The general mitochondrial processing peptidase from potato is an integral of cytochrome c reductase of the respiratory chain. EMBO J. 11, 3219 – 3227.

Braun HP, Zabaleta E (2007) Carbonic anhydrase subunits of the mitochondrial NADH dehydrogenase complex (complex I) in plants. Physiol. Plant. 129, 114 – 122.

Cardol P, Vanrobaeys F, Devreese B, Van Beeumen J, Matagne RF, Remacle C (2004) Higher plant-like subunit composition of mitochondrial complex I from Chlamydomonas reonhardtii: 31 conserved components among eukaryotes. Biochim. Biophys. Acta. 1658, 212 – 224.

Chance B, Williams GR (1955) A method for the localization of sites for oxidative phosphorylation. Nature 176, 250 – 254.

Considine MJ, Holtzapffel RC, Day DA, Whelan W, Millar AH (2002) Molecular distinction between alternative oxidase from monocots and dicots. Plant Physiol 129, 949 – 953.

Cruciat CM, Brunner S, Baumann F, Neupert W, Stuart RA (2000) The cytochrome bc1 and cytochrome c oxidase complexes associate to form a single supercomplex in yeast mitochondria. J. Biol. Chem. 275, 18093 – 18098.

Dudkina NV, Eubel H, Keegstra W, Boekema EJ, Braun HP (2005a) Structure of a mitochondrial supercomplex formed by respiratory-chain complexes I and III. PNAS 102, 3225 – 3229.

Dudkina NV, Heinemeyer J, Keegstra W, Boekema, EJ, Braun HP (2005b) Structure of dimeric ATP synthase from mitochondria: An angular association of monomers induces the strong curvature of the inner membrane. FEBS Lett. 579, 5769 – 5772.

Dudkina NV, Sunderhaus S, Braun HP, Boekema EJ (2006) Characterization of dimeric ATP synthase and cristae membrane ultra structure from *Saccharomyces* and *Polytomella* mitochondria. FEBS Lett. 580, 3427 – 3432.

Dudkina NV, Sunderhaus S, Boekema EJ, Braun HP (2008) The higher level of organization of the oxidative phosphorylation system: mitochondrial supercomplexes. J. Bioenerg. Biomembr. in press.

Engelman DM (2005) Membranes are more mosaic than fluid. Nature 438, 578 – 580.

Eubel H, Jänsch L, Braun HP (2003) New insights into the respiratory chain of plant mitochondria. Supercomplexes and a unique composition of complex II. Plant Physiol. 133, 274 – 286.

Eubel H, Braun HP, Millar AH (2005) Blue-native PAGE: a tool for analyses of protein-protein interactions. Plant Methods 1:11.

Fowler LR, Hatefi Y (1961) Reconstitution of the electron transport system (III. Reconstitution of DPNH oxidase, succinate oxidase, and DPNH, succinic oxidase). Biochem. Biophys. Res. Comm. 5, 203 – 208.

Fowler LR, Richardson SH (1961) Studies on the electron transport system (L. On the mechanism of reconstitution of the mitochondrial electron transfer system). J. Biol. Chem. 278, 456 – 463.

Fujikawa-Adachi K, Nishimori I, Taguchi T, Onishi S (1999) Human mitochondrial carbonic anhydrase VB. J. Biol. Chem. 274, 21228 – 21233.

Ghandur MS, Parkkila, AK, Parkkila S, Waheed A, Sly WS (2000) Mitochondrial carbonic anhydrase in the nervous system: Expression in neuronal and glial cells. J Neuroch 75, 2212 – 2220.

Gibernau M, Macquart D, Przetak G (2004) Pollination in the genus *Arum* – a review. Aroideana 27, 148 – 166.

Grant NM, Miller RE, Watling JR, Robinson SA (2008) Synchronicity of thermogenetic activity, alternative pathway respiratory flux, AOX protein content, and carbohydrates in receptacle tissues of sacred lotus during floral development. J. Exp. Bot. 59, 705 – 714.

Gray MW, Burger G, Lang FB, (2001) The origin and early evolution of mitochondria. Genome Biology 2: reviews 1018.1 – 1018.5.

Grigorieff N (1998) Three-dimensional structure of bovine NADH:ubiquinone oxidorecductase (complex I) at 22Å. J. Mol. Biol. 277, 1033 – 1046.

Guenebaut V, Schlitt A, Weiss H, Leonard K, Friedrich T (1998) Consistent structure between bacterial and mitochondrial NADH:ubiquinone oxidoreductase (complex I). J. Mol. Biol. 276, 105 – 112.

Hackenbrock CR, Chazotte B, Gupte SS (1986) The random collision model and a critical assessment of diffusion and collision in mitochondrial electron transport. J. Bioenerg. Biomembr. 18, 331 – 368.

Hatefi Y, Haavik AG, Jurtschuk P (1961) Studies on the electron transport system (XXX. DPNH-cytochrome c reductase I). Biochim. Biophys. Acta 52, 106 – 118.

Hatefi Y, Haavik AG, Griffiths DE (1962) Studies on the electron transfer system (XL. Preparation and properties of mitochondrial DPNH.coenzym q reductase). J. Biol. Chem. 237, 1676 – 1680.

Heazlewood JL, Howell KA, Millar AH (2003) Mitochondrial complex I from *Arabidopsis* and rice: orthologs of mammalian and fungal components coupled with plant specific subunits. Biochim. Biophys. Acta 1604, 159 – 169.

Henry RP (1996) Multiple roles of carbonic anhydrases in cellular transport and metabolism. Annu. Rev. Physiol. 58, 523 – 538.

Hewett-Emmett D, Tashian RE (1996) Functional diversity, conservation and convergence in the evolution of the α-, β- and γ- carbonic anhydrase gene families. Mol. Phylogenet. Evol. 5, 50 – 77.

Juszczuk IM, Rychter AM (2003) Alternative Oxidase in higher plants. Acta Biochim. Polonica 50: 1257 – 1271.

Kruft V, Eubel H, Jänsch L, Werhahn W, Braun HP (2001) Proteomic approach to identify novel mitochondrial proteins in *Arabidopsis*. Plant Physiol 127, 1694 – 1710.

Lee AG (2004) How lipids affect the activities of integral membrane proteins. Biochim. et Biophys. Acta 1666, 62 – 87.

Lenaz G, Genova ML (2007) Kinetics of integrated electron transfer in the mitochondrial respiratory chain: random collision vs. solid state electron channeling. Am. J. Physiol. Cell Physiol. 292, C1221 – C1239.

Logan C (2006) The mitochondrial compartment. J. Exp. Bot. 57, 1225 – 1243.

Matsuno-Yagi A, Yagi T (2001) Introduction: Complex I – an L-shaped box. J. Bioenerg. Biomembr. 33, 155 – 157.

McGinn PJ, Morel FM (2008) Expression and regulation of carbonic anhydrases in the marine diatom *Thalassiosira pseudonana* and in natural phytoplankton assemblages from Great Bay New Jersey. Plant Physiol. 133, 78 – 91.

McMahon HT, Gallop JL (2005) Membrane curvature and mechanisms of dynamic cell membrane remodeling. Nature 438, 590 – 596.

Meldrum NU, Roughton FJ (1933) Carbonic anhydrase: its preparation and properties. J. Physiol. 80, 113 – 141.

Millar AH, Wiskich JT, Whelan J, Day DA (1993) Organic acid activation of the alternative oxidase of plant mitochondria. FEBS Lett. 329, 259 – 262.

Millar AH, Mittova V, Kiddle G, Heazlewood JL, Bartoli CG, Theodoulou FL, Foyer CH (2003) Control of ascorbate synthesis by respiration and its implications for stress response. Plant Physiol. 133, 443 – 447.

Møller IM (2001) Plant mitochondria and oxidative stress: electron transport, NADPH turnover and metabolism of reactive oxygen species. Annu. Rev. Plant Physiol. Plant Mol. Biol. 52, 561 – 591.

Moroney JV, Bartlett SG, Samuelsson G (2001) Carbonic anhydrases in plants and algae. Plant Cell Envir. 24, 141 – 153.

Parisi G, Perales M, Fornasari MS, Colaneri A, Gonzalez-Schain N, Gomez-Casati D, Zimmermann S, Brennicke A, Araya A, Ferry JG, Echave J, Zabaleta E (2004) Gamma carbonic anhydrases in plant mitochondria. Plant Mol. Biol. 55, 192 – 207.

Paumard P, Vaillier J, Coulary B, Schaeffer J, Soubannier V, Mueller DM, Brethes D, di Rago J-P, Velours J (2002) The ATP-Synthase is involved in generating mitochondrial cristae morphology. EMBO J. 21, 221 – 230.

Perales M, Parisi G, Fornasari MS, Colaneri A, Villareal F, Gonzalez-Schain N, Echave J, Gomez-Casati D, Braun HP, Araya A, Zabaleta E (2004) Gamma carbonic anhydrase like complex interact with plant mitochondrial complex I. Plant Mol. Biol. 56, 947 – 957.

Perales M, Eubel H, Heinemeyer J, Colaneri A, Zabaleta E, Braun HP (2005) Disruption of a nuclear gene encoding a mitochondrial gamma-type carbonic anhydrase reduces complex I and supercomplex I+III_2 levels and alters mitochondrial physiology in *Arabidopsis*. J. Mol. Biol. 350, 263 – 277.

Rademacher M, Ruiz T, Clason T, Benjamin S, Brandt U, Zickerman V (2006) The Three dimensional structure of complex I from *Yarrowia lipolytika*: A highly dynamic enzyme. J. Struct. Biol. 154, 269 – 279.

Raskin I, Ehmann A, Melander WR, Meeuse BJD (1987) Salicylic acid: A natural inhibitor of heat production in Arum lilies. Science 237, 1601 – 1602.

Rhoads DM, McIntosh L (1992) Salicylic acid regulation of respiration in higher plants: alternative oxidase expression. Plant Cell 4, 1131 – 1139.

Sagan L (1967) On the origin of mitosing cells. J. Theor. Biol. 14, 255 – 274.

Schägger H, von Jagow G (1991) Blue native electrophoresis for isolation of membrane protein complexes in enzymatically active form. Anal. Biochem. 199, 223 – 231.

Schägger H, Pfeiffer K (2000) Supercomplexes in the respiratory chains of yeast and mammalian mitochondria. EMBO J. 19, 1777 – 1783.

Schägger H (2001a) Blue native gels to isolate protein complexes from mitochondria. Methods Cell Biol. 65, 231 – 244.

Schägger H (2001b) Respiratory chain supercomplexes. IUBMB Life 52, 119 – 128.

Schägger H, Pfeiffer K (2001) The ratio of oxidative phosphorylation complexes I – V in bovine heart mitochondria and the composition of respiratory chain supercomplexes. J. Biol. Chem. 276, 37861 – 37867.

Schlame M (2008) Cardiolipin synthesis for the assembly of bacterial and mitochondrial membranes. J. Lipid Res. 49, 1607 – 1620.

Seymour RS (2001) Biophysics and physiology of temperature regulation in thermogenetic flowers. Bioscience Reports 21, 223 – 236.

Seymour RS, White CR, Gibernau M (2003) Heat reward for insect pollinators. Nature 426, 243 – 244.

Siedow JN (1982) The nature of cyanide-resistant pathway in plant mitochondria. Recent Adv. Phytochem. 16, 47 – 83.

Siedow JN, Umbach AL (2000) The mitochondrial cyanide resistant oxidase: structural conservation amid regulatory diversity. Biochim. Biophys. Acta 1459, 432 – 439.

Singer SJ, Nicholson GL (1972) The fluid mosaic model of the structure of membranes. Science 175, 720 – 731.

Sunderhaus S, Dudkina NV, Jänsch L, Klodmann J, Heinemeyer J, Perales M, Zabaleta E, Boekema EJ, Braun H.-P. (2006) Carbonic anhydrase subunits form a matrix exposed domain attached to the membrane arm of mitochondrial complex I in plants. J. Biol. Chem. 281, 6482 – 6488.

Tripp BC, Smith K, Ferry JG (2001) Carbonic anhydrase: New insights for an ancient enzyme. J. Biol. Chem. 52, 48615 – 48618.

Umbach AL, Siedow JN (1993) Covalent and noncovalent dimers of the cyanide-resistant alternative oxidase protein in higher plant mitochondria and their relationship to enzyme activity. Plant Physiol. 103, 845 – 854.

Vanlerberghe GC, McIntosh L (1997) Alternative Oxidase: From gene to function. Annu. Rev. Plant Physiol. Plant Mol. Biol. 48, 703 – 734.

Voeltz GK, Prinz WA (2007) Sheets, ribbons and tubules – how organellars get their shape. Nature 8, 258 – 264.

Wagner AM, Krab K, Wagner MJ, Moore AL (2008) Regulation of thermogenesis in flowering Araceae: Thr role of alternative oxidase. Biochim. Biophys. Acta 1777, 993 – 1000.

Werhahn W, Braun HP (2002) Biochemical dissection of the mitochondrial proteome from *Arabidopsis thaliana* by three-dimensional gel electrophoresis. Electrophoresis 23, 640 – 646.

Wittig I, Braun HP, Schägger H (2006) Blue native PAGE. Nature Protocols 1, 418 – 428.

Zerbetto E, Vergani V, Dabbeni-Sala F (1997) Quantification of muscle mitochondrial oxidative phosphorylation enzymes by histochemical staining of blue native polyacrylamide gels. Electrophoresis 18, 2059 – 2064.

Chapter 2

Carbonic Anhydrase Subunits form a Matrix-exposed Domain Attached to the Membrane Arm of Mitochondrial Complex I in Plants.

THE JOURNAL OF BIOLOGICAL CHEMISTRY VOL. 281, NO. 10, pp. 6482–6488, March 10, 2006
© 2006 by The American Society for Biochemistry and Molecular Biology, Inc. Printed in the U.S.A.

Carbonic Anhydrase Subunits Form a Matrix-exposed Domain Attached to the Membrane Arm of Mitochondrial Complex I in Plants*[S]

Received for publication, October 25, 2005, and in revised form, December 30, 2005 Published, JBC Papers in Press, January 4, 2006, DOI 10.1074/jbc.M511542200

Stephanie Sunderhaus[‡], Natalya V. Dudkina[§], Lothar Jänsch[¶], Jennifer Klodmann[‡], Jesco Heinemeyer[‡], Mariano Perales[‖], Eduardo Zabaleta[‖], Egbert J. Boekema[§], and Hans-Peter Braun[‡1]

From the [‡]Institut für Angewandte Genetik, Universität Hannover, Herrenhäuser Strasse 2, D-30419 Hannover, Germany, the [§]Department of Biophysical Chemistry, Groningen Biomolecular Sciences and Biotechnology Institute, University of Groningen, Nijenborgh 4, 9747 AG Groningen, The Netherlands, [¶]Gesellschaft für Biotechnologische Forschung, Mascheroder Weg 1, D-38124 Braunschweig, Germany, and the [‖]Instituto de Investigaciones Biológicas, Facultad de Ciencias Exactas y Naturales, Universidad Nacional de Mar del Plata, Funes 3250, 7600 Mar del Plata, Argentina

Complex I of Arabidopsis includes five structurally related subunits representing γ-type carbonic anhydrases termed CA1, CA2, CA3, CAL1, and CAL2. The position of these subunits within complex I was investigated. Direct analysis of isolated subcomplexes of complex I by liquid chromatography linked to tandem mass spectrometry allowed the assignment of the CA subunits to the membrane arm of complex I. Carbonate extraction experiments revealed that CA2 is an integral membrane protein that is protected upon protease treatment of isolated mitoplasts, indicating a location on the matrix-exposed side of the complex. A structural characterization by single particle electron microscopy of complex I from the green alga Polytomella and a previous analysis from Arabidopsis indicate a plant-specific spherical extra-domain of about 60 Å in diameter, which is attached to the central part of the membrane arm of complex I on its matrix face. This spherical domain is proposed to contain a heterotrimer of three CA subunits, which are anchored with their C termini to the hydrophobic arm of complex I. Functional implications of the complex I-integrated CA subunits are discussed.

Carbonic anhydrases (CA)[2] are zinc-containing enzymes that catalyze the reversible interconversion of CO_2 and HCO_3^-. In higher plants, carbonic anhydrases have been localized to the chloroplast stroma and to the cytoplasm; in algae additionally to the mitochondrion (reviewed in Moroney *et al.*, Ref. 1)). Chloroplast carbonic anhydrases are important for efficient delivery of CO_2 to ribulose-bisphosphate carboxylase/oxygenase (RubisCO). In contrast, the physiological role of carbonic anhydrases of other subcellular compartments is still a matter of debate. Structurally, carbonic anhydrases can be divided into three families termed α, β, and γ, which evolved independently (2). The chloroplast carbonic anhydrases belong to the β family. Homologs of carbonic anhydrases from all three families were identified in the course of the Arabidopsis genome sequencing project (1, 3), but so far have not been physiologically characterized.

Recently, γ-type carbonic anhydrases were found to be localized within plant mitochondria attached to complex I of the respiratory chain. This complex was first purified about 10 years ago from plants (Refs. 4–8, reviewed in Rasmusson *et al.* Ref. 9). Many of the characterized subunits were found to be homologous to subunits of complex I from fungi and animals, but some did not exhibit any significant sequence identity, *e.g.* an "unknown 29-kDa protein" of potato complex I (5). Systematic identification of complex I proteins in Arabidopsis, rice, and Chlamydomonas led to the discovery of up to 5 subunits related to the "unknown 29-kDa protein" within this respiratory complex of these organisms (10, 11).[3] Based on sequence comparisons, these subunits were initially proposed to be called "ferripyochelin-binding proteins." However, later it became clear that these identifications were based on a falsely annotated data base entry (12). Instead, significant sequence identity was discovered to the prototype γ-carbonic anhydrase of the Archaebacterium *Methanosarcina thermophila* (12). Computer modeling using the crystal structure of the archaebacterial γ-carbonic anhydrase revealed that at least three of the five plant-specific complex I subunits of Arabidopsis have a conserved active site (12). They are called carbonic anhydrase 1 (CA1) (At1g19580), CA2 (At1g47260), and CA3 (At5g66510) in Arabidopsis. Two further related complex I subunits of Arabidopsis have a less conserved primary structure and are termed carbonic anhydrase-like protein 1 (CAL1) (At5g63510) and CAL2 (At3g48680) (13).

The physiological role of CA2 and CA3 in plant mitochondria was addressed with the use of Arabidopsis knock-out lines (14). Surprisingly, the phenotype of the mutants was not distinguishable from a wild-type line under all conditions tested, which might be a consequence of redundant activities of the five related complex I subunits. However, suspension cell cultures of the knock-out lines had a reduced growth rate. Furthermore, complex I levels were clearly reduced in mutant lines, indicating that the CA subunits are important for complex I assembly. The genes encoding CA1 and CA2 were found to be down-regulated when Arabidopsis plants are grown under elevated CO_2 concentrations, supporting a role of these proteins in mitochondrial one-carbon metabolism. Possibly the CA subunits play important roles in the context of photorespiration, which leads to the liberation of large amounts of CO_2 in plant mitochondria, especially under high light conditions (14).

* This work was supported by Grant Br1829-7/1 from the Deutsche Forschungsgemeinschaft. The costs of publication of this article were defrayed in part by the payment of page charges. This article must therefore be hereby marked "*advertisement*" in accordance with 18 U.S.C. Section 1734 solely to indicate this fact.

[S] The on-line version of this article (available at http://www.jbc.org) contains supplemental Fig. S1.

[1] To whom correspondence should be addressed. E-mail: braun@genetik.uni-hannover.de.

[2] The abbreviations used are: CA, carbonic anhydrase; Tricine, *N*-[2-hydroxy-1,1-bis(hydroxymethyl)ethyl]glycine; MOPS, 4-morpholinepropanesulfonic acid; EM, electron microscopy; ANT, adenine nucleotide translocator; SOD, superoxide dismutase; PMSF, phenylmethylsulfonyl fluoride.

[3] H. P. Braun, unpublished results.

The location of the carbonic anhydrase subunits within mitochondrial complex I so far is unknown. The CAL1 and CAL2 subunits of Arabidopsis were shown to interact with CA2 using the yeast two-hybrid system (13). Very recently, the projection structure of Arabidopsis complex I was resolved by electron microscopy and single particle analysis (15). Interestingly, it shows an extra matrix-exposed domain, which is attached to the membrane arm of this complex. Here we present evidence that CA2 forms part of this extra-domain: CA2 cannot be detached from mitochondrial membranes by carbonate extraction, was identified by mass spectrometry to form part of the membrane arm of complex I and is shown to be localized on the matrix-exposed side of this arm by protease protection experiments with isolated mitoplasts. Location of the carbonic anhydrase domain of complex I was confirmed by a structural analysis of this complex from Polytomella by electron microscopy and single particle analysis.

MATERIALS AND METHODS

Cultivation of Arabidopsis and Polytomella—Arabidopsis cell suspension cultures were established as described by May and Leaver (16). Cells were cultivated in 500-ml flasks containing 100 ml of medium (0.316% (w/v) B5 medium, 3% (w/v) sucrose, 0.0001% (w/v) 2,4 dichlorphenoxyacetic acid, 0.00001% (w/v) kinetin, pH 5.75) at 25 °C, and 90 rpm in the dark. Cells were transferred into fresh medium all 7 days. The starting material for mitochondrial isolation was ~100 × *g* cells.

Polytomella spp. (198.80, E. G. Pringsheim) was obtained from the "Sammlung von Algenkulturen der Universität Göttingen" (SAG) (epsag.uni-goettingen.de/html/sag.html). Cells were cultivated in 2.5-liter culture flasks containing 1200 ml of medium (0.2% (w/v) sodium acetate, 0.1% (w/v) yeast extract, 0.1% (w/v) tryptone) for 4–5 days at 25 °C in the dark without shaking. The starting material for mitochondrial isolations was ~100 × *g* cells.

Isolation of Mitochondria from Polytomella—Mitochondria from Polytomella were purified as outlined in Dudkina *et al.* (17). Organelles were resuspended in resuspension buffer (0.4 M mannitol, 1 mM EGTA, 10 mM Tricine, 0.1 mM PMSF, pH 7.2) at a protein concentration of 10 mg/ml, divided into 100-μl aliquots, and stored at −80 °C.

Isolation and Subfractionation of Mitochondria from Arabidopsis—Mitochondria from Arabidopsis were purified as outlined in Werhahn *et al.* (18). Organelles were resuspended in resuspension buffer (0.4 M mannitol, 1 mM EGTA, 10 mM Tricine, 0.2 mM PMSF, pH 7.2) and either stored at −80 °C or directly used for the generation of mitochondrial subfractions. In the latter case, mitochondria were sedimented by centrifugation for 10 min at 12 000 × *g* and resuspended in resuspension buffer without mannitol at a protein concentration of 10 mg/ml. Mitochondria were broken by sonication with a Ultrasonic cell disruptor (Misonix Inc.) in four intervals of 10 s. Unbroken mitochondria were sedimented by centrifugation for 7 min at 5000 × *g* and discarded. The supernatant was centrifuged at 150,000 × *g* for 90 min. The resulting pellet contains the mitochondrial membranes whereas the supernatant contains the soluble proteins of the mitochondrial matrix and the intermembrane space. The pellet was resuspended with resuspension buffer at a protein concentration of 10 mg/ml. Membrane and soluble fractions were divided into aliquots and stored at −80 °C. The purity of subfractions was analyzed by two-dimensional blue-native PAGE (see below) or by immunoblotting experiments using antibodies directed against marker proteins of the mitochondrial membrane and soluble fractions (see "Results").

Carbonate Extraction—For carbonate extraction, mitochondrial membranes were resuspended in carbonate buffer (0.1 M Na_2CO_3, 0.1 mM PMSF, pH 11.5) at a protein concentration of 10 mg/ml and incubated for 5 min at 4 °C. Afterward the membranes were again sedimented by ultracentrifugation for 90 min at 150,000 × *g*. The pellet was finally resuspended in resuspension buffer at a protein concentration of 10 mg/ml and divided into aliquots (membranes with integral membrane proteins); the supernatant was directly divided into aliquots (peripheral membrane proteins). All aliquots were stored at −80 °C.

Protease Protection Experiments—Mitoplasts (mitochondria lacking the outer membrane) were generated from isolated mitochondria to obtain topological information on inner membrane proteins: first mitochondria were sedimented by centrifugation and resuspended in swelling buffer (5 mM potassium phosphate, pH 7.2) at a protein concentration of 5 mg/ml. Subsequently the outer mitochondrial membrane was selectively ruptured by treatment with a Teflon homogenizer (20 strokes). Resulting mitoplasts and outer membrane fragments were next separated by sucrose gradient ultracentrifugation (step gradient of 60%, 32%, and 15% sucrose in 1 mM EDTA, 10 mM MOPS, pH 7.2) for 1 h at 92,000 × *g*. Mitoplasts are enriched at the 32/60% interphase of the gradients. They were purified from sucrose by dilution with resuspension buffer, sedimentation by centrifugation for 10 min at 12,000 × *g*, and again resuspended in resuspension buffer at a protein concentration of 10 mg/ml. For protease protection experiments, 250-μl mitoplasts were combined with 10 μl of protease solution (0.1% proteinase K in 10 mM Tris-HCl, pH 7.2) and incubated for 30 min on ice. The reaction is stopped by addition of 2.5 μl of PMSF solution (200 mM PMSF). Fractions were either directly analyzed by one-dimensional SDS-PAGE and immunoblotting (see below) or stored at −80 °C.

Gel Electrophoresis Procedures and Immunoblotting—One-dimensional SDS-PAGE was carried out according to Schägger *et al.* (19), one-dimensional blue-native PAGE and two-dimensional blue-native/SDS-PAGE according to Heinemeyer *et al.* (20), and two-dimensional blue-native/blue-native PAGE as outlined by Sunderhaus *et al.* (21). Proteins were either visualized by Coomassie Blue-colloidal staining (22, 23), in-gel NADH dehydrogenase activity staining (24), or blotted onto nitrocellulose filters. Blots were incubated overnight with different antibodies directed against the mitochondrial adenine nucleotide translocator (ANT), the mitochondrial superoxide dismutase (SOD), and the C-terminal half of the mitochondrial CA (At1g47260) from Arabidopsis (14). Visualization of immune-positive bands was performed using biotinylated secondary antibodies, avidin, and horseradish peroxidase (Vectastain ABC kit, Vector Labs). Selected protein complexes were cut out from Coomassie Blue-stained two-dimensional blue-native/blue-native gels and subunits were identified by mass spectrometry (25).

Purification of Complex I from Polytomella—Complex I from Polytomella was purified as outlined in Dudkina *et al.* (15) for the corresponding protein complex from Arabidopsis. About 1 mg of Polytomella mitochondria (100 μg of mitochondrial protein) was redissolved in digitonin solubilization buffer (5.0% digitonin, 30 mM HEPES, 150 mM potassium acetate, pH 7.4). Solubilized protein complexes were subsequently separated by sucrose gradient ultracentrifugation (gradients of 0.3–1.5 M sucrose/15 mM Tris base, pH 7.0, 20 mM KCl/0.2% digitonin) for 20 h at 150,000 × *g*. Fractions were removed from the gradient from bottom to top. The protein complex content of the fractions was analyzed by one-dimensional blue-native PAGE and two-dimensional blue-native/SDS-PAGE (see above). Complex I-containing fractions were used for EM analyses.

Electron Microscopy and Image Analysis—Negatively stained specimens were prepared with 2% uranyl acetate on glow-discharged carbon-coated copper grids. Images were recorded with a Gatan 4K slow-scan CCD camera on a Philips CM12 electron microscope. 2000 × 2000 pixel images were recorded at ×77,400 magnification with a pixel size of 15

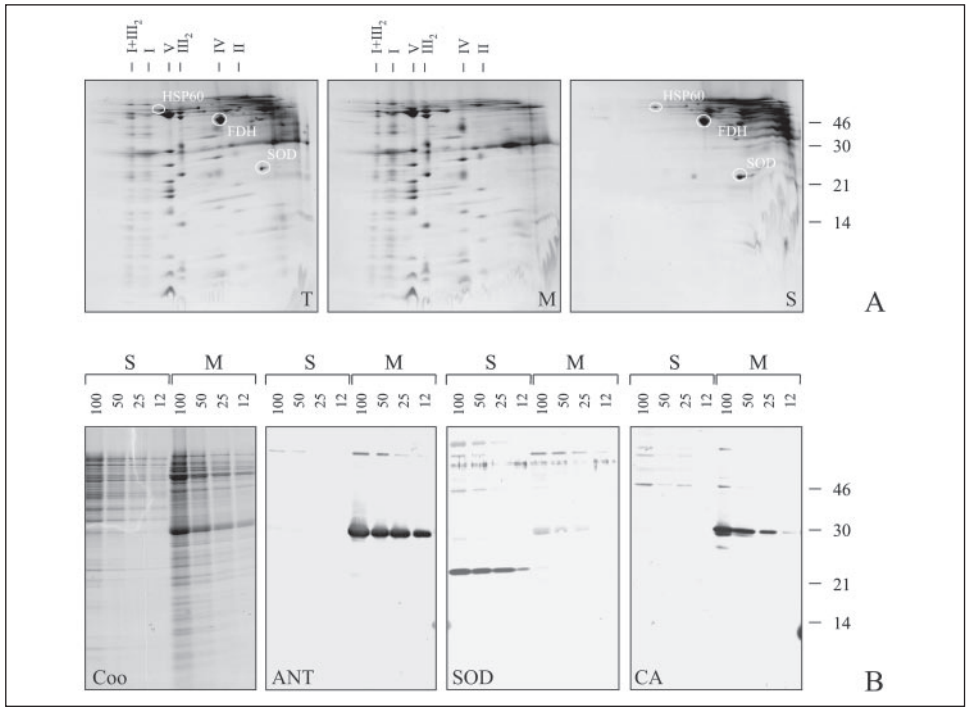

FIGURE 1. **Submitochondrial localization of the carbonic anhydrase CA2.** Mitochondria were isolated and subfractionated into a membrane and a soluble fraction as described under "Materials and Methods." *A*, documentation of the purity of the subfractions by two-dimensional blue-native/SDS-PAGE. *T*, total mitochondrial protein; *M*, protein of the membrane fraction; *S*, protein of the soluble fraction. Identities of membrane-bound protein complexes are given above the gels (*I*, complex I; *II*, complex II; III_2, dimeric complex III; *IV*, complex IV; *V*, ATP synthase complex; $I+III_2$, supercomplex formed by complex I and dimeric complex III) and identities of soluble protein complexes directly on the two-dimensional gels (*HSP60*, heat stress protein *60*, *FDH*, formate dehydrogenase). The molecular masses of standard proteins are given to the *right* (in kDa). *B*, immunological localization of carbonic anhydrase. Varying amounts of protein (indicated *above* the gels in μg) of the soluble (*S*) and the membrane (*M*) fraction were resolved by one-dimensional SDS-PAGE and Coomassie-stained (*Coo*) or blotted onto nitrocellulose. Proteins of interest were detected using antibodies directed against ANT (membrane marker), SOD (matrix marker), and CA. Molecular masses of standard proteins are given to the *right* of the gels (in kDa).

μm and a binning factor of 2, corresponding to a size of 3.85 Å at the specimen level. Single particle projections were extracted from images and analyzed with Groningen image processing (Grip) software on a PC cluster. Images were subsequently subjected to multireference alignment, multivariate statistical analysis, and hierarchical classification as described before (15). Resolution of averaged single particle two-dimensional projections was measured according to van Heel (26).

RESULTS

The Carbonic Anhydrase CA2 of Arabidopsis Is an Integral Membrane Protein—Complex I of plants purified by chromatographic or electrophoretic procedures was shown to include carbonic anhydrase subunits. Deletion of the gene encoding CA2 drastically reduces complex I levels in Arabidopsis, indicating an integral position of this protein within this respiratory complex. However, a more loosely binding of the carbonic anhydrase subunits to complex I so far cannot be excluded. Therefore, localization of the carbonic anhydrases was immunologically tested using submitochondrial fractions. The following results are based on an antibody directed against the C-terminal half of CA2 (At1g47260), which previously was shown to be monospecific for the CA2 protein (14).

Mitochondria from Arabidopsis were subfractionated into a membrane (M) and a soluble (S) fraction as described under "Materials and Methods." The purity of the generated fractions was tested by two-dimensional blue-native PAGE (Fig. 1*A*). The respiratory protein complexes, which were identified on the basis of their subunit compositions (27), were exclusively present in the membrane fraction. In contrast the formate dehydrogenase complex, the HSP60 complex and the SOD of the mitochondrial matrix were absent in this fraction but present in the soluble fraction. The purity of the mitochondrial subfractions was confirmed by one-dimensional SDS-PAGE and immunoblotting using antibodies directed against ANT (marker for the mitochondrial membrane fraction) and SOD (marker for the soluble mitochondrial fraction) (Fig. 1*B*). ANT exclusively was recognized in the membrane fraction, SOD in the soluble fraction. In conclusion, the generated subfractions can be considered to be very pure.

In a parallel immunoblotting experiment, CA2 was only detectable in the membrane fraction. Probing the 12-μg sample of the membrane fraction gave a clear signal on the immunoblot, whereas no signal was observed in the corresponding 100-μg sample of the soluble fraction (Fig. 1*B*, *right immunoblot*). This suggests that CA2 is a membrane protein.

In the next step, carbonate extraction was employed to test whether CA2 is an integral membrane protein or associated to the surface of the membrane. Mitochondria were isolated from Arabidopsis and subfractionated into a soluble fraction (SP), a fraction containing peripheral membrane proteins (PMP), and a fraction containing integral membrane proteins (IMP) as described under "Materials and Methods." All three subfractions have a very distinct composition of proteins as monitored by one-dimensional SDS-PAGE in combination with Coomassie Blue-staining (Fig. 2). Parallel immunoblotting experiments were carried out to monitor the purity of the generated subfractions. As expected, only SOD is present in the soluble fraction and ANT in the fraction of integral membrane proteins. Similarly, CA2 was nearly exclusively present in the fraction of integral membrane proteins. We conclude that CA2 is an integral membrane protein.

The Carbonic Anhydrase CA2 Forms Part of the Membrane Arm of Complex I—Complex I has an L-like shape. The matrix arm, which is responsible for NADH oxidation, protrudes into the matrix. It is attached to a membrane arm responsible for the proton translocation activity of complex I. The location of CA2 with respect to these two arms was investigated by blue-native/blue-native PAGE in combination with in-gel NADH oxidation activity staining and mass spectrometry. Proteins normally are localized on a diagonal line on gel systems if the same buffer and detergent conditions were used for both dimensions. However, in an alternative approach of blue-native/blue-native PAGE, the first gel dimension is carried out in the presence of digitonin, which is for the most part mild for protein solubilization, and the second gel dimension in the presence of dodecylmaltoside, which is slightly less mild (28). Protein complexes specifically destabilized in the presence of the second detergent were divided on this two-dimensional gel system into subcomplexes of enhanced electrophoretic mobility, which are vis-

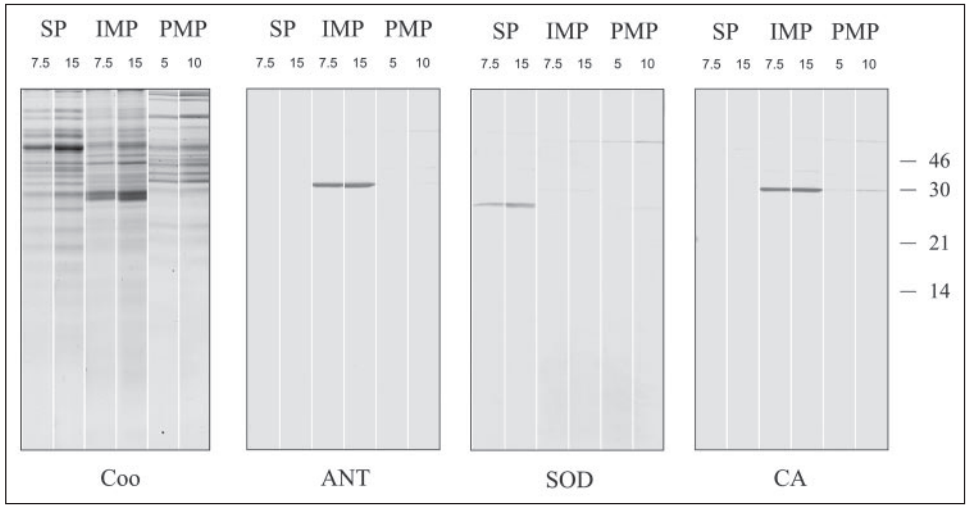

FIGURE 2. **Analysis of the anchoring of carbonic anhydrase CA2 within the inner mitochondrial membrane by carbonate extraction.** Peripheral and integral membrane proteins were separated by carbonate treatment and subsequent centrifugation as described under "Materials and Methods." Two different protein amounts (indicated *above* the gels in μg) of fractions containing soluble mitochondrial proteins (*SP*), integral membrane proteins (*IMP*), and peripheral membrane proteins (*PMP*) were separated by one-dimensional SDS-PAGE and Coomassie Blue-stained (*Coo*) or blotted onto nitrocellulose. Proteins of interest were immunodetected using antibodies directed against SOD (matrix marker), ANT (membrane marker), and CA. The molecular masses of standard proteins are given to the *left* of the Coomassie Blue-stained gel.

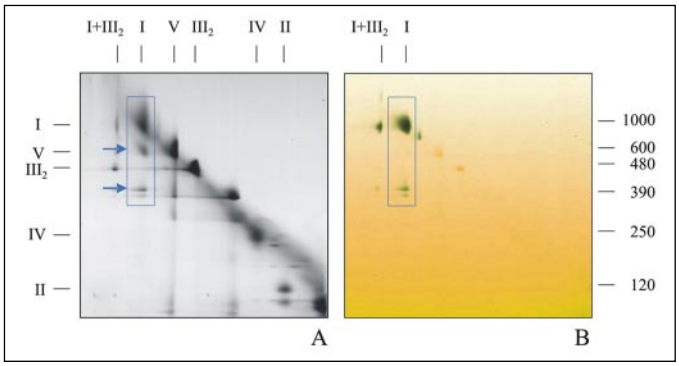

FIGURE 3. **Partial division of complex I from Arabidopsis into two subcomplexes.** Total mitochondrial membrane protein of Arabidopsis was resolved by two-dimensional blue-native/blue-native PAGE. First dimension blue-native PAGE was carried out in the presence of digitonin, second dimension blue-native PAGE in the presence of dodecylmaltoside. *A*, Coomassie Blue-stained two-dimensional gel; *B*, complex I activity-stained gel (NADH oxidation). Identities of protein complexes are given on *top* of the gels and to the *left* of the Coomassie Blue-stained gel; molecular masses of standard protein complexes are given to the *right* of the activity-stained gel. Complex I and its subcomplexes of 600 and 400 kDa (*arrows*) are marked by a *box*.

ible beneath the diagonal line. Using this gel system, complex I of Arabidopsis (1000 kDa) partially becomes divided into a 600- and a 400-kDa subcomplex (Fig. 3). For unknown reasons, the 400-kDa complex in part gets further divided into a 380-kDa complex. The 400/380-kDa complexes represent the matrix arm of complex I as shown by in-gel NADH oxidation activity staining (Fig. 3). We conclude that the 600-kDa complex must represent the membrane arm.

To localize CA2 within complex I, the two 600- and 400-kDa subcomplexes were directly cut out from the two-dimensional blue-native/blue-native gel, trypsinated, and analyzed by liquid chromatography in combination with tandem mass spectrometry (Table 1). 19 different proteins could be identified forming part of the 600-kDa complex, 16 of which were previously known (Ref. 10 and references within) and 3 of which were described for the first time (At1g14450, At4g00585, At1g67350). As expected, several of the subunits forming part of the 600-kDa subcomplex of complex I from Arabidopsis are homologous to complex I subunits from beef and *Neurospora crassa* known to be present in the membrane arm. Furthermore, 4 of the 5 CA subunits (γCA1, γCA2, γCA3, γCAL2) were identified forming part of the 600-kDa complex. In contrast, no CA subunits were identified within the 400-kDa subcomplex, which includes 4 known proteins of the matrix arm (Table 1). We conclude that the CA subunits of complex I from Arabidopsis are integral membrane proteins, which form part of the membrane arm of this complex. This result was confirmed by immunoblotting experiments using two-dimensional blue-native/blue-native gels (data not shown).

The Carbonic Anhydrase CA2 Is Localized on the Matrix-exposed Side of the Membrane Arm of Complex I—The topological localization of CA2 within the membrane arm of complex I was addressed by protease protection experiments using isolated mitoplasts (mitochondria lacking the outer mitochondrial membrane). Mitoplasts of Arabidopsis were incubated with proteinase K as outlined under "Materials and Methods." Subsequently, proteins of protease-treated and untreated mitoplasts were analyzed by SDS-PAGE and immunoblotting (Fig. 4). As expected, SOD was protease-protected, because it was localized within the mitochondrial matrix. ANT was accessible to protease digestion. As known from the crystal structure of this protein from beef, ANT is composed of six membrane-spanning helices (29). The N and the C terminus as well as two internal loops are exposed to the intermembrane space. Therefore, degradation of ANT upon protease treatment of mitoplasts into several distinct fragments is expected. In contrast, the 30-kDa CA2 proved to be protease-protected. Only one very faint degradation product was visible on the corresponding immunoblot at 28 kDa (Fig. 4). We conclude that CA2 is an integral membrane protein of the membrane arm of complex I, which is localized on the matrix side of this arm. Possibly a small part (2 kDa) of the protein protrudes into the intermembrane space.

Polytomella Also Has the Matrix-exposed Extra-domain of Complex I—Single particle electron microscopy is a suitable technique for a direct structural characterization of CA subunits within complex I. Previously, EM data from Arabidopsis revealed a spherical extra matrix-exposed domain, which is attached to the central part of the membrane arm (15). Most likely the extra-domain represents the carbonic anhydrase subunits of complex I. This hypothesis was tested with an alga species. The green alga Chlamydomonas was recently reported to also include homologous CA subunits within complex I (11). It therefore should also have an extra CA domain. This was investigated using purified mitochondria from *Polytomella spp.*, a non-green alga of the Chlamydomonaceae closely related to *Chlamydomonas reinhardtii*. Analysis of the mitochondria by two-dimensional blue-native/SDS-PAGE allowed us to identify the known respiratory protein complexes of Polytomella (30–32): dimeric complexes III and V, two forms of complex IV, and complex I. Complex I is partially divided into a smaller

TABLE 1

Identified subunits of the 600- and 400-kDa subcomplexes of complex I

Protein complex[a]	Accession numbers[b]	Proteins[c]	Calc mol. mass[d]	MOWSE score[e]	Coverage[f]
600 kDa	At1g47260	NADH-DH carbonic anhydrase subunit	30.0	391	13
	At3g48680	NADH-DH carbonic anhydrase subunit	28.0	153	5
	At2g33220	NADH-DH B 16.6 subunit (*N. crassa*)	16.1	124	6
	At1g04630	NADH-DH B 16.6 subunit (*N. crassa*)	16.1	124	6
	At2g27730	NADH-DH 16 kDa (*Solanum tuberosum*)	11.9	123	2
	At5g66510	NADH-DH carbonic anhydrase subunit	27.8	105	4
	At2g02050	NADH-DH CI-B18 (beef)	11.7	88	5
	At1g14450	Unknown protein	8.2	85	3
	At1g19580	NADH-DH carbonic anhydrase subunit	30.0	84	4
	At4g34700	NADH-DH chain CI-B22 (*N. crassa*)	13.6	73	3
	At4g16450	NADH-DH 20.9-kDa chain (*N. crassa*)	11.4	73	3
	At1g67350	Unknown protein	15.2	59	3
	At2g31490	NADH-DH subunit (*Arabidopsis thaliana*)	8.2	57	2
	At3g18410	NADH-DH 14-kDa subunit (*S. tuberosum*)	12.4	56	1
	At1g49140	NADH-DH PDSW subunit (beef)	12.5	56	1
	At2g47690	NADH-DH 15-kDa subunit (beef)	14.0	55	2
	AtMg01120	NADH-DH, subunit 1	36.0	49	1
	At4g00585	Unknown protein	9.8	49	1
	At2g42310	NADH-DH subunit (*A. thaliana*)	12.6	41	2
400 kDa	At5g37510	NADH-DH, 76-kDa chain precursor protein	81.5	187	6
	At2g20360	NADH-DH, 40-kDa chain (*N. crassa*) = 39-kDa protein	43.9	104	3
	nad7	NADH-DH, subunit 7 = nuoD	44.6	72	2
	At5g52840	NADH-DH 22.5-kDa subunit (*S. tuberosum*) 13-kDa-B subunit (B13) (beef)	19.2	32	2

[a] Protein complexes were directly excised from the Coomassie Blue-stained BN / BN gel shown in Fig. 3.
[b] Accession numbers corresponding to TAIR (www.arabidopsis.org/).
[c] Protein identities based on sequence identity to complex I subunits from other organisms as revealed by BLAST searches.
[d] Calculated molecular mass of the identified precursor proteins (in kDa).
[e] MOWSE score from the MASCOT software package. (www.matrixscience.com/).
[f] Number of matching peptides.

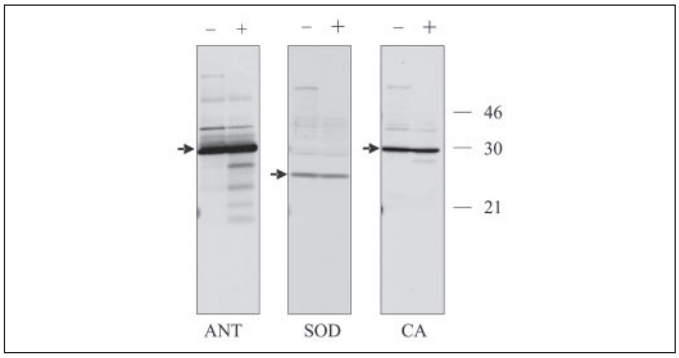

FIGURE 4. **Topographical analysis of carbonic anhydrase CA2 by protease protection experiments.** Mitoplasts (mitochondria lacking the outer membrane) were incubated with proteinase K as described under "Materials and Methods." Total mitochondrial protein of untreated (−) and treated (+) fractions was resolved by SDS-PAGE and blotted onto nitrocellulose. Proteins of interest were identified by immunodetection using antibodies directed against ANT (marker for an integral inner membrane protein accessible for protease digestion), SOD (marker for a matrix protein inaccessible for protease digestion), and CA.

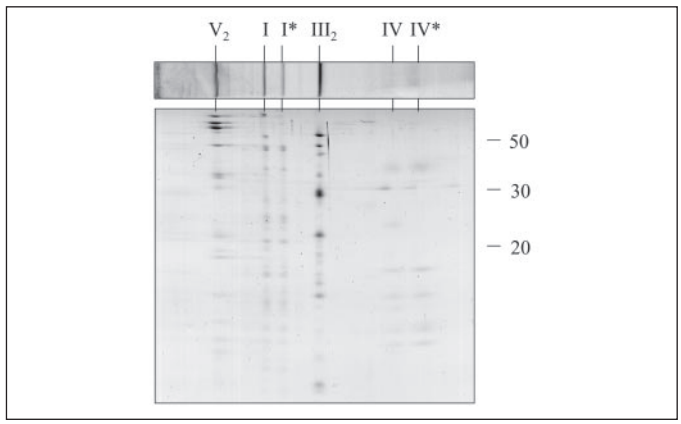

FIGURE 5. **Two-dimensional resolution of mitochondrial protein complexes from Polytomella.** Isolated mitochondria from Polytomella were solubilized with 5% digitonin as described under "Materials and Methods." Proteins were separated by one-dimensional blue-native PAGE (gel stripe on *top*) and subunits of the protein complexes by a second gel dimension in the presence of SDS. Molecular masses of standard proteins are given to the *right* of the gel and identities of protein complexes on *top*. V_2, dimeric ATP synthase; *I*, complex I; *I**, subcomplex of complex I lacking subunits of the NADH oxidizing domain; III_2, dimeric complex III; *IV*, complex IV; *IV**, subcomplex of complex IV.

form, which lacks the large subunits of the NADH oxidation domain (*complex I** in Fig. 5).

For EM analysis of complex I, mitochondrial protein complexes were solubilized using digitonin and separated by sucrose density ultracentrifugation. Complex I-containing fractions of the gradient were directly analyzed by EM in combination with single particle analysis (Fig. 6). A subset of 6,500 side view projections was analyzed. Four different projection views could be distinguished, which represent the larger and the smaller form of complex I from both sides, respectively (Fig. 6, *panels a*, *b*, *d*, and *e*). In these views the stronger stain-excluding membrane-bound arm with a length of 210 Å runs horizontal and the hydrophilic arm almost vertical. The smaller particle, which lacks part of the matrix arm (Fig. 6, *panels a* and *b*) is more abundant than the intact particle (Fig. 6, *panels d* and *e*). A fifth projection class represents a top view of the Polytomella complex I (Fig. 6*c*). From this perspective, the membrane arm is slightly bent, which previously was reported for the Arabidopsis supercomplex consisting of complex I and dimeric complex III (Fig. 6, *panel f* and Ref. 15). The best projection maps of Fig. 6, *panels b* and *c* have a resolution of about 17 Å.

All the side view projections of Polytomella complex I show the matrix-exposed extra-domain at the center of the membrane arm of the complex (Fig. 6, *panels a–f*, *white arrows*). The side views indicate that this spherical domain has a diameter of about 60 Å in both Polytomella (Fig. 6, *panels a* and *e*) and Arabidopsis (Fig. 6, *panels g* and *h*). In our hypothesis it contains a heterotrimer of different carbonic anhydrase subunits, as discussed below. To verify this hypothesis we did an additional single particle electron microscopy study on purified complex I

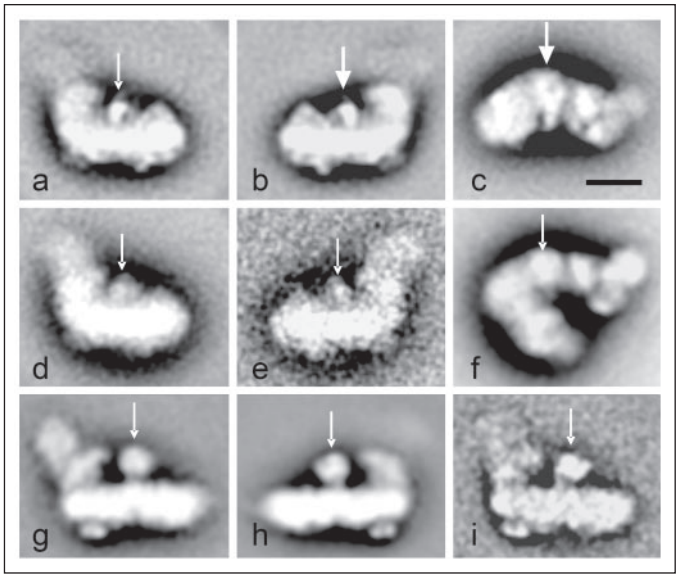

FIGURE 6. **Structure of complex I from Polytomella spp.** A data set of 11,000 single particle projections was analyzed by multireference alignment and multivariate statistical analysis. A total of 6581 projections could be assigned to side views of the larger and smaller form of complex I in two different positions, respectively (*panel a*, average of 1449 projections; *panel b*, average of 4608 projections; *panel d*, average of 512 projections; *panel e*, average of 16 projections). 1366 projections represent a *top* view (*panel c*). *Panel f*, averaged projection map of top view projections of I-III$_2$ supercomplex particles from Arabidopsis; *panels g* and *h*, average of side view projections of a complete complex I and complex I lacking a part of the NADH-oxidizing domain from Arabidopsis (taken from Dudkina *et al.* (15), Fig. 2, *panels d* and *e*); *panel i*, total sum of 318 projections of complex I in a side view position from an Arabidopsis mutant lacking the At1g47260 gene encoding CA2. The plant-specific carbonic anhydrase domain is indicated by an *arrow*. The *bar* equals 10 nm.

from an Arabidopsis knock-out mutant of gene At1g47260, encoding the CA2 subunit. The total sum of 318 projections represents a complex I particle, which is very similar or identical to the wild type (Fig. 6, *panel i*). Most likely, other structurally related CA subunits of complex I are compensating for the absence of CA2.

DISCUSSION

The subunit composition of complex I is well known for several organisms (33–35). In eukaryotes, 40–45 subunits form part of this complex, many of which have a conserved primary structure in fungi and animals. In contrast, complex I from plants includes quite a number of plant-specific subunits, most strikingly a group of 3–5 structurally related γ-carbonic anhydrases (10, 11). Using a monospecific antibody directed against CA2, this protein was shown to be an integral membrane protein, which is attached to the membrane arm of complex I on its matrix side. These results nicely fit to a special structural feature of plant complex I. In contrast to bacteria, fungi, and animals, Arabidopsis complex I has an extra spherical matrix-exposed domain attached to the central part of its membrane arm (15). This extra-domain now was confirmed for green algae, which also are known to include the plant-specific carbonic anhydrase subunits (11).

Topology of Carbonic Anhydrase Subunits of Arabidopsis Complex I—Based on carbonate extraction, CA2 is anchored to the inner mitochondrial membrane by hydrophobic interaction. Protease protection experiments reveal anchoring of the protein by a region close to one of its termini. Because the N-terminal two-thirds of the protein has clear homology to the hydrophilic carbonic anhydrase domain of the prototype γ-carbonic anhydrase from *M. thermophila*, anchoring of CA2 to the membrane most likely is mediated by its C terminus. Strikingly, compared with the *M. thermophila* enzyme, CA1, CA2, and CA3 have a C-terminal extension of 27–47 amino acids (supplementary Fig. S1).

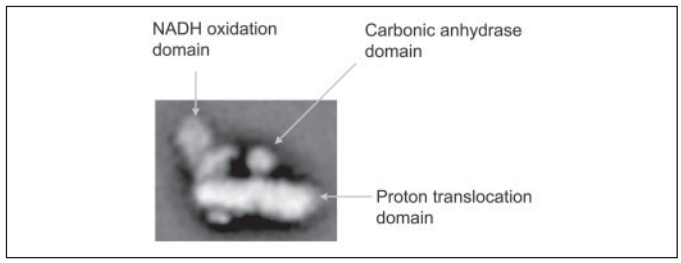

FIGURE 7. **Domain structure of plant complex I.**

The 2-kDa segment of CA2 accessible by proteolysis during protease protection experiments probably is represented by this C-terminal extension, which is exposed to the mitochondrial intermembrane space. In contrast, the main part of the 30-kDa CA2 protein is not degraded during protease protection experiments and seems to form a carbonic anhydrase domain of about 25 kDa on the matrix side of the inner membrane.

We speculate that the spherical extra-domain of Arabidopsis complex I represents the plant-specific carbonic anhydrase subunits of this complex. The extra-domain has a diameter of about 6 nm, corresponding to a molecular mass of ~75 kDa, which could include three carbonic anhydrase domains. X-ray crystallography of the γ-carbonic anhydrase of the Archeon *M. thermophila* has revealed a homotrimeric structure of this enzyme with dimensions of 65 × 65 × 70 Å (36), compatible to the diameter of the extra-domain found by EM. The γ-carbonic anhydrase subunits of Arabidopsis have a rather high homology to the γ-carbonic anhydrase of *M. thermophila* and even show immune cross-reactivity to antiserum raised against this γ-CA (12). It therefore is very likely that the complex I-integrated γ-carbonic anhydrase domain of Arabidopsis also forms a trimeric structure. However, information on the precise anchoring of the CA subunits to complex I in plants has to await further structural investigation.

Upon EM analysis, the spherical extra-domain is the only visible difference between complex I from plants and other eukaryotes on the matrix side of the membrane arm of complex I. It therefore is unlikely that the CA subunits are represented by a different region of the membrane arm on its matrix surface. However, EM analysis of complex I of an Arabidopsis knock-out mutant of the gene encoding CA2 yielded a complex I particle, which is (almost) identical to the wild type (Fig. 6, *panel i*). We interpret that the absence of one of the five complex I-included CA or CAL subunits can be compensated by the remaining proteins. Indeed, cells of the Arabidopsis knock-out mutant clearly have reduced levels of complex I, which nevertheless has a normal subunit composition (14). We speculate that the CA subunits form a heterotrimeric domain and that different CA or CAL subunits can replace each other. The biological reason for the occurrence of five structurally related CA or CAL subunits within Arabidopsis complex I remains to be established.

In summary we conclude that the Arabidopsis complex I is composed of three different subcomplexes: the main matrix-exposed domain constituting the NADH oxidation activity, the membrane arm involved in proton translocation across the inner mitochondrial membrane, and the spherical extra matrix domain most likely constituting a γ-type carbonic anhydrase domain (Fig. 7).

Physiological Role of Carbonic Anhydrases in Plant Mitochondria—Although the spherical domain is attached to complex I by a very thin stalk, this extra-domain is very tightly attached to the respiratory complex and not ripped off by biochemical extractions like carbonate treatment. Interestingly, complex I from Arabidopsis has a cavity directly opposite to the point of attachment of the spherical domain. Possibly

the γ-carbonic anhydrase domain of complex I is physiologically linked to a pore-like structure within complex I involved in proton translocation. In cyanobacteria, CO_2 hydration also takes place at the cytoplasmic face of a homologous NADH dehydrogenase complex and is thought to be linked to proton translocation activity of this complex (reviewed in Badger and Price, Ref. 37). This NADH-linked carbonic anhydrase constitutes an important part of a CO_2-concentrating mechanism in cyanobacteria, which is very important for photosynthesis. In contrast, plant mitochondria have to handle excess CO_2 that is liberated during the citric acid cycle and other catabolic reactions within these organelles and additionally during photorespiration. Indirect involvement of mitochondrial CAs in photorespiration is supported by the down-regulation of CA genes when plants are cultivated in the presence of elevated CO_2 concentration (14). It will be interesting to further explore the physiological role of the complex I-integrated mitochondrial γ-carbonic anhydrases in higher plants.

REFERENCES

1. Moroney, J. V., Bartlett, S. G., and Samuelsson, G. (2001) *Plant Cell Environ.* **24,** 141–153
2. Hewett-Emmett, D., and Tashian, R. E. (1996) *Mol. Phylogenet. Evol.* **5,** 50–77
3. The Arabidopsis Genome Initiative (2000) *Nature* **408,** 796–815
4. Leterme, S., and Boutry, M. (1993) *Plant Physiol.* **102,** 435–443
5. Herz, U., Schroder, W., Lidell, A., Leaver, C. J., Brennicke, A., and Grohmann, L. (1994) *J. Biol. Chem.* **269,** 2263–2269
6. Rasmusson, A. G., Mendel-Hartvig, J., Moller, I. M., and Wiskich, J. T. (1994) *Physiol. Plant* **90,** 607–615
7. Trost, P., Bonora, P., Scagliarini, S., and Pupillo, P. (1995) *Eur. J. Biochem.* **234,** 452–458
8. Jänsch, L., Kruft, V., Schmitz, U. K., and Braun, H. P. (1996) *Plant J.* **9,** 357–368
9. Rasmusson, A. G., Heiser, V. V., Zabaleta, E., Brennicke, A., and Grohmann, L. (1998) *Biochim. Biophys. Acta* **1364,** 101–111
10. Heazlewood, J. L., Howell, K. A., and Millar, A. H. (2003) *Biochim. Biophys. Acta (Bioenergetics)* **1604,** 159–169
11. Cardol, P., Vanrobaeys, F., Devreese, B., van Beeuman, J., Matagne, R. F., and Remacle, C. (2004) *Biochim. Biophys. Acta* **1658,** 212–224
12. Parisi, G., Perales, M., Fornasari, M. S., Maria, S., Colaneri, A., Gonzalez-Schain, N., Gomez-Casati, D., Zimmermann, S., Brennicke, A., Araya, A., Ferry, J.G., Echave, J., and Zabaleta, E. (2004) *Plant Mol. Biol.* **55,** 193–207
13. Perales, M., Parisi, G., Fornasari, M. S., Colaneri, A., Villarreal, F., Gonzalez-Schain, N., Gómez-Casati, D., Braun, H. P., Araya, A., Echave, J., and Zabaleta, E. (2004) *Plant Mol. Biol.* **56,** 947–957
14. Perales, M., Eubel, H. Heinemeyer, J., Colaneri, A., Zabaleta, E., and Braun, H.P. (2005) *J. Mol. Biol.* **350,** 263–277
15. Dudkina, N. V., Eubel, H., Keegstra, W., Boekema, E. J., and Braun, H. P. (2005a) *Proc. Natl. Acad. Sci. U. S. A.* **102,** 3225–3229
16. May, M. J., and Leaver, C. J. (1993) *Plant Physiol.* **103,** 621–627
17. Dudkina, N. V., Heinemeyer, J., Keegstra, W., Boekema, E. J., and Braun, H. P. (2005b) *FEBS Lett.* **579,** 5769–5772
18. Werhahn, W., Niemeyer, A., Jänsch, L., Kruft, V., Schmitz, U. K., and Braun, H. P. (2001) *Plant Physiol.* **125,** 943–954
19. Schägger, H., and von Jagow, G. (1987) *Anal. Biochem.* **166,** 368–379
20. Heinemeyer, J., Lewejohann, D., and Braun, H. P. (2005) in *Plant Proteomics* (Thiellement, H., ed) Humana Press, Totowa, in press
21. Sunderhaus, S., Eubel, H., and Braun, H. P. (2005) in *Mitochondrial Genomics and Proteomics Protocols* (Leister, D and Herrmann, J. H., eds), Humana Press, Totowa in press
22. Neuhoff, V., Stamm, R., and Eibl, H. (1985) *Electrophoresis* **6,** 427–448
23. Neuhoff, V., Stamm, R., Pardowitz, I., Arold, N., Ehrhardt, W., and Taube, D. (1990) *Electrophoresis* **11,** 101–117
24. Zerbetto, E., Vergani, L., and Dabbeni-Sala, F. (1997) *Electrophoresis* **18,** 2059–2064
25. Heinemeyer, J., Eubel, H., Wehmhöner, D., Jänsch, L., and Braun, H. P. (2004) *Phytochemistry* **65,** 1683–1692
26. van Heel, M. (1987) *Ultramicroscopy* **21,** 95–100
27. Eubel, H., Jänsch, L., and Braun, H.P. (2003) *Plant Physiol.* **133,** 274–286
28. Schägger, H., and Pfeiffer, K. (2000) *EMBO J.* **19,** 1777–1783
29. Pebay-Peyroula, E., Dahout-Gonzalez, C., Kahn, R., Trezeguet, V., Lauquin, G. J., and Brandolin, G. (2003) *Nature* **426,** 39–44
30. Van Lis, R., Atteia, A., Mendoza-Hernandez, G., and Gonzalez-Halphen, D. (2003) *Plant Physiol.* **132,** 318–330
31. Atteia, A., van Lis, R., Mendoza-Hernandez, G., Henze, K., Martin, W., Riveros-Rosas, H., and Gonzalez-Halphen, D. (2003) *Plant Mol. Biol.* **53,** 175–188
32. Van Lis, R., Mendoza-Hernandez, G., and Gonzalez-Halphen, D. (2005) *Biochim. Biophys. Acta* **1708,** 23–34
33. Carroll, J., Fearnley, I. M., Shannon, R. J., Hirst, J., and Walker, J. E. (2003) *Mol. Cell. Proteomics* **2,** 117–126
34. Abdrakhmanova, A., Zickermann, V., Bostina, M., Radermacher, M., Schägger, H., Kerscher, S., and Brandt, U. (2004) *Biochim. Biophys. Acta* **1658,** 148–156
35. Friedrich, T., and Böttcher, B. (2004) *Biochim. Biophys. Acta* **1608,** 1–9
36. Iverson, T. M., Alber, B. E., Kisker, C., Ferry, J. G., and Rees, D. C. (2000) *Biochemistry* **39,** 9222–9231
37. Badger, M. R., and Price, G. D. (2003) *J. Exp. Botany* **383,** 609–622

Chapter 3

Characterization of Dimeric ATP Synthase and Cristae Membrane Ultrastructure from *Saccharomyces* and *Polytomella* Mitochondria.

FEBS Letters 580 (2006) 3427–3432

Characterization of dimeric ATP synthase and cristae membrane ultrastructure from *Saccharomyces* and *Polytomella* mitochondria

Natalya V. Dudkina[a], Stephanie Sunderhaus[b], Hans-Peter Braun[b], Egbert J. Boekema[a,*]

[a] *Department of Biophysical Chemistry, GBB, University of Groningen, Nijenborgh 4, 9747 AG Groningen, The Netherlands*
[b] *Institute for Plant Genetics, Faculty of Natural Sciences, Universität Hannover, Herrenhäuser Str. 2, 30419 Hannover, Germany*

Received 8 March 2006; revised 20 April 2006; accepted 21 April 2006

Available online 12 May 2006

Edited by Richard Cogdell

Abstract **There is increasing evidence now that F_1F_0 ATP synthase is arranged in dimers in the inner mitochondrial membrane of several organisms. The dimers are also considered to be the building blocks of oligomers. It was recently found that the monomers in beef and the alga *Polytomella* ATP synthase dimer make an angle of ~40° and ~70°, respectively. This arrangement is considered to induce a strong local bending of the membrane. To further understand the packing of dimers into oligomers we performed an electron microscopy analysis of ATP synthase dimers purified from *Saccharomyces cerevisiae*. Two types of dimers were found in which the angle between the monomers is either ~90° or ~35°. According to our interpretation, the wide-angle dimers (70–90°) are "true-dimers" whereas the small-angle dimers (35–40°) rather are "pseudo-dimers", which represent breakdown products of two adjacent true dimers in the oligomer. Ultrathin sectioning of intact *Polytomella* mitochondria indicates that the inner mitochondrial or cristae membrane is folded into lamellae and tubuli. Oligomers of ATP synthase can arrange in a helical fashion in tubular-shaped cristae membranes. These results strongly support the hypothesized role of ATP synthase oligomers in structural determination of the mitochondrial inner membrane.**
© 2006 Federation of European Biochemical Societies. Published by Elsevier B.V. All rights reserved.

Keywords: ATP synthase; Dimer; Electron microscopy; Mitochondria; *Saccharomyces cerevisiae*; *Polytomella*

1. Introduction

The proton F_1F_0 ATP synthase is a ubiquitous enzyme that is found in virtually all living organisms. It is a multi-subunit complex of about 600 kDa involved in rotary catalysis. In prokaryotes the enzyme consists of an F_0 intrinsic membrane domain with three different subunits named a, b and c and an extramembranous F_1 domain (or headpiece), including a central stalk, with five different subunits α, β, γ, δ and ε. Three α and β subunits shape the F_1 headpiece; the γ, and ε are present in single copies in the central stalk. Most of the F_0 domain is formed by a multimer of 10 c subunits. The c-subunit multimer of the F_0 domain and the $\alpha_3\beta_3$ F_1 headpiece are linked by the central stalk and additionally by a peripheral stalk composed of two b subunits. The peripheral stalk is connected to the top of the $\alpha_3\beta_3$ F_1 headpiece via the δ subunit. During catalysis a proton membrane gradient drives the rotation of the ring of multiple copies of the c subunit [1]. This results in a clockwise rotation of the γ subunit of the F_1-ATPase and in the synthesis of ATP.

Mitochondrial F_1F_0 ATP synthases contain the same eight subunits, though some have a different name such as the OSCP subunit, which is the counterpart of the prokaryotic δ subunit. There are at least eight small subunits in addition to those of the prokaryotic enzyme [2]. In *Saccharomyces cerevisiae* there is one additional subunit located in the central stalk (the mitochondrial specific ε subunit). Most of the remaining ones are located in the F_0 domain (d, e, f, g, h, i and k) where they are positioned close to the peripheral stalk. Atomic resolution structures have revealed the folding of the α, β, γ, δ and ε subunits of the F_1 domain [3,4] and based on biochemical studies there is a recent lower resolution model for the arrangement of the four subunits consisting the peripheral stalk or stator in beef [5]. There is, however, no detailed structural information of the many (small) subunits of bovine or yeast ATP synthase, which form the F_0 domain outside the subunit c multimer.

Although the proton ATP synthase is catalytically active in its monomeric form a dimeric ATP synthase supercomplex from yeast mitochondria has been characterized by BN/SDS PAGE [6] and other techniques. This supercomplex includes the above-mentioned small subunits f, i, e, g, and k, the latter three of which are thought to be involved in dimer formation. Recent data show that yeast cells deficient in the dimer-specific subunits e or g lack dimeric ATP synthase [7,8]. Some data also point to an involvement of one of the subunits of the peripheral stalk, subunit b, in dimer formation [9]. Similar dimeric ATP synthase supercomplexes were found in a wide range of organisms such as beef [10], *Arabidopsis* [11], *Chlamydomonas* [12] and *Polytomella* [13,14].

Several biochemical studies indicate in addition to the dimeric conformation a further packing of ATP synthase into oligomers. The oligomerization of the ATP synthase has been proposed to determine mitochondrial morphogenesis [7,8,14]. Yeast mutants that lack the ATP synthase subunits e or g show a different type of folding of the inner mitochondrial or cristae membrane. This membrane is heavily folded, but mutants show an onion-like packing of cristae membranes. A GTPase named Mgm1p serves as a regulator of subunit e stability, ATP synthase assembly and cristae morphology [15]. The only

*Corresponding author. Fax: +33 503634800.
E-mail address: e.j.boekema@rug.nl (E.J. Boekema).

0014-5793/$32.00 © 2006 Federation of European Biochemical Societies. Published by Elsevier B.V. All rights reserved.
doi:10.1016/j.febslet.2006.04.097

direct evidence for ATP synthase oligomers was obtained in an electron microscopy study by using rapid-frozen deep-etched mitochondria from the unicellular freshwater organism *Paramecium* [16]. One of the best ways to study subcellular structures by electron microscopy is to embed them without chemical fixation in amorphous ice and to perform a three-dimensional reconstruction by electron tomography [17,18]. But for relatively large objects like mitochondria it remains particularly difficult to obtain a resolution sufficient to see the packing of individual copies of the major protein complexes like the ATP synthases, because the attainable resolution is directly related the size of the object [19]. In the best current available reconstructions the F_1 headpieces come into focus, but they do not show how the oxidative phosphorylation complexes are precisely organized [17].

Until now a low-resolution structural characterization of the ATP synthase dimer has been carried out in parallel for two different species: beef [20] and the colorless alga *Polytomella* [14]. In both cases it was found that the two F_1F_0 monomers are making an unexpected angle which was ~40° in the case of beef and ~70° for *Polytomella*. Because of this angle the membrane around the F_0 parts of the dimer is curved. It was concluded that this kink drives the mitochondrial cristae membrane to adopt a local curvature [14,20]. A major difference between the two dimers, however, is a difference of ~30° between the two angles. This discrepancy may be explained by the fact that the two species are not closely related and have a different subunit composition. But it may also be possible that the association of monomers in the dimers is different. To get further insight into the dimer configuration we performed single particle electron microscopy analysis on a third species, the yeast *S. cerevisiae*. Since *Polytomella* ATP synthase dimers were found to be unusually stable [14], additional ultrathin sectioning of these mitochondria was performed to investigate the overall membrane packing of the oxidative phosphorylation complexes. The analysis of the yeast dimers indicates that detergent solubilization of mitochondrial membranes leads actually to two distinct types of dimers, either with an angle of about 90° between the long axes of the F_1F_0 monomers or with an angle of 35°. Both types of dimers are considered to originate from an oligomeric organization of ATP synthases in rows. Ultrathin-sectioning and negative staining of osmotically shocked *Polytomella* mitochondria show that such oligomers are (partly) arranged in a helical fashion in tubular-shaped cristae membranes.

2. Materials and methods

2.1. Cultivation of *Polytomella spp. and* Saccharomyces cerevisiae

Polytomella spp. (198.80, E.G. Pringsheim) was obtained from the "Sammlung von Algenkulturen der Universität Göttingen" (Germany) and cultivated as described in Dudkina et al. [14]. *S. cerevisiae* (strain Y187) was cultivated in YPD medium. For mitochondrial isolations, cells were transferred into lactate medium (2.6 mM glucose, 7.3 mM KH_2PO_4, 18.7 mM NH_4Cl, 4.5 mM $CaCl_2$, 8.6 mM NaCl, 2.9 mM MgCl, 2.2% lactate).

2.2. Preparation of mitochondria

Mitochondria of *Polytomella* were isolated by differential centrifugation and Percoll density gradient ultracentrifugation as outlined previously [14]. Isolation of yeast mitochondria was based on differential centrifugations and sucrose gradient ultracentrifugation as described by Meissinger et al. [21]. Mitochondria were shock-frozen using liquid nitrogen and stored at −80 °C until use.

2.3. Purification of dimeric ATP synthase

The membrane-bound protein complexes of yeast and *Polytomella* were solubilized using digitonin solution (5% detergent, 30 mM HEPES, 150 mM K-acetate, 10% glycerine, pH 7.4) and separated by sucrose gradient ultracentrifugation (gradients of 0.3–1.5 M sucrose, 15 mM Tris base, pH 7.0, 20 mM KCl, 0.2% digitonin; centrifugation for 17 H at 150,000 × *g*/4 °C). Afterwards the gradients were fractionated and the protein complex compositions of the fractions analyzed by 1D Blue-native PAGE [22].

2.4. Electron microscopy

Selected fractions of the gradients including dimeric ATP synthase were directly used for electron microscopy and single particle analyses [23]. For ultrathin sectioning, *Polytomella* mitochondria were isolated according to [14], pelleted and double fixed with glutaraldehyde and osmium tetroxide. Fixed mitochondria were dehydrated with acetone and embedded in Epon. Ultrathin sections were made on an ultramicrotome and double stained with uranyl acetate and lead citrate.

For studying the localization of the oxidative phosphorylation system in the inner membrane before detergent disruption *Polytomella* mitochondria were osmotically shocked by diluting them 10× in distilled water on electron microscopy grids and directly stained with uranyl acetate.

3. Results

3.1. Purification of yeast ATP synthase dimers

Solubilization of isolated yeast mitochondria by digitonin and analysis of the solubilized protein complexes by 2D Blue native/SDS PAGE allowed to monitor the known complexes of the respiratory chain (Fig. 1). In accordance with previous publications [6], ATP synthase is present in two forms, a monomeric complex of about 500 kDa and a dimeric complex of about 1000 kDa. In-between, supercomplexes of dimeric complex III and one or two copies of monomeric complex IV are visible. Furthermore, two forms of dimeric complex III are present below the monomeric ATP synthase complex, which represent the intact dimer and a subcomplex of the dimer lacking the Rieske FeS subunit and another 8.5 kDa subunit. Both subunits are known to easily get detached from the dimeric complex III [24]. The ratio of monomeric and dimeric ATP synthase very much depends on the detergent used for solubilization [6]. The dimer is best stabilized in the presence of low Triton X-100 concentrations. However, digitonin and dodecylmaltoside also proved to be suitable detergents for ATP synthase supercomplex stabilization [10].

In contrast, ATP synthase of *Polytomella* is exclusively visible in the dimeric form on 2D Blue native/SDS gels independently of the type of non-ionic detergent used for solubilization (Fig. 1, [13,14,25]). The extraordinary stability of the dimer most likely is due to an additional large subunit called "mitochondrial ATP synthase associated protein" (MASAP), which runs at 60 kDa on the second gel dimension (Fig. 1).

For successive EM analysis of yeast ATP synthase, Blue-native PAGE was substituted by sucrose density gradient ultracentrifugation to obtain protein complexes in solution. The gradients were fractionated and small aliquots of the fractions were analyzed by Blue-native PAGE to monitor their protein complex composition. A fraction close to the bottom of the gradients (fraction 5) included pure ATP synthase dimers. The corresponding fractions were directly used for EM and single particle analysis.

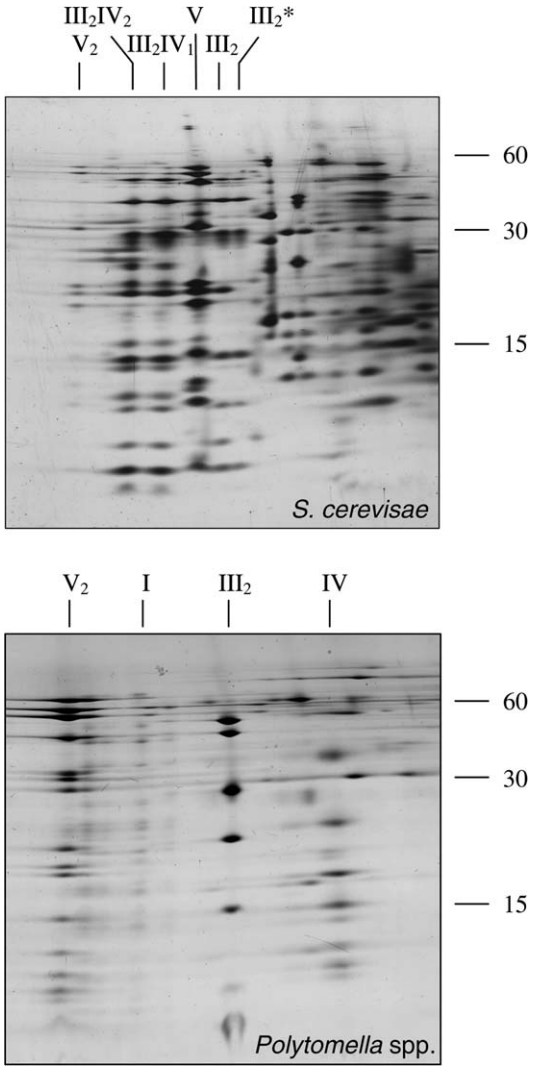

Fig. 1. Separation of OXPHOS complexes from *Saccharomyces cerevisiae* and *Polytomella* spp. by 2D Blue-native/SDS–PAGE. Mitochondrial proteins were solubilized with digitonin (5 g per g protein) as described under experimental procedures. Identities of the protein complexes are given above the gels and molecular masses of standard proteins to the right (in kDa). V_2: dimeric ATP synthase; I: complex I; III_2: dimeric complex III; III_2*: subcomplex of dimeric complex III lacking the FeS subunit; III_2IV_2: supercomplex composed of dimeric complex III and two copies of complex IV; III_2IV_1: supercomplex composed of dimeric complex III and one copy of monomeric complex IV; IV: complex IV.

3.2. Structural analysis of yeast ATP synthase dimers by electron microscopy

Negatively stained specimens of the fractions were found to contain large numbers of dimeric ATP synthase molecules (Fig. 2). The only obvious contamination was the supercomplexes of complex III and IV, but because the latter looks quite different and because the shape of the ATP synthase dimers is very characteristic, it was possible to select a rather homogeneous data set of 20,000 single particle projections. Single particle analysis showed the presence of seven different views, representing two types of ATP synthase dimers and their apparent breakdown fragments. The main difference between the two types of dimers is in the angle between the monomers, which is either about 90° (Fig. 3(A)) or 35° (Fig. 3(E)). A smaller difference is in the total width of the F_0 domains in projection, which is larger in the wide-angle dimers. Both angles are found to remain in particles missing one headpiece (Fig. 3(B), (C), (F) and (G)) and even both headpieces (Fig. 3(D)). The ratio between the two types of dimers, including their fragments, is about 1:1.

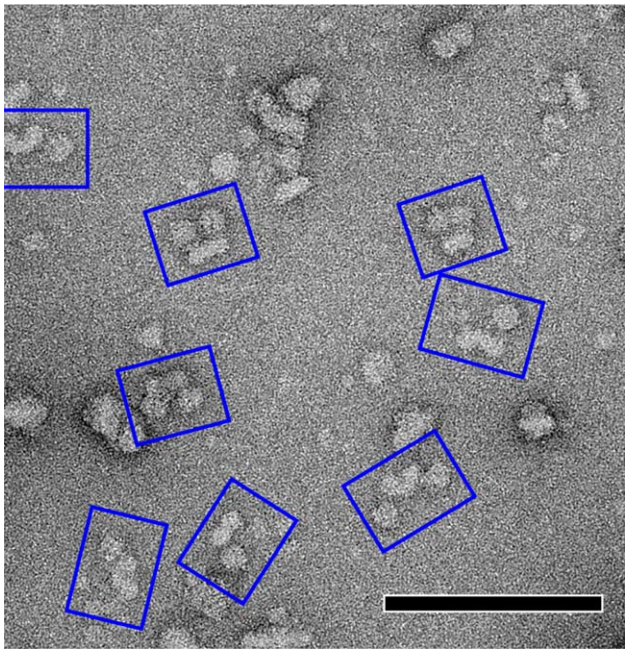

Fig. 2. Electron micrograph of membrane proteins from the fraction 5 obtained by sucrose gradient centrifugation. Blue boxes indicate ATP synthase dimers, unassigned proteins could be partly the supercomplex of complexes III and IV (see text). The space bar is 100 nm. (For interpretation of the references to color in this figure legend, the reader is referred to the web version of this article.)

The peripheral stalk of the yeast dimer appears faint (white arrows; left headpieces in Fig. 3(A) and (B)) or is absent (all other headpieces). This is a striking difference with the previously analyzed *Polytomella* dimer (Fig. 3(H)). Another difference is at the top of the F_1 headpiece because the yeast F_1 headpiece is clearly seen to be blunt in all views. In the best-resolved headpiece of the particle of Fig. 3(C) there is a stain accumulation at the site of the tip (white arrowhead) at where the OSCP subunit should be present. The absence of (most of) the OSCP subunit explains the absence of the stator because the stator needs OSCP for binding to the headpiece. Despite the large number of particles analyzed the resolution was low in comparison to *Polytomella* and the best resolution of about 30 Å was obtained for one of the fragments (Fig. 3(C)). This low resolution is likely due to flexibilities in the dimer such as small angular deviations between two monomers or a movement between the F_0 and F_1 domains because of the absence of the stator in most monomers. A further difference with *Polytomella* is in the membrane part; in yeast dimers the width is somewhat larger (Fig. 3(A)) or smaller (Fig. 3(B)) than in of those of *Polytomella* (Fig. 3(H)).

3.3. Cristae morphology

Electron microscopy analysis of thin-sectioned *Polytomella* mitochondria shows it is a spherical organelle of approximately 3 μm in diameter (Fig. 4(A)). Two types of cristae membranes could be observed in these mitochondria. There are lamellae

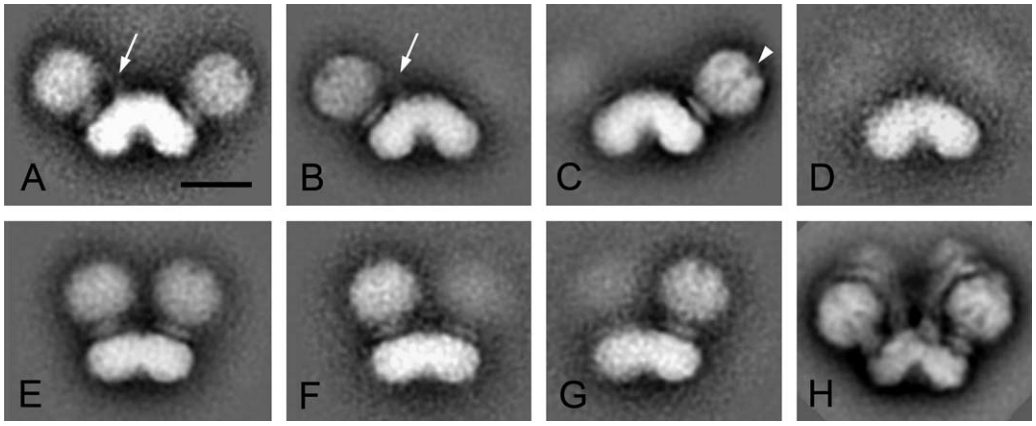

Fig. 3. Projection maps of purified dimeric ATP synthase complexes from *S. cerevisiae* (A–G) obtained by single particle averaging. A, E – complete dimers; B, C, F, G – dimeric ATP synthase fragments lacking one F_1 headpiece; D – fragment of supercomplex lacking two F_1 headpieces; H – complete ATP synthase dimer from *Polytomella* (from Dudkina et al. 2005). White arrows indicate the stator at the right side of the left headpiece; white arrowhead indicates the absence of the OSCP subunit. The bar is 10 nm.

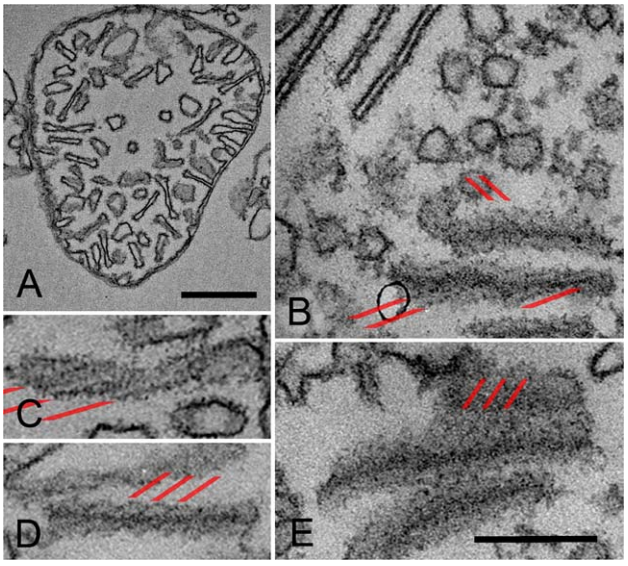

Fig. 4. Electron microscopy of ultrathin-sectioned *Polytomella* mitochondria. (A) Overview of a mitochondrion. The bar is 1 μm. (B–E) Selected higher-magnification parts of thin-sections showing lamellae (B) and mostly tubular cristae membranes with some periodicity in the arrangement of protein complexes (B–E). The red bars indicate the angle between the periodic ordering and the long axis of the tubules. The bar for frames B–E is 500 nm. (For interpretation of the references to color in this figure legend, the reader is referred to the web version of this article.)

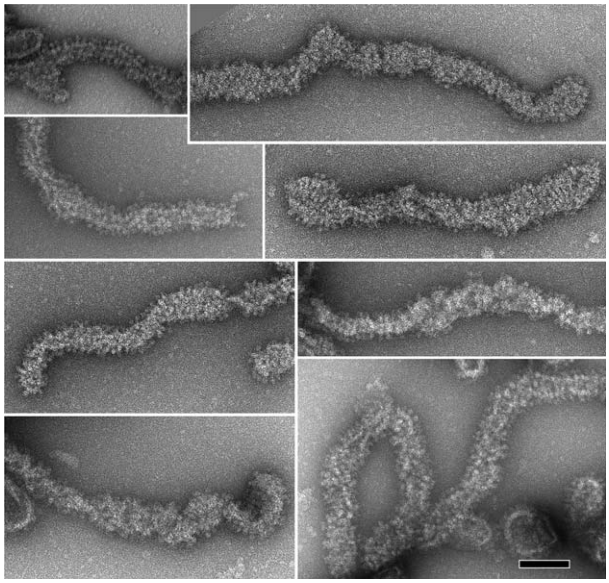

Fig. 5. Negatively stained mitochondrial tubular cristae fragments of *Polytomella*. The largest protruding densities are ATP synthase headpieces, which are especially dominant in the upper left electron micrograph. The space bar for all frames is 100 nm.

with a spacing of about 25 nm between the membranes (upper left corner, Fig. 4(B)) and tubes with a diameter of 60 nm or more. In several of the tubes that run parallel to the sectioning direction a kind periodicity in the arrangement of protein complexes is visible (red bars, Fig. 4(B–E)). Although individual complexes are not well visible it appears that this ordering of protein complexes makes an angle with the long axis of the tubules, as indicated by the red bars. Because the resolution in the sections was low we also applied negative staining with uranyl acetate on osmotically shocked mitochondria. Similar rods with a diameter of 60–90 nm are present in osmotically shocked mitochondria (Fig. 5). In some of the tubules the ATP synthase headpieces are well resolved (upper left frame, Fig. 5), but no visible ordering of proteins seems to be preserved. The fact that the observed ordering makes an angle with the long axis of the tubules from the thin sections is typical for a helical ordering of protein complexes. Since the complexes were metal stained, the stronger stained dark zones should represent ATP synthase complexes, because the ATP synthase headpieces protrude at least two times farther away from the membrane as any of the complexes I–IV. Hence, the tubules seen in the sectioned *Polytomella* mitochondria are interpreted as composed of helically arranged rows of ATP synthase complexes separated by zones occupied by the respiratory complexes I–IV.

4. Discussion

In this report, we present an analysis of ATP synthase dimers isolated from *S. cerevisiae* mitochondria by electron

microscopy and single particle image analysis in combination with the ultrathin sectioning and negative staining of the whole mitochondria from the alga *Polytomella*. The aim of this analysis is the detection of the way in which ATP synthase dimers/oligomers are organized in the mitochondrial inner membrane. We analyzed the projection structure of the yeast ATP synthase dimer in which complete dimers and fragments missing one or both of the F_1 parts clearly indicate that the interaction between the monomers occurs by their F_0 parts. The monomers make an angle between of either about 90° or 35°, but other angles were not observed (Fig. 3). In *Polytomella* there appears to be only one type of ATP synthase dimer (Fig. 3(H), [14]), in which the angle is about 70°. This causes the membrane-embedded F_0 parts to have a different orientation, but otherwise they look quite similar. In the case of the bovine ATP synthase there are only dimers with a small (40°) angle between the monomers [20], quite similar to the 35° angle observed in yeast particles (Fig. 3(E–G)). Both small angle dimers show the absence of stators in projection, which could mean that they are not visible because of an overlap-situation with the headpieces. But because the large angle yeast particles appear to lack most of the stators, it could well be that the same is true for the small angle dimers. The loss of stators might be caused by the low abundance of the OSCP subunit. It is possible that this subunit is partly lost during EM specimen preparation due to the high (5%) digitonin concentration or more likely a lower stability of the yeast ATP synthase dimers. However, the absence or presence of the stator and the OSCP subunit do not appear to have a major effect on the overall shape of the dimers, because even in the absence of one or two complete F_1 headpieces the angle between the F_0 parts is maintained.

The question now arises what makes the ATP synthase dimer to appear seemingly in two conformations. Until now several studies, as well as our results (see below), point to oligomerization of ATP synthases and thus dimeric supercomplexes are thought to be the building blocks of ATP synthase oligomers. According to our scheme (Fig. 6), we propose that two types of dimers appear as breakdown products of oligomers after detergent solubilization of cristae membranes. This could lead to "true-dimers" with an observed angle of 70° or 90° and to "pseudo-dimers" with angle of 35° or 40° consisting of two neighbour monomers from two broken native dimers, as depicted in the scheme. The fact that the two types of dimers appear rather than a change in the angular position of the monomers is clear from the width of the F_0 parts. The F_0 part from the true-dimers (Fig. 3(A)) is about 40% wider than in the pseudo-dimers (Fig. 3(E)). The fact that the pseudo-dimers were not observed in *Polytomella* could have to do with the fact that the intra-dimeric interaction in the ATP synthase oligomers is much stronger than the inter-dimeric interaction. It would also be worthwhile to re-examine the beef dimers to see if any type of wide-angle dimers is present at low frequency. Finally, a lower intra-dimeric interaction could correlate with the low abundance of intact stators in yeast (Fig. 3) and bovine dimers [14,20] and the high abundance in *Polytomella* [14], where the stator is very pronounced by the presence of MASAP protein in its upper part. Biochemical data also indicate that dimer specific subunits of yeast are attached to the stator close to the F_0 part [2].

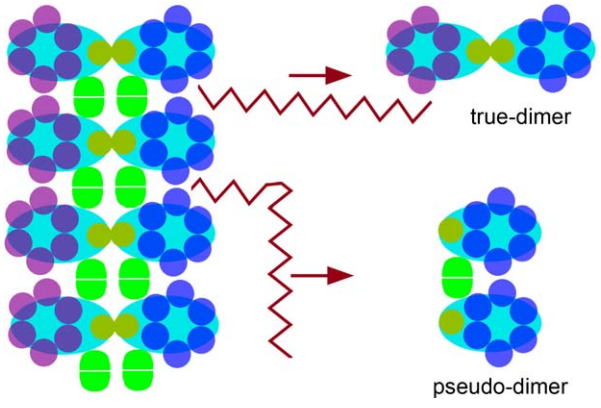

Fig. 6. A model for the arrangement of ATP synthases dimers into multimers. Oligomers consist of dimeric ATP synthases. The oligomers can break down by detergent incubation into "true-dimers" or into "pseudo-dimers". The latter actually consist of two monomers from the neighbouring dimers, symbolized by a blue and purple set of $\alpha_3\beta_3$ subunits. Ochre and bright green densities symbolize dimer- and interdimer specific subunits, respectively.

Supporting evidence for the scheme of Fig. 6 is presented in a BN-PAGE analysis of mammalian mitochondria which resulted in several types of ATP synthase multimers [26]. About 30–35% of total ATP synthase was obtained as three low-mobility species with apparent molecular masses of ~1500, ~2300, and ~2900 kDa, and the remainder as monomeric ATP synthase (~750 kDa). These low-mobility species represented dimeric ATP synthase, as well as trimeric and tetrameric ATP synthase [26]. The trimeric ATP synthase fragments can now be explained as an expected breakdown product if the strength of inter- and intra-dimeric interactions are about equal. The position of the small mitochondrial ATP synthase subunits b, e, f, g, i and k around the dimer interface is not precisely known. It is not yet possible to propose their role in intra- and interspecific dimer contacts. But recently it was proposed that subunits e and g are important in interspecific interaction [7,8]. This is a further support for the interpretation of the two different types of dimers as being different breakdown products of oligomers.

Because the best current available reconstructions [17] do not show how the oxidative phosphorylation complexes are precisely organized we used classical ultrathin sectioning to get hints about the packing of proteins in the mitochondria membrane. Sectioning of *Polytomella* mitochondria indicates a helical packing of cristae membrane proteins in tubules (Fig. 4). Because these tubular membranes are full of oxidative phosphorylation complexes as shown by additional negative staining of osmotically shocked mitochondria from *Polytomella* (Fig. 5) these data clearly hint to an oligomeric organization of ATP synthases in a helical fashion. The observation of rows of ATP synthases arranged in a helical way was previously demonstrated at higher resolution for mitochondria from the unicellular freshwater organism *Paramecium* by rapid-freeze deep-etch electron microscopy [16,27]. The latter studies indicated that ATP synthase dimerization and the cristae morphology are linked to each other. Yeast mutants devoid of dimer-specific subunits were shown unable to form dimeric ATP synthase and comprise mitochondria with drastically changed morphology [7,8]. Instead of the characteristic highly folded inner membrane architecture, the cristae, the membranes consist of atypical "onion-like" structures. Similar

mitochondrial morphology was observed in yeast cells containing in vivo cross-linked F_1-headpieces [28]. The presence of a surprisingly large angle of 90° between two membrane parts of neighbouring monomers in yeasts nicely confirms the hypothesis that ATP synthase supercomplexes are essential for the inner membrane folding.

Acknowledgements: We thank Mr. Ruby Kalicharan for expert technical assistance. H.P.B. acknowledges a grant of the Deutsche Forschungsgemeinschaft (Br1829-7/1) and E.J.B. grants of the Dutch science foundation NWO-CW.

References

[1] Stock, D., Leslie, A.G.W. and Walker, J.E. (1999) Molecular architecture of the rotary motor in ATP synthase. Science 286, 1700–1705.
[2] Devenish, R.J., Prescott, M., Roucou, X. and Nagley, P. (2000) Insights into ATP synthase assembly and function through the molecular genetic manipulation of subunits of the yeast mitochondrial enzyme complex. Biochim. Biophys. Acta 1458, 428–442.
[3] Abrahams, J.P., Leslie, A.G., Lutter, R. and Walker, J. (1994) Structure at 2.8 Å resolution of F_1-ATPase from bovine heart mitochondria. Nature 370, 621–628.
[4] Stock, D., Gibbons, C., Arechaga, I., Leslie, A.G.W. and Walker, J.E. (2000) Rotary mechanism of ATP synthase. Curr. Opin. Struct. Biol. 10, 672–679.
[5] Walker, J.E. and Dickson, V.K. The peripheral stalk of the mitochondrial ATP synthase. Biochim. Biophys. Acta (in press).
[6] Arnold, I., Pfeiffer, K., Neupert, W., Stuart, R.A. and Schägger, H. (1998) Yeast mitochondrial F_1F_0-ATP synthase exists as a dimer: identification of three dimer-specific subunits. EMBO J. 17, 7170–7178.
[7] Paumard, P., Vaillier, J., Coulary, B., Schaeffer, J., Soubannier, V., Mueller, D.M., Brethes, D., di Rago, J.P. and Velours, J. (2002) The ATP synthase is involved in generating mitochondrial cristae morphology. EMBO J. 21, 221–230.
[8] Giraud, M.F., Paumard, P., Soubannier, V., Vaillier, J., Arselin, G., Salin, B., Schaeffer, J., Brèthes, D., di Rago, P. and Velours, J. (2002) Is there a relationship between the supramolecular organization of the mitochondrial ATP synthase and the formation of cristae? Biochim. Biophys. Acta 1555, 174–180.
[9] Gavin, P.D., Prescott, M. and Devenish, R.J. (2005) Yeast F_1F_0-ATP synthase complex interactions in vivo can occur in the absence of the dimer specific subunit e. J. Bioenerg. Biomembr. 37, 55–66.
[10] Schägger, H. and Pfeiffer, K. (2000) Supercomplexes in the respiratory chains of yeast and mammalian mitochondria. EMBO J. 19, 1777–1783.
[11] Eubel, H., Jänsch, L. and Braun, H.P. (2003) New insights into the respiratory chain of plant mitochondria: supercomplexes and a unique composition of complex II. Plant Physiol. 133, 274–286.
[12] Van Lis, R., Atteia, A., Mendoza-Hernandez, G. and Gonzalez-Halphen, D. (2003) Identification of novel mitochondrial protein components of *Chlamydomonas reinhardtii*. A proteomic approach. Plant Physiol. 132, 318–330.
[13] Atteia, A., van Lis, R., Mendoza-Hernandez, G., Henze, K., Martin, W., Riveros-Rosas, H. and Gonzalez-Halphen, D. (2003) Bifunctional aldehyde/alcohol dehydrogenase (ADHE) in chlorophyte algal mitochondria. Plant Mol. Biol. 53, 175–188.
[14] Dudkina, N.V., Heinemeyer, J., Keegstra, W., Boekema, E.J. and Braun, H.P. (2005) Structure of dimeric ATP synthase from mitochondria: an angular association of monomers induces the strong curvature of the inner membrane. FEBS Lett. 579, 5769–5772.
[15] Amutha, B., Gordon, D.M., Gu, Y. and Pain, D. (2004) A novel role of Mgm1p, a dynamin-related GTPase, in ATP synthase assembly and cristae formation/maintenance. Biochem. J. 381, 19–23.
[16] Allen, R.D., Schroeder, C.C. and Fok, A.K. (1989) An investigation of mitochondrial inner membranes by rapid-freeze deep-etch techniques. J. Cell Biol. 108, 2233–2240.
[17] Nicastro, D., Frangakis, A.S., Typke, D. and Baumeister, W. (2000) Cryo-electron tomography of *Neurospora* mitochondria. J. Struct. Biol. 149, 48–56.
[18] Beck, M., Förster, F., Ecke, M., Plitzko, J.M., Melchior, F., Gerisch, G., Baumeister, W. and Medalia, O. (2004) Nuclear pore complex structure and dynamics revealed by cryoelectron tomography. Science 306, 1387–1390.
[19] Klug, A. and Crowther, R.A. (1972) Three-dimensional image reconstruction from the viewpoint of information theory. Nature 238, 435–440.
[20] Minauro-Sanmiguel, F., Wilkens, S. and Garcia, J.J. (2005) Structure of dimeric mitochondrial ATP synthase: novel F_0 bridging features and the structural basis of mitochondrial cristae biogenesis. Proc. Natl. Acad. Sci. 102, 12356–12358.
[21] Meisinger, C., Pfanner, N. and Truscott, K.N. (2006) Isolation of yeast mitochondria. Methods Mol. Biol. 313, 33–39.
[22] Schägger, H. and von Jagow, G. (1991) Blue native electrophoresis for isolation of membrane–protein complexes in enzymatically active form. Anal. Biochem. 199, 223–231.
[23] Dudkina, N.V., Eubel, H., Keegstra, W., Boekema, E.J. and Braun, H.P. (2005) Structure of a mitochondrial supercomplex formed by respiratory chain complexes I and III. Proc. Natl. Acad. Sci. USA 102, 3225–3229.
[24] Geier, B., Schägger, H., Brandt, U., Colson, A.M. and von Jagow, G. (1992) Point mutation in cytochrome *b* of the yeast ubihydroquinone:cytochrome-*c* oxidoreductase causing myxothiazol resistance and facilitated dissociation of the iron–sulfur subunit. Eur. J. Biochem. 208, 375–380.
[25] Van Lis, R., Mendoza-Hernandez, G. and Gonzalez-Halphen, D. (2005) Divergence of the mitochondrial electron transport chains from the green alga *Chlamydomonas reinhardtii* and its colorless close relative *Polytomella* sp.. Biochim. Biophys. Acta 1708, 23–34.
[26] Krause, F., Reifschneider, N.F., Goto, S. and Dencher, N.A. (2005) Active oligomeric ATP synthases in mammalian mitochondria. Biochem. Biophys. Res. Commun. 329, 583–590.
[27] Allen, R.D. (1995) Membrane tubulation and proton pumps. Protoplasma 189, 1–8.
[28] Gavin, P.D., Prescott, M., Luff, S.E. and Devenish, R.J. (2004) Cross-linking ATP synthase complexes in vivo eliminates mitochondrial cristae. J. Cell Sci. 117, 2233–2243.

Chapter 4

Two-dimensional Blue Native/Blue Native Polyacrylamide Gel Electrophoresis for the Characterization of Mitochondrial Protein Complexes and Supercomplexes.

Methods in Molecular Biology: Mitochondrial Genomics and Proteomics Protocols
(Humana Press)

Two dimensional blue native / blue native polyacrylamide gel electrophoresis for the characterization of mitochondrial protein complexes and supercomplexes

Stephanie Sunderhaus, Holger Eubel and Hans-Peter Braun

Prof. Dr. Hans-Peter Braun
Abteilung Angewandte Genetik
Naturwissenschaftliche Fakultät
Universität Hannover
Herrenhäuser Str. 2
30419 Hannover, Germany

Tel: +49 5117622674
Fax: +49 5117623608
braun@genetik.uni-hannover.de

Running head: 2D blue native / blue native PAGE

Key words: Blue-native polyacrylamide gel electrophoresis (BN-PAGE), digitonin, in gel enzyme assay, membrane proteins, mitochondria, protein complexes, protein supercomplexes, respiratory chain

Abstract

Blue-native polyacrylamide gel electrophoresis (BN PAGE) employs the blue wool dye Coomassie for labeling of proteins and protein complexes under native conditions. Electrophoresis under native conditions subsequently allows resolving proteins and protein complexes according to their molecular mass. BN-PAGE can be combined with second gel dimensions for extended analyses. Best known is the 2D BN / SDS PAGE system, which allows resolution of subunits of protein complexes. Recently, a 2D BN / BN PAGE system was suggested, which proved to be useful for investigating the substructure of protein complexes and protein supercomplexes. Basis of this 2D system is a variation in the conditions used for the two BN gel dimensions. Here we present a basic protocol for the analysis of mitochondrial fractions by 2D BN / BN PAGE. The 2D BN / BN system is compatible with in gel enzyme activity stainings, because both gel dimensions are carried out under native conditions.

Introduction

Blue-native polyacrylamide gel electrophoresis (BN-PAGE) is based on incubation of proteins with Coomassie-blue. Coomassie belongs to the trimethylmethane dye family and was used as a wool dye since the late 19th century. Due to its efficient and specific binding to proteins it was introduced in biochemistry to visualize proteins on gels after electrophoresis and later to photometrically determine protein concentrations [1,2]. Coomassie is a negatively-charged compound which carefully introduces charges into proteins and protein complexes. Because of this property it was suggested to be used for protein labeling prior to electrophoretic separations [3]. Coomassie does not denature proteins. In combination with non-ionic detergents, BN-PAGE proved to be an ideal tool for the analysis of membrane bound protein complexes, especially for those of mitochondria [3]. Even supramolecular assemblies of membrane bound mitochondrial protein complexes were shown to be stable during BN-PAGE, if the membrane solubilization step is carried out under very mild conditions [4]. Classically, a first Blue-native gel dimension is combined with SDS-PAGE as a second gel dimension, which allows to separate subunits of protein complexes. On the resulting gels, subunits of protein complexes form vertical rows. Detailed protocols for 2D BN / SDS PAGE were published recently [5-7].

Five years ago, a novel two-dimensional gel electrophoresis system was suggested which is based on BN-PAGE for both gel dimensions [4]. If the two gel dimensions are carried out under identical conditions, protein complexes form a diagonal line on the resulting 2D gels. However, if conditions of the second dimension BN-PAGE are slightly less gentle than conditions of the first dimension BN-PAGE, protein complexes are dissected into subcomplexes, which are visible underneath this diagonal line. 2D BN / BN PAGE proved to be a very powerful tool for the investigation of the protein complex composition of supercomplexes or the subcomplex composition of protein complexes. It successfully was used to characterize the supramolecular structure of the protein complexes of the oxidative phosphorylation (OXPHOS) system in mitochondria [4, 6, 8-14] and of the photosynthetic electron transport system in chloroplasts [15]. Conditions to be varied between the two BN gel dimensions can refer to detergent type (e.g. digitonin / dodecylmaltoside), detergent concentration (e.g. 0.5 / 2.0 % dodecylmaltoside), temperature (e.g. 4° / 20°C) or presence of chaotropic compounds (absence / presence of urea). 2D BN / BN PAGE is compatible with in gel enzyme stainings, allowing to determine the activity of supramolecular assemblies of protein complexes as well

as the activities of subcomplexes of protein complexes (Fig. 1). In this chapter, we present a basic protocol for the analysis of mitochondrial protein complexes by BN / BN PAGE, which is based on detergent variation between the two BN gel dimensions. The presented protocol also is suitable for the analysis of other organell fractions or bacteria.

2. Materials

2.1. Preparation of BN gels for first and second gel dimensions

1. Acrylamide solution: 49.5 %, acryl / bisacryl = 32 / 1 (AppliChem, Darmstadt, Germany)
2. Gel buffer BN (6x): 1.5 M amino caproic acid, 150 mM BisTris, pH 7.0 (adjust at 4°C)

2.2. Sample preparation

1. Digitonin solubilization solution: 5.0 % digitonin (e.g. Fluka, Buchs, Switzerland), 30 mM HEPES, 150 mM potassium acetate, 10 % (v/v) glycerol, pH 7.4 (adjust at 4°C). This buffer should be freshly prepared and shortly heated to 98°C to dissolve the detergent. Add PMSF directly before use (final concentration: 2 mM; stock solution: 200 mM PMSF [w/v] in EtOH)
2. Coomassie-blue solution: 5 % Coomassie G 250 (e.g. Merck, Darmstadt, Germany), 750 mM amino caproic acid

2.3. First dimension BN-PAGE

1. Cathode buffer BN (5x): 250 mM Tricine, 75 mM BisTris, 0.1 % (w/v) Coomassie G 250 (e.g. Merck, Darmstadt, Germany), pH 7.0 (adust at 4°C)
2. Anode buffer BN (6x): 300 mM BisTris, pH 7.0 (adjust at 4°C)

2.4. Transfer of gel stripes of first gel dimensions onto second gel dimensions

1. 1x Cathode buffer BN + dodecylmaltoside: 50 mM Tricine, 15 mM BisTris, 0.03% dodecylmaltoside, 0.02 (w/v) Coomassie G 250 (e.g. Merck, Darmstadt, Germany), pH 7.0 (adjust at 4°C)

2.5. Second dimension BN-PAGE

1. Agarose solution: 1.5 % (w/v) Agarose
2. Cathode buffer BN + dodecylmaltoside: (see 2.4.)
3. Anode buffer BN (6x): (see 2.3.)

2.6. Enzyme activity staining procedures of 2D BN / BN gels

1. Phosphate buffer stock solution: 1M phosphate, pH 7.4
2. DAB stock solution: 0.1 M 3,3'-diamino benzidine tetrahydrochloride dihydrate
3. KCN stock solution: 1 M KCN
4. EDTA stock solution: 0.1 M EDTA
5. Tris stock solution: 2 M Tris-HCl, pH 7.4
6. Cytochrome c oxidase staining solution: 10 mM Phosphate buffer, pH 7.4, 0.1 % (w/v) DAB, 7.5 % (w/v) sucrose, 19 U/ml catalase and 16 mM cytochrome c (Sigma-Aldrich, St. Louis, MO, USA)
7. Succinate dehydrogenase staining solution: 50 mM Phosphate buffer, pH 7.4, 84 mM succinic acid, 0.2 mM N-Methylphenazonium methyl sulfate (Fluka, Buchs, Switzerland), 0.2 % Nitro tetrazolium blue (Fluka, Buchs, Switzerland), 4.5 mM EDTA, 10 mM KCN
8. NADH dehydrogenase staining solution: 0.1 M Tris-HCl, pH 7.4, 0.14 mM NADH, 0.1 % Nitro tetrazolium blue (Fluka, Buchs, Switzerland)
9. Fixing solution: 40 % (v/v) methanol, 10 % (w/v) acetic acid

3. Methods

Digitonin currently is considered to be the mildest detergent for mitochondrial research, which better stabilizes most supramolecular structures than Triton X100, dodecylmaltoside or other non-ionic detergents. In the protocol given below, first dimension BN-PAGE is therefore carried out after membrane solubilization using digitonin and second dimension BN-PAGE after incubation of the gel stripe of the first gel dimension with dodecylmaltoside. However, numerous variations of this experimental design are possible (*see* Note 1)

3.1. Preparation of BN gels for first and second gel dimensions

Best resolution capacity of BN gels is achieved if the electrophoretic separation distance is > 12 cm. The following instructions refer to the Protean II electrophoresis unit (BioRad, Richmond, Ca, USA; dimensions 0.1 x 16 x 20 cm for the gel of the first dimension, 0.15 x 16 x 20 cm for the gel of the second dimension). However, units from other manufacturers are of comparable suitability for BN-PAGE, e.g. the Hoefer SE-400 or SE-600 gel systems (Amersham Biosciences, Uppsala, Sweden). Usage of gradient gels is recommended, because molecular masses of protein complexes can vary between 50 kDa and several thousand kDa. *(see* Note 2)

First dimension gel (thickness of the gel: 1.0 mm)

1. Prepare a 4.5 % separation gel solution by mixing 1.2 ml Acrylamide solution with 2.2 ml Gel buffer BN and 10.0 ml ddH_2O
2. Prepare a 16 % separation gel solution by mixing 4.5 ml Acrylamide solution with 2.2 ml Gel buffer BN, 4.0 ml ddH_2O and 2.7 ml glycerol
3. Transfer the two gel solutions into the two chambers of a gradient former and connect the gradient former via a hose and a needle with the space in-between two glass plates, which are pre-assembled in a gel casting stand. Gradient gels can either be pored from the top (16 % gel solution has to enter the gel sandwich first) or from the bottom (4.5 % gel solution has to enter first). Poring gradient gels at 4°C is recommended to avoid premature polymerization.
4. Add APS and TEMED to the two gel solutions (60 µl 10 % APS / 6 µl TEMED to the 4.5 % gel solution, 40 µl APS / 4 µl TEMED to the 16 % gel solution)
5. Pour the gradient gel, leaving space for the stacking gel, and overlay with ddH_2O. The gel should polymerize in about 60 minutes
6. Pour off the ddH_2O
7. Prepare the stacking gel solution by mixing 1.2 ml Acrylamide solution, 2.5 ml Gel buffer BN and 11.3 ml ddH_2O
8. Add 65 µl APS and 6.5 µl TEMED and pour the stacking gel around an inserted the comb. The stacking gel should polymerize within 30 minutes.

Second dimension gel (thickness of the gel: 1.5 mm)

1. Prepare a 5.0 % separation gel solution by mixing 2.0 ml Acrylamide solution with 3.3 ml Gel buffer BN and 14.7 ml ddH_2O
2. Prepare a 20 % separation gel solution by mixing 8.0 ml Acrylamide solution with 3.3 ml Gel buffer BN, 4.7 ml ddH_2O and 4.0 ml glycerol
3. Transfer the two gel solutions into the two chambers of a gradient former as described for the first dimension gel
4. Add APS and TEMED to the two gel solutions (90 µl 10 % APS / 9 µl TEMED to the 5 % gel solution, 50 µl APS / 5 µl TEMED to the 20 % gel solution)
5. Pour the gradient gel, leaving space for the stacking gel, and overlay with ddH_2O. The gel should polymerize in about 60 minutes
6. Pour off the ddH_2O
7. Prepare the stacking gel solution by mixing 1.2 ml Acrylamide solution, 2.5 ml Gel buffer BN, 1.7 ml glycerol and 9.6 ml ddH_2O
8. Add 65 µl APS and 6.5 µl TEMED and cast the stacking gel until 1 cm below the upper edge of the inner glass plate (do not insert a comb). Overlay with ddH_2O. The stacking gel should polymerize within 30 minutes. Finally remove the overlaying water.

Gels for both gel dimensions should be prepared one day before usage and should be stored at 4°C.

3.2. Sample preparation

All steps of the sample preparation should be carried out at 4°C.

1. Prepare mitochondria of interest (*see* Note 3)
2. Determine the protein concentration, e.g. according to Lowry [16].
3. Adjust the protein concentration to 10 µg / µl
4. Centrifuge 50 µl fractions (about 0.5 mg protein) for 10 minutes at 15 000 xg to sediment organelles
5. Resuspended pellets in 50 µl Digitonin solubilization solution
6. Incubate the fractions for 20 minutes on ice

7. Centrifuge the fractions for 20 minutes at 20 000 xg to remove insoluble material
8. Supplement the fractions with 2.5 µl Coomassie-blue solution
9. Load 30 - 50 µl of the supernatants (corresponding to about 0.3 – 0.5 mg mitochondrial protein) directly into the wells of a BN gel (protein amounts are adjusted to allow staining of gels by Coomassie; if silver staining shall be applied, protein amounts can be reduced by factor 10).

3.3. First dimension BN-PAGE

1. Prepare 1xAnode and 1xCathode buffers BN by diluting the corresponding stock solutions
2. Carefully remove the comb of the first dimension BN gel
3. Assemble the gel electrophoresis unit, add 1xCathode and 1xAnode buffers BN to the upper and lower chambers of the gel unit. Cool down the unit to 4°C
4. Load Coomassie-blue pre-treated protein samples (see 3.2.) into the gel wells
5. Connect the gel unit to a power supply. Start electrophoresis at constant voltage (100V for 45 minutes) and continue at constant current (15 mA for about 5 hours, *see* Note 4). Electrophoresis should be carried out at 4°C. Blue gel bands should already be visible during the electrophoresis run.

3.4. Transfer of gel stripes of first gel dimensions onto second gel dimensions

1. Cut out a lane of the first dimension BN gel
2. Incubate the gel stripe for 10 minutes in Cathode buffer BN + dodecylmaltoside at 4°C

3.5. Second dimension BN-PAGE

1. Assemble the gel electrophoresis unit and transfer the gel stripe of the first gel dimension onto a second dimension gel. Make sure it is placed centrally and that is has close contact to the second dimension gel. Fix the gel stripe with 1.5 % agarose solution (boil the solution before use and allow it to cool down to approximately 45°C). (*see* Note 5)
2. Prepare 1xAnode buffer BN by diluting the corresponding stock solution
3. Add 1x Cathode buffer BN + dodecylmaltoside and 1xAnode buffer BN to the upper and lower chambers of the gel unit.

4. Connect the gel unit to a power supply. Start electrophoresis at constant voltage (100V for 45 minutes) and continue at constant current (15 mA for 6 - 12 hours, *see* Note 6). Electrophoresis should be carried out at 4°C. Blue gel spots should already be visible during the electrophoresis run.

3.6. Enzyme activity staining procedures of 2D BN / BN gels

After completion of the electrophoresis run, 2D BN / BN gels can be stained using Coomassie colloidal [17, 18] or silver [19] (*see* Notes 7 and 8). However, since both gel dimensions are carried out under native conditions, 2D BN / BN PAGE also is compatible with in gel enzyme activity stainings [20, 21]. Three classical in gel staining procedures for enzymes of the respiratory chain are given below (activity staining procedures for several other enzymes can be found in the literature).

1. incubate the gel with ddH_2O for two times 10 minutes
2. incubate the gel with 100 ml freshly prepared staining solution (Cytochrome c oxidase staining solution, or Succinate dehydrogenase staing solution, or NADH dehydrogenase staining solution) Staining takes minutes until hours depending on the abundance of the stained enzyme.
3. Stop the reaction by transferring the gel into Fixing solution (*see* Notes 9 and 10).

4. Notes

1. Conditions to be varied in the two gel dimensions of BN / BN PAGE can refer to detergent type, detergent concentration, temperature, presence of chaotropic compounds and others. Conditions to monitor dissection of supercomplexes into protein complexes and / or dissection of protein complexes into subcomplexes should be optimized for the mitochondria of interest.
2. If very large protein complexes (>3 MDa) have to be resolved, the acrylamide gradient gel of the BN gel dimension can be substituted by a 2.5 % agarose gel prepared in Gel buffer BN [22].

3. Alternatively, mitochondrial subfractions can be used as starting material for BN / BN PAGE, e.g. an inner membrane or a matrix fraction.
4. Electrophoresis should not be carried out for more than 5 hours, because protein complexes might get stuck in the pores of the gradient polyacrylamide gel, which might prevent migration of the complexes into the second gel dimension. In general, 2/3 completion of the electrophoresis run is sufficient for protein complex resolution on the first gel dimension.
5. Transfer of a lane of a BN gel onto a second gel dimension is proposed to be carried out by fixing a lane of a first dimension BN gel onto a pre-poured BN gel for second gel dimension. By using this procedure, time between first and second gel dimension is minimized, which is advantageous for activity stainings of 2D BN / BN gels. However, physical contact between the lane of the first dimension gel and the second dimension gel might be better if the lane of the second gel dimension is embedded into the stacking gel of the second gel dimension (see [5-7] for corresponding protocols). On the other hand, TEMED and APS of the gel solution for the second gel dimension can diffuse into the gel stripe of the first gel dimension, which usually greatly reduces enzymatic activities. Therefore, this procedure should only be applied for 2D BN / BN gels in combination with Coomassie and silver staining.
6. Electrophoresis of the second gel dimension should be carried out for 6-12 hours or longer. Often, sharpness of protein spots is best after long electrophoresis, because protein complexes get stuck into the pores of the gradient gel of the second gel dimension at defined polyacrylamide concentrations.
7. Protein complexes resolved on 2D BN / BN gels also can be blotted onto membranes. Short pre-blots should be carried out to electrophoretically de-stain gels from excess of Coomassie-blue [23]. Alternatively, the Cathode-buffer BN can be replaced by a Cathode buffer BN without Coomassie blue after 50 % completion of the electrophoresis run of the second BN gel dimension. Furthermore, protein complexes excised from 2D BN / BN gels also can be separated on a third gel dimension, which is carried out in the presence of SDS [4].
8. Protein complexes resolved by 2D BN / BN PAGE also can be cut out and prepared for analysis by mass spectrometry. Usually the subunits of protein complexes are first fragmented by Trypsin. Afterwards, peptides are best analyzed by coupled liquid choromatography and electrospray tamdem mass spectrometry (LC-MS/MS).

9. Alternatively, in gel activity staining also can be stopped by adding inhibitors of the monitored enzymes
10. If 2D BN / BN gels shall be Coomassie or silver stained after activity staining, wash the gels several times with ddH_2O before fixation to remove proteins of the activity staining solutions. This will reduce background staining of the gels.

Acknowledgments:

This work was supported by the Deutsche Forschungsgemeinschaft (grant Br 1829 – 7/1)

References

[1] Groth, S.F., Webster, R.G. and Datyner, A. (1963) Two new staining procedures for quantitative estimation of proteins on electrophoretic stripes. *Biochim. Biophys. Acta* **71**, 377-391.

[2] Bradford, M. (1976) A rapid and sensitive method for the quantitation of microgram quantities of protein utilizing the principle of protein-dye binding. *Anal. Biochem*. **72,** 248-254.

[3] Schägger, H, and von Jagow, G. (1991) Blue native electrophoresis for isolation of membrane protein complexes in enzymatically active form. *Anal. Biochem.* **199**, 223-231.

[4] Schägger, H. and Pfeiffer, K. (2000) Supercomplexes in the respiratory chain of yeasts and mammalian mitochondria. *EMBO J.* **19**, 1777-1783.

[5] Schägger, H. (2001a) Blue-native gels to isolate protein complexes from mitochondria. *Meth. Cell Biol.* **166**, 231-244.

[6] Schägger, H. (2003) Blue native electrophoresis. In: Membrane protein purification and crystallization: A practical guide. C. Hunte, G. von Jagow and H. Schägger (eds), Academic Press, London, UK, pp. 105-130.

[7] Heinemeyer, J., Lewejohann, D. and Braun, H.P. (2005) Blue-native gel electrophoresis for the characterization of protein complexes in plants. In: Methods in Molecular Biology: Plant Proteomics, H. Thiellement, V. Méchin, C. Damerval and M. Zivy (eds), Humana press, in press.

[8] Schägger H and Pfeiffer K. (2001) The ratio of oxidative phosphorylation complexes I-V in bovine heart mitochondria and the composition of respiratory chain supercomplexes.
J. Biol. Chem. **276**, 37861-37867.

[9] Schägger, H. (2001b) Respiratory chain super complexes. *IUBMB Life* **52**, 119-128.

[10] Schägger, H. (2002) Respiratory supercomplexes of mitochondria and bacteria. *Biochim. Biophys. Acta* **1555**, 154-159.

[11] Eubel, H., Jänsch, L. and Braun, H.P. (2003) New insights into the respiratory chain of plant mitochondria: supercomplexes and a unique composition of complex II. *Plant Physiol.* **133**, 274-286.

[12] Eubel, H., Heinemeyer, J. and Braun, HP. (2004) Identification and characterization of respirasomes in potato mitochondria. *Plant Physiol.* **134**, 1450-1459.

[13] Millar, A.H., Eubel, H., Jänsch, L., Kruft, V., Heazlewood, L. and Braun, H.P. (2004) Mitochondrial cytochrome c oxidase and succinate dehydrogenase contain plant-specific subunits. *Plant Mol. Biol.* **56**, 77-89.

[14] Krause, F., Reifschneider, N.H., Vocke, D., Seelert, H., Rexroth, S. & Dencher, N.A. (2004) "Respirasome"-like supercomplexes in green leaf mitochondria of spinach. *J. Biol. Chem.* **279**, 48369-48375.

[15] Heinemeyer, J., Eubel, H., Wehmhöner, D., Jänsch, L. and Braun, H.P. (2004) Proteomic approach to characterize the supramolecular organization of photosystems in higher plants. *Phytochemistry* **65**, 1683-1692.

[16] Lowry, O.H., Rosebrough, N.J., Farr, A.L. and Randall, R.J. (1951) Protein measurement with the Folin phenol reagent. *J. Biol. Chem.* **193**, 265-275.

[17] Neuhoff, V., Stamm, R. and Eibl, H. (1985) Clear background and highly sensitive protein staining with Coomassie Blue dyes in polyacrylamide gels: A systematic analysis. *Electrophoresis* **6**, 427-448.

[18] Neuhoff, V., Stamm, R., Pardowitz, I., Arold, N., Ehrhardt, W. and Taube, D. (1990) Essential problems in quantification of proteins following colloidal staining with Coomassie Brilliant Blue dyes in polyacrylamide gels, and their solution. *Electrophoresis* **11**, 101-117.

[19] Heukeshoven, J. & Dernick, R. (1986) Silver staining of proteins. In: BJ Radola, ed., Elektrophoresis Forum ’86, Technische Universität München, p. 22-27.

[20] Grandier-Vazeille, X. and Guerin, M. (1996) Separation by blue native and colorless native polyacrylamide gel electrophoresis of the oxidative phosphorylation complexes

of yeast mitochondria solubilized by different detergents: specific staining of the different complexes. *Anal. Biochem.* **242**, 248-254.

[21] Zerbetto, E., Vergani, L. and Dabbeni-Sala, F. (1997) Quantitation of muscle mitochondrial oxidative phosphorylation enzymes via histochemical staining of blue native polyacrylamide gels. *Electrophoresis* **18**, 2059-2064.

[22] Henderson, N.S., Nijtmans, L.G., Lindsay, J.G., Lamantea, E., Zeviani, M. and Holt, I.J. (2000) Separation of intact pyruvate dehydrogenase complex using blue native agarose gel electrophoresis. *Electrophoresis* **21**, 2925-2931.

[23] Jänsch, L., Kruft, V., Schmitz, U.K. and Braun, H.P. (1996) New insights into the composition, molecular mass and stoichiometry of the protein complexes of plant mitochondria. *Plant J.* **9**, 357-368.

Figure legend:

Resolution of mitochondrial protein complexes from Arabidopsis by two-dimensional BN / BN PAGE. Proteins were solubilized by Digitonin solubilization solution. A: 2D BN / BN gel after Coomassie-staining, B: 2D BN / BN gel after activity staining for NADH dehydrogenase (complex I). The numbers to the right refer to the molecular masses of standard proteins. I+III_2: supercomplex composed of complexes I and III_2; I: NADH dehydrogenase (complex I); V: ATP synthase (complex V); III_2: dimeric cytochrome c reductase (complex III); IV: cytochrome c oxidase (complex IV), II: succinate dehydrogenase (complex II). Note: activity staining allows to visualize the singular and the supercomplex-bound form of complex I. Furthermore, complex I is partially dissected into fragments of 600 kDa (hydrophobic arm) and 400 kDa (matrix exposed arm). The 400 kDa arm includes the NADH oxidizing domain and therefore is also labeled by activity staining, whereas the 600 kDa arm is not.

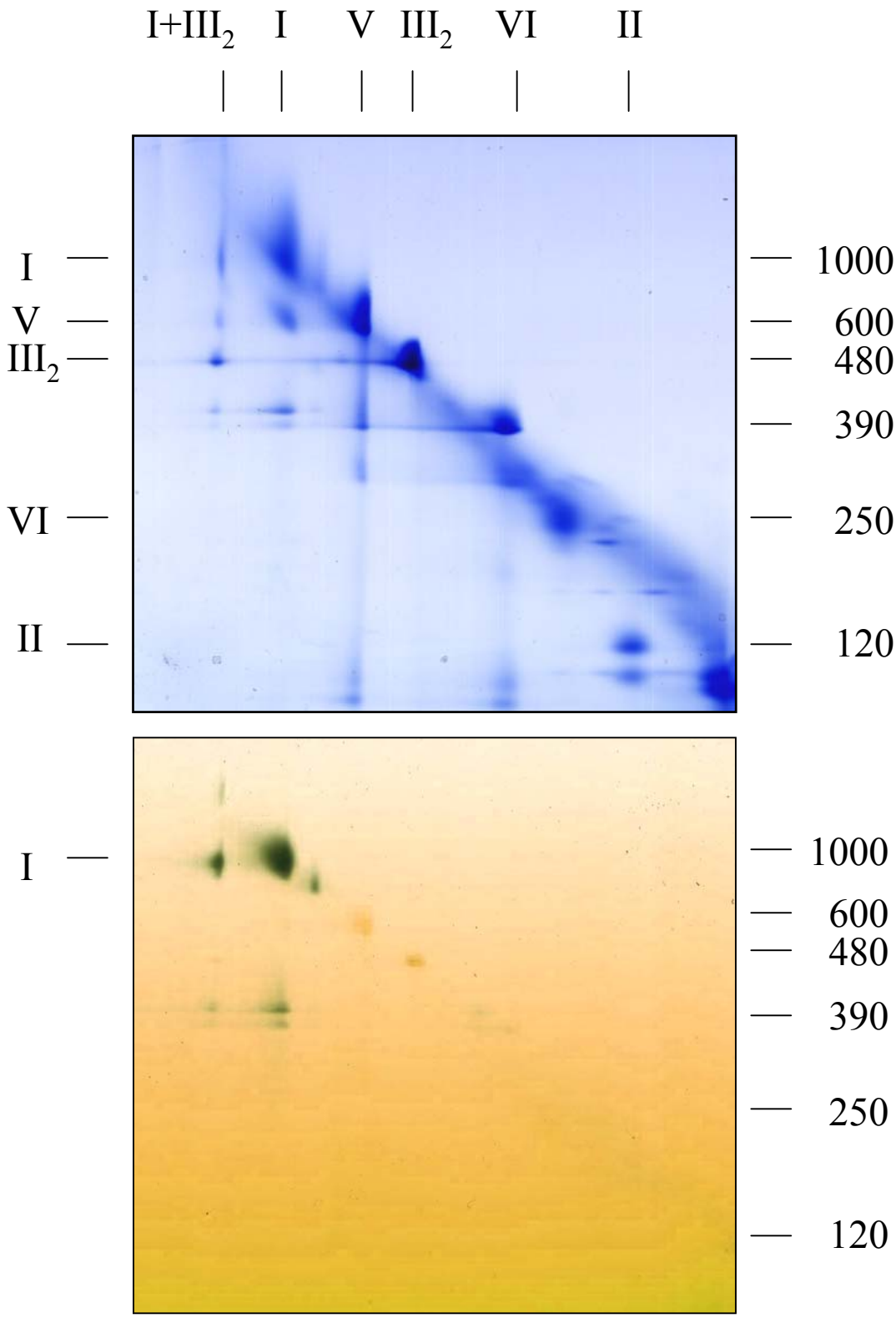
I+III2
I
V
III2
VI
II
I
V
III2
VI
II
1000
600
480
390
250
120
I
1000
600
480
390
250
120

Chapter 5

The Higher Level of Organization of the Oxidative Phosphorylation System: Mitochondrial Supercomplexes.

AUTHOR'S PROOF

J Bioenerg Biomembr
DOI 10.1007/s10863-008-9167-5

The higher level of organization of the oxidative phosphorylation system: mitochondrial supercomplexes

Natalya V. Dudkina · Stephanie Sunderhaus · Egbert J. Boekema · Hans-Peter Braun

Received: 28 June 2008 / Accepted: 20 July 2008
© The Author(s) 2008. This article is published with open access at Springerlink.com

Abstract The organization of the oxidative phosphorylation (OXPHOS) system within the inner mitochondrial membrane appears to be far more complicated than previously thought. In particular, the individual protein complexes of the OXPHOS system (complexes I to V) were found to specifically interact forming defined supramolecular structures. Blue-native polyacrylamide gel electrophoresis and single particle electron microscopy proved to be especially valuable in studying the so-called "respiratory supercomplexes". Based on these procedures, increasing evidence was presented supporting a "solid state" organization of the OXPHOS system. Here, we summarize results on the formation, organisation and function of the various types of mitochondrial OXPHOS supercomplexes.

Keywords Supercomplexes · Respirasome · Electron microscopy · Mitochondria · Oxidative phosphorylation

UNCORRECTED PROOF

Introduction

Respiration is the primary process for energy conversion in eukaryotes and is performed in mitochondria. Five membrane-embedded enzymes constitute an oxidative phosphorylation (OXPHOS) system in the inner mitochondrial membrane. Four of these protein complexes compose the "respiratory chain" and are involved in electron transfer reactions, which in three cases are coupled to proton translocation across the inner mitochondrial membrane. The resulting proton gradient is used by the ATP synthase complex for the phosphorylation ADP. Complex I or NADH dehydrogenase is the main entrance point of electrons to the respiratory chain. It uses NADH molecules generated by catabolic reactions within the mitochondrial matrix as a source of electrons and transfers them to ubiquinone within the membrane. Succinate dehydrogenase or complex II represents an alternative entrance point of electrons to the respiratory chain, which transfers electrons from succinate to ubiquinone and directly connects the Krebs cycle to the respiratory chain. This electron transfer is not coupled to proton translocation. The central component of the OXPHOS system, cytochrome *c* reductase or complex III, is a functional dimer. It transfers electrons from reduced ubiquinone (which is referred to as "ubiquinol") to cytochrome *c* – a small mobile electron carrier associated with the outer surface of the inner membrane. Complex IV or cytochrome *c* oxidase represents the terminal complex of the respiratory chain and was described as a monomer upon solubilization of the inner mitochondrial membrane by mild detergent treatment but as a dimer within protein crystals. It catalyses electron transfer from cytochrome *c* to molecular oxygen thereby reducing the latter to water. By translocating protons across the inner mitochondrial membrane this complex makes a final contribution to the proton gradient across the inner membrane, which is used by the ATP synthase (complex V) for ATP formation. The ATP synthase is composed of two domains: a hydrophobic F_0 membrane part that is

N. V. Dudkina · E. J. Boekema (✉)
Electron microscopy group, Groningen Biomolecular Sciences and Biotechnology Institute, University of Groningen, Nijenborgh 4,
9747 AG Groningen, The Netherlands
e-mail: e.j.boekema@rug.nl

S. Sunderhaus · H.-P. Braun
Institute for Plant Genetics, Faculty of Natural Sciences, Leibniz Universität Hannover,
Herrenhäuser Str. 2,
30419 Hannover, Germany

AUTHOR'S PROOF JnlID 10863_ArtID 9167_Proof# 1 - 02/09/2008

connected to a water-soluble F_1-headpiece by two stalks. In a nutshell, the proton gradient across the membrane domain triggers the rotation of the subunit c ring within the F_0 and γ, δ and ε within F_1, which causes the phosphorylation of ADP.

For a long time the "fluid-state" model was believed to be the best description of the organization of the OXPHOS system (Fig. 1a); it postulates that the respiratory chain complexes freely diffuse in the membrane and that electron transfer takes place on the basis of random collisions. This model is based on the finding that all individual protein complexes of the OXPHOS system can be purified in enzymatically active form and on lipid dilution experiments (reviewed in Hackenbrock et al. 1986).

In the last decade more and more evidences were published pointing to stable interactions of the OXPHOS complexes in the form of defined supercomplexes (Fig. 1b): (1) Flux control experiments proved that the respiratory chain is organized in one functional unit (Boumans et al. 1998; Bianchi et al. 2004). (2) Point mutations within genes encoding subunits of one OXPHOS complex affect the stability of another OXPHOS complex (Acin-Perez et al. 2004; Diaz et al. 2006). (3) Supercomplexes can be separated by blue native PAGE (Schägger and Pfeiffer 2000; Eubel et al. 2003). (4) Supercomplexes are active by *in-gel* activity measurements within blue native gels (Schägger and Pfeiffer 2000; Eubel et al. 2004a). (5) Oxygen uptake by isolated mitochondria of potato correlate with the abundance of supercomplexes (Eubel et al. 2004a). (6) EM structures revealed very defined interactions of OXPHOS complexes within respiratory supercomplexes (Dudkina et al. 2005a, b; Minauro-Sanmiguel et al. 2005; Schäfer et al. 2006; Heinemeyer et al. 2007).

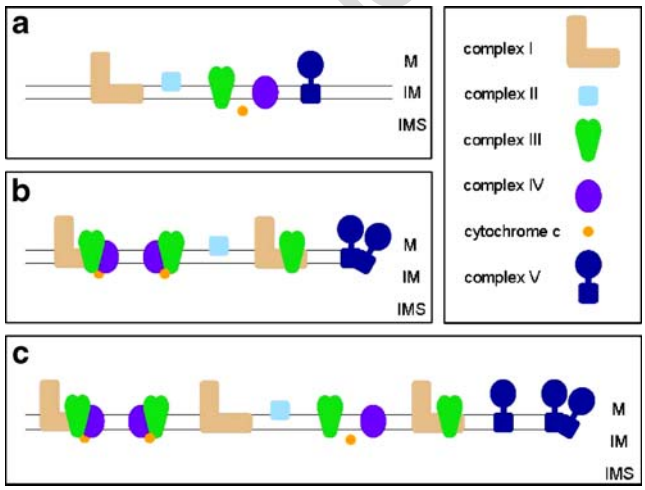

Fig. 1 Models of the mitochondrial OXPHOS system. **a** The "fluid state model". **b** Defined interactions of OXPHOS complexes within supercomplexes as predicted by the "solid state model". **c** Integrated model of the OXPHOS system. *M* Matrix; *IM* inner mitochondrial membrane; *IMS* mitochondrial intermembrane space

The complexes I, III and IV were found to form different types of supercomplexes in a wide range of organisms (reviewed in Dudkina et al. 2006a). Since the various OXPHOS complexes differ in abundance they are considered to not completely incorporate in supermolecular structures. Rather, OXPHOS supercomplexes and single OXPHOS complexes co-exist within the inner mitochondrial membrane (Fig. 1c). Furthermore, association of OXPHOS complexes into supercomplexes and dissociation supercomplexes into OXPHOS complexes is considered to be a dynamic process, which depends on the physiological state of a cell.

Remarkably, complex II was never observed to be included in any respiratory chain supercomplex if analyzed by Blue native PAGE or single particle EM. It is noteworthy that the succinate dehydrogenase is part of the citric acid cycle and that its electron transfer function towards complex III is not a crucial function to be incorporated in a supercomplex.

Respiratory chain complexes and supercomplexes

Supercomplexes involved in the proton gradient: I, I+III_2, III_2+$IV_{1,2}$, I+III_2 +IV

Complex I is the largest complex of the respiratory chain which catalyzes the transfer of two electrons from NADH to ubiquinone and couples it to the translocation of four protons across the inner mitochondrial membrane. The extensively studied bovine heart mitochondria complex I is made of 45 different protein subunits (Carroll et al. 2003). Fourteen homologous "core subunits" are present in all organisms including prokaryotes and chloroplast complex I and constitute the "minimal enzyme". Other additional subunits have been depicted as "peripheral". Structural studies describe complex I as a typical L-shaped molecule consisting of a large membrane arm and hydrophilic arm which runs perpendicular and protrudes far into the matrix (reviewed in Yagi and Matsuno-Yagi 2003). Some peripheral subunits may provide specific features to complex I in certain organisms such as an unique matrix-exposed carbonic anhydrase domain in *Arabidopsis* (Sunderhaus et al. 2006) and *Zea mays* (Peters et al. 2008) or the unknown protrusion at the tip of the membrane arm of complex I from *Yarrowia lipolytica* (Radermacher et al. 2006). A similar additional density at the matrix side was found at the membrane arm tip of complex I from bovine heart mitochondria (Fig. 2a), which was not previously shown in the 3D model at 18 Å deriving from cryo-EM preparation (Grigorieff 1998). The presented bovine negative stain maps are more consistent with other 2D and 3D electron microscopy data than the cryo-EM structure. A prominent

UNCORRECTED PROOF

AUTHOR'S PROOF
JrnlID 10863_ArtID 9167_Proof# 1 - 02/09/2008

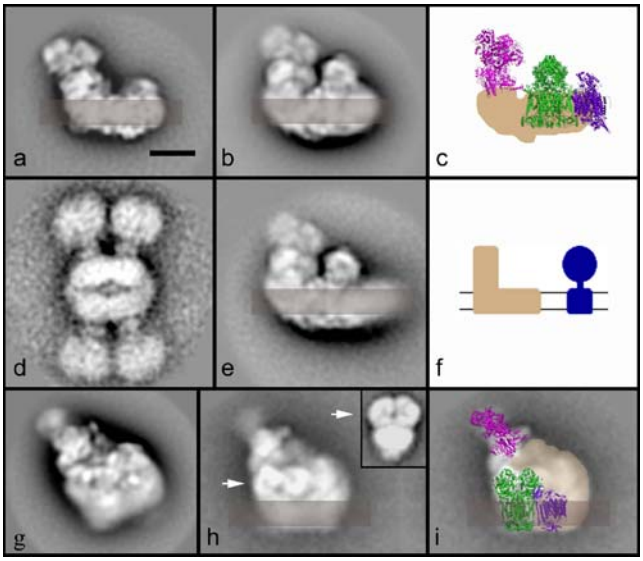

Fig. 2 Structure of the complex I and its supercomplexes from bovine heart mitochondria. Supercomplexes were obtained by solubilization of isolated mitochondria with dodecylmaltoside (7.5 g/g) and digitonin (25 g/g) followed by purification via sucrose gradient ultracentrifugation (S. Sunderhaus and N.V. Dudkina, unpublished data) **a** Side-view of complex I. Position of the membrane is indicated in semi-transparent brown. **b** Side-view of the I + III_2 supercomplex. **c** Modelling of the respirasome. X-ray structures of the hydrophilic domain of complex I from *Thermus thermophilus* (*pink*, Sazanov and Hinchliffe 2006), bovine cytochrome *c* reductase (*green*, Iwata et al. 1998) and bovine cytochrome *c* oxidase (*purple*, Tsukihara et al. 1996) were used. The membrane arm of complex I is given in beige. **d** An aggregate of two dimeric ATP synthases on the same scale as the complex I supercomplexes. e Side view of the I + III_2 supercomplex with a larger membrane part, likely representing the I + III_2 + IV supercomplex or respirasome. **f** Scheme emphasizing that ATP synthase and complex I have the same height. **g** Respirasome in an intermediate orientation on the carbon support film. **h** The same respirasome as in (**e**), but prepared using deep negative stain. This reveals the position of cytochrome *c* reductase within the I + III_2 + IV supercomplex (*white arrow*). The *insert* in the *upper right corner* is purified cytochrome *c* reductase complex from *Arabidopsis* in a similar position (Dudkina et al. 2005a). **i** Model of the respirasome in the intermediate orientation. The position of complex III_2 is according to (**e**); the hydrophilic arm of complex I was generated from the X-ray data of *T. thermophilus* by turning it aproximately 30° away from a side-view orientation and the remainder of the supercomplex are complex I densities (*transparent beige*). The location of complex IV is still uncertain. The *bar* of the EM frames is 10 nm

feature are the overall dimensions of complex I; it is noteworthy that the height of complex I is comparable to the height of the ATP synthase monomer (Fig. 2a,d,f), which is neglected in most textbook illustrations.

In a wide range of organisms complex I was found to form a stable association with the dimeric cytochrome *c* reductase complex which can be easily purified in active form from the membrane after detergent extraction. The first I + III_2 supercomplex maps were described for *Arabidopsis* (Dudkina et al. 2005a) and for *Z. mays* (Peters et al. 2008). Within the supercomplex the dimeric complex III is bound at the tip of the membrane arm of complex I. The top-view projection map of the supercomplex is not completely parallel to the membrane plane although the side view map of the I+III_2 supercomplex rather indicates a parallel position of the long axes of the peripheral complex I arm and complex III_2 with respect to the inner membrane.

In potato (Eubel et al. 2004a, b), spinach (Krause et al. 2004) and *Asparagus* (Dudkina et al. 2006a) complex III_2 was found to associate with one or two copies of complex IV. The structure of the mitochondrial III_2 + $IV_{1,2}$ supercomplex was first studied in *Saccharomyces cerevisiae* because this organism lacks complex I (Heinemeyer et al. 2007). From different maps a pseudo-atomic model could be generated. It shows that two monomeric complex IV copies are attached on both sides of dimeric complex III with their convex side facing complex III_2, which is the opposite to the side involved in the formation of complex IV dimers as described by X-ray crystallography. This attachment is mediated by cardiolipids (Zhang et al. 2002). Formation of the III_2 + $IV_{1,2}$ supercomplex most likely has important functional implications, because the electron transport between complexes III and IV can be optimized by a contraction of cytochrome *c* movement between these two complexes. Moreover, in the presence of complex I it can form a more complicated structure, the "respirasome", a supercomplex uniting complexes I, III and IV. The respirasome is able to carry out full respiration autonomously in the presence of the mobile electron carriers ubiquinone and cytochrome *c*.

Recent experiments with bovine heart mitochondria show that digitonin efficiently extracts complex I but mostly in combination with other respiratory chain complexes, in particular as a I + III_2 + IV supercomplex (S. Sunderhaus and N.V. Dudkina, unpublished data). Projection maps were assigned to single complex I (Fig. 2a), the I + III_2 supercomplex (Fig. 2b), the I + III_2 + IV supercomplex or respirasome (Fig. 2e) and to tilted positions of the same particle (Fig. 2g,h), as obtained previously (Schäfer et al. 2006). Microscopy specimens were made by standard negative staining, but by using deep negative staining, which results in respirasomes fully embedded in the stain layer. Under these conditions, features of the hydrophilic parts of the core 1 and 2 subunits of complex III_2 became more prominent (arrows, Fig. 2h). This leads to an unambiguous identification of the complex III_2 position within the respirasome. The difference in length between the membrane arms of Fig. 2b and e is interpreted to be complex IV.

By using the X-ray structures of complexes III, IV and the peripheral arm of complex I we could determine the positions of these single complexes within the 2D maps of the respirasome (Fig. 2c,i). Although the hydrophilic arm of

UNCORRECTED PROOF

AUTHOR'S PROOF JnlID 10863_ArtID 9167_Proof# 1 - 02/09/2008

Thermus thermophius complex I is built up of less subunits than in bovine it resembles its overall shape in side-view orientation (Fig. 2c). The position of complex III_2 was determined exactly due to the well recognizable features of core 1 and 2 subunits of this complex. The smaller complex IV is placed at the tip of the membrane arm of complex I, because there is a striking difference in the length of the membrane part of supercomplex (Fig. 2b,e). The exact *rotational orientation*, however, is unclear because the complex IV is mostly embedded into the membrane and because there are only two different views of the respirasome. The exact *position* is, however, different between yeast and bovine, as we will explain here: In the some specific side view maps on which the yeast model was based (Heinemeyer et al. 2007), the core 1 and 2 subunits of complex III_2 and the complex IV monomers are in non-overlapping positions. The side view map of the bovine I+III_2+IV supercomplex, however, shows the core 1 and 2 subunits in an overlap position, which is only possible by rotating the complex III dimer about 90° in the membrane plane. Because the complex IV monomer is mostly if not all in a non-overlapping position (Fig. 2c) this implies that it binds at a different position. Complex IV is placed next to the complex III_2 within the bovine respirasome model from Fig. 2c and the remainder densities belong to complex I.

Finally, both monomers of the complex III dimer can be an attachment site for the complex I, because they are identical. But remarkably, in the *Arabidopsis* I + III_2 supercomplex only one of the sites is occupied. This could be an effect of a non-stoichiometric presence of complexes I and III, because it appears that in potato indeed two copies of complex I can bind to complex III_2 (J.B. Bultema, R. Kouřil, unpublished data).

Previous inhibitor titration experiments showed that cytochrome *c* does not exhibit pool behavior in yeast and that the whole respiratory chain of yeast behaves like a single functional unit (Boumans et al. 1998). Wittig et al. 2006 proposed that the respirasome is the unit of a higher level organization of the respiratory chain into long "string"-like megastructures. Our data on bovine supercomplexes, where high numbers of respirasomes were found after mild detergent solubilization, are in line with this suggestion. Such an organization makes the electron transfer rate through the OXPHOS system more efficient and, thus, provides a basis for most effective respiration.

Supercomplexes using the proton gradient: dimeric ATP synthase

The composition of dimeric F_0F_1 ATP synthase from bovine and yeast has been studied in detail (reviewed in Wittig and Schägger 2008). The water-soluble F_1-part is mostly constituted of three α and three ß subunits. It is connected to the ring-like subunit c oligomer of the F_0-part by a central stalk consisting of γ, δ and ε subunits and by a peripheral stalk made from subunits OSCP (Su 5), b, d, F6 (h) (different names of the yeast counterparts in brackets). In addition, the F_0-part is composed of subunits a (Su 6), A6L (Su 8), e, f, g. The yeast protein has two specific subunits i and k.

The first biochemical evidence about a dimeric organization of the ATP synthases complex in yeast came from the BN-PAGE work of Arnold et al. 1998. The supercomplex includes dimer specific subunits named e, g and k, which were not detected in monomers. Later, dimers were described in beef, Arabidopsis and several other organisms by the same technique (Schägger and Pfeiffer 2000; Eubel et al. 2003). Recently, low-resolution 2D structures of dimeric ATP synthase were solved in bovine (Minauro-Sanmiguel et al. 2005), the colorless green alga *Polytomella* (Dudkina et al. 2005b) and *S. cerevisiae* (Dudkina et al. 2006b). In all organisms studied until now two monomers associate via the membrane F_0 parts and make an angle of 35–90°. Dimeric ATP synthase from green algae (Fig. 3e) seems to be the most stable one and is represented exclusively by molecules with an angle of 70°. These data, together with BN-PAGE evidences of trimeric and tetra-

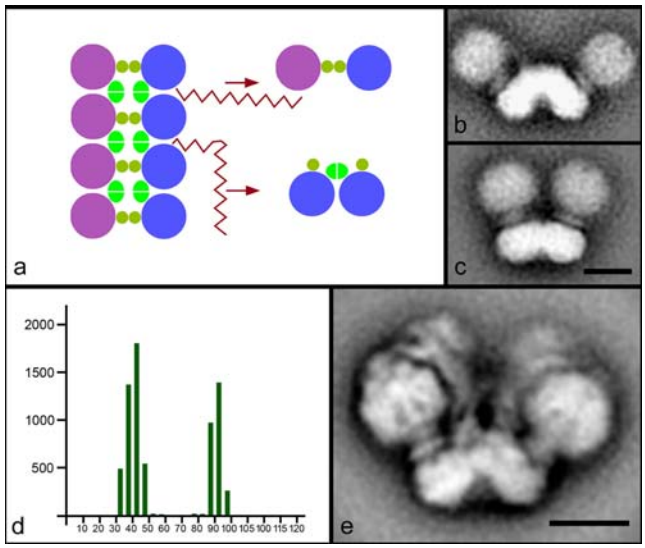

Fig. 3 Dimers and multimers of ATP synthase. **a** Scheme of the multimeric chain of ATP synthases in mitochondria, which can be disrupted by detergent in two ways giving small and large angle dimers. *Purple* and *blue circles* symbolize monomeric ATP synthase complexes and ochre and *bright green* represent dimer-specific subunits. In mitochondria of *S. cerevisiae* the large angle dimers of 90° (**b**) and small angle dimers of 35° (**c**) were found in similar proportions. **d** Distribution of angles between the monomers of dimeric ATP synthase from *S. cerevisiae*. y-axis: number of particles; x-axis: size of the angle in degrees. **e** Dominant projection map of dimeric ATP synthase from *Polytomella* which corresponds to a stable dimer in which the monomers exclusively make an angle of 70°. The *bars* are 10 nm

UNCORRECTED PROOF

AUTHOR'S PROOF

meric organizations of mammalian ATP synthases (Krause et al. 2005), give support for an oligomeric arrangement of ATP synthases in the membrane. The presence of rows of ATP synthase dimers was previously demonstrated in mitochondria of *Paramecium* by rapid-freeze deep-etch electron microscopy (Allen et al. 1989) and in yeast mitochondria by ultrasectioning and negative staining of osmotically shocked *Polytomella* mitochondria (Dudkina et al. 2006b). Recently, new supporting data based on electron cryo-tomography were presented which show that the ATP synthases of mammalian mitochondria are arranged in long rows of dimers located at the apex of cristae membranes (Strauss et al. 2008).

In our scheme of the multimeric chain of ATP synthase complexes in mitochondria (Fig. 3a) we try to explain the difference in angle between two types of monomers. The two types are products of detergent disruption that may happen in two different ways. Chains can be disrupted to give a large angle dimer (70–90°) or a small angle dimer (35–40°) that differ in the interface. In mitochondria of *S. cerevisiae* the large angle dimers of 90° (Fig. 3b) and small angle dimers of 35° (Fig. 3c) are represented in similar numbers (Fig. 3d), which indicates the interactions between monomers within both types of dimers have an equal stability. In the case of *Polytomella* the presence of only 70° dimers suggests that the interaction between two neighboring monomers of the dimers is very weak and can be easily broken by detergent, likely due to the presence of unique dimer specific subunits in this organism (Vázquez-Acevedo et al. 2006). Although originally only dimers of 40° were reported in bovine (Minauro-Sanmiguel et al. 2005) we could observe small amounts of dimers with an angle of 90° (N.V. Dudkina, unpublished data), which also was reported in the recent study on intact bovine mitochondria (Strauss et al. 2008). The large angle dimers were also found in mitochondria of *Z. mays* (N.V. Dudkina, unpublished data).

Though the EM studies provide the first look on the structural organization of dimeric ATP synthase, they do not give a clear statement about the dimer interface. Wittig and Schägger (2008) summarize the most recent data about the monomer–monomer and dimer–dimer interaction. The dimer specific subunits e and g, as well as the subunits a, b, h and i of the monomer, stabilize the monomer–monomer interface. These data are in agreement with electron microscopy results showing that the dimerization occurs via the membrane F_0- and peripheral stalk parts (Dudkina et al. 2005b, 2006b). The dimer–dimer interface is less well understood. Subunits e, f, g, Su 8 (A6L), transmembrane helixes of the a-subunit not involved in monomer–monomer interaction, as well as carriers for inorganic phosphate and for ADP/ATP are candidates for the oligomerization of ATP synthases.

The angle between two monomers in a dimer provides direct evidence that oligomerization of ATP synthases leads to the curvature of the inner mitochondrial membrane. Ultractructural studies on yeast null mutants of dimer specific e and g subunits which lack the dimeric state of ATP synthases indicated that their mitochondria exhibit unusual onion-shape morphology without any membrane foldings (Paumard et al. 2002; Giraud et al. 2002). This strongly suggests that dimerization of ATP synthases is essential for cristae morphology. The recent study on bovine and rat mitochondria proved that the ATP synthases in mammalian mitochondrial membranes are organized in long ribbons of dimers and, furthermore, the mitochondrial cristae act as proton traps and, as a result, ATP synthases may optimize their own performance under proton-limited conditions (Strauss et al. 2008).

Perspectives and open questions

Membrane proteins are difficult objects for any high-resolution structural investigation but the first low-resolution data are a good initial point on the way to high-resolution 3D structures. It is relatively easy to obtain medium-resolution maps of the dimeric ATP synthase. Unfortunately, only a low resolution 3D structure of a respirasome is available up to now (Schäfer et al. 2007). At a resolution around 30 Å, as obtained in the 3D structure, it is impossible to fit unambiguously the X-ray structures of single complexes. At least a resolution of about 15 Å or better is necessary for the precise modeling, as was obtained in some of our beef 2D maps. 2D maps, however, have the disadvantage that the complexes are often only present in a very limited number of orientations, with the exception of the yeast supercomplex $III_2 + IV_{1,2}$ (Heinemeyer et al. 2007). Hence, higher 2D and 3D resolution is needed to solve the single complexes interfaces within the supercomplex. Currently there are two methods to obtain higher resolution structures of such complexes: crystallization of the rather stable supercomplexes and merging of EM and X-ray data. In dimeric ATP synthase specific subunits must be responsible for the tilt of the membrane domain. There are now several proteins known in which some of the membrane spanning α-helices make large angles within proteins, e.g. LHCII (Liu et al. 2004). A next step in dimeric ATP synthase research would be to reveal such α-helices that make large angles between different subunits and thereby contribute in membrane bending.

Acknowledgements We thank Dr. Roman Kouřil for discussion. We also gratefully acknowledge funding by the Netherlands organization of scientific research (NWO) and by the Deutsche Forschungsgemeinschaft (grants Br1829-7/3 and Br1829-8/1).

UNCORRECTED PROOF

AUTHOR'S PROOF JnlID 10863_ArtID 9167_Proof# 1 - 02/09/2008

Open Access This article is distributed under the terms of the Creative Commons Attribution Noncommercial License which permits any noncommercial use, distribution, and reproduction in any medium, provided the original author(s) and source are credited.

References

Acín-Pérez R, Bayona-Bafaluy M, Fernández-Silva P, Moreno-Loshuertos R, Pérez-Martos A, Bruno C, Moraes C, Enríquez J (2004) Mol Cell 13:805–815

Allen RD, Schroeder CC, Fok AK (1989) J Cell Biol 108:2233–2240

Arnold I, Pfeiffer K, Neupert W, Stuart RA, Schägger H (1998) EMBO J 17:7170–7178

Bianchi C, Genova ML, Castelli GP, Lenaz G (2004) J Biol Chem 279:36562–36569

Boumans H, Grivell LA, Berden JA (1998) J Biol Chem 273:4872–4877

Carroll J, Fearnley IM, Shannon RJ, Hirst J, Walker JE (2003) Mol Cel Proteomics 2:117–126

Diaz F, Fukui H, Garcia S, Moraes CT (2006) Mol Cell Biol 26:4872–4881

Dudkina NV, Eubel H, Keegstra W, Boekema EJ, Braun HP (2005a) Proc Natl Acad Sci U S A 102:3225–3229

Dudkina NV, Heinemeyer J, Keegstra W, Boekema EJ, Braun HP (2005b) FEBS Lett 579:5769–5772

Dudkina NV, Heinemeyer J, Sunderhaus S, Boekema EJ, Braun HP (2006a) Trends Plant Sci 11:232–240

Dudkina NV, Sunderhaus S, Braun HP, Boekema EJ (2006b) FEBS Lett 580:3427–3432

Eubel H, Jänsch L, Braun HP (2003) Plant Physiol 133:274–286

Eubel H, Heinemeyer J, Braun HP (2004a) Plant Physiol 134:1450–1459

Eubel H, Heinemeyer J, Sunderhaus S, Braun HP (2004b) Plant Physiol Biochem 42:937–942

Giraud MF, Paumard P, Soubannier V, Vaillier J, Arselin G, Salin B, Schaeffer J, Brethes D, di Rago P, Velours J (2002) Biochim Biophys Acta 1555:174–180

Grigorieff N (1998) J Mol Biol 277:1033–1046

Hackenbrock CR, Chazotte B, Gupte SS (1986) J Bioenerg Biomembr 18:331–368

Heinemeyer J, Braun HP, Boekema EJ, Kouřil R (2007) J Biol Chem 282:12240–12248

Iwata S, Lee JW, Okada K, Lee JK, Iwata M, Rasmussen B, Link TA, Ramaswamy S, Jap BK (1998) Science 281:64–71

Krause F, Reifschneider NH, Vocke D, Seelert H, Rexroth S, Dencher NA (2004) J Biol Chem 279:48369–48375

Krause F, Reifschneider NH, Goto S, Dencher NA (2005) Biochem Biophys Res Commun 329:583–590

Liu Z, Yan H, Wang K, Kuang T, Zhang J, Gui L, An X, Chang W (2004) Nature 428:287–292

Minauro-Sanmiguel F, Wilkens S, García JJ (2005) Proc Natl Acad Sci U S A 102:12356–12358

Paumard P, Vaillier J, Coulary B, Schaeffer J, Soubannier V, Mueller DM, Brethes D, di Rago JP, Velours J (2002) EMBO J 21:221–230

Peters K, Dudkina NV, Jänsch L, Braun HP, Boekema EJ (2008) Biochim Biophys Acta 1777:84–93

Radermacher M, Ruiz T, Clason T, Benjamin S, Brandt U, Zickermann V (2006) J Struct Biol 154:269–279

Sazanov LA, Hinchliffe P (2006) Science 311:1430–1436

Schäfer E, Seelert H, Reifschneider NH, Krause F, Dencher NA, Vonck J (2006) J Biol Chem 281:15370–15375

Schäfer E, Dencher NA, Vonck J, Parcej DN (2007) Biochemistry 46:12579–12585

Schägger H, Pfeiffer K (2000) EMBO J 19:1777–1783

Strauss M, Hofhaus G, Schröder RR, Kühlbrandt W (2008) EMBO J 27:1154–1160

Tsukihara T, Aoyama H, Yamashita E, Tomizaki T, Yamaguchi H, Shinzawa-Itoh K, Nakashima R, Yaono R, Yoshikawa S (1996) Science 272:1136–1144

Vázquez-Acevedo M, Cardol P, Cano-Estrada A, Lapaille M, Remacle C, González-Halphen D (2006) J Bioenerg Biomembr 38:271–282

Wittig I, Schägger H (2008) Biochim Biophys Acta in press Q3

Wittig I, Carrozzo R, Santorelli FM, Schägger H (2006) Biochim Biophys Acta 1757:1066–1072

Yagi T, Matsuno-Yagi A (2003) Biochemistry 42:2266–2274

Zhang M, Mileykovskaya E, Dowhan W (2002) J Biol Chem 277:43553–43556

UNCORRECTED PROOF

Chapter 6

Supramolecular Structure of the OXPHOS System
in Highly Thermogenic Tissue
of *Arum maculatum.*

Supramolecular Structure of the OXPHOS System in Highly Thermogenic Tissue of *Arum maculatum*

Stephanie Sunderhaus and Hans-Peter Braun

Institute for Plant Genetics, Faculty of Natural Sciences, Leibniz Universität Hannover, Herrenhäuser Str. 2, D-30419 Hannover, Germany

ABSTRACT

The protein complexes of the mitochondrial respiratory chain associate in defined ways forming supramolecular structures called respiratory supercomplexes or respirasomes. In plants, additional oxidoreductases participate in respiratory electron transport, e.g. the so-called "alternative NAD(P)H dehydrogenases" or the extra terminal oxidase called "Alternative Oxidase" (AOX). These additional enzymes were previously reported not to form part of respiratory supercomplexes. However, formation of respiratory supercomplexes might indirectly affect alternative respiration because electrons can be channeled within the supercomplexes, which reduces access of the alternative enzymes towards their electron donating substrates. Here we report an investigation on the supramolecular organization of the respiratory chain in thermogenic *Arum maculatum* appendix mitochondria, which is known to have a highly active AOX for heat production. Investigations based on mild membrane solubilization by digitonin and protein separation by blue native PAGE revealed a very special organization of the respiratory chain in *Arum*, which strikingly differs to the one described for the model plant *Arabidopsis thaliana*: (i) complex I is not present in monomeric form, but exclusively forms part of a $I+III_2$ supercomplex, (ii) the III_2+IV and $I+III_2+IV$ supercomplexes are detectable but of low abundance, (iii) complex II has fewer subunits than in *Arabidopsis*, and (iv) complex IV is mainly present as a monomer in the larger form termed "complex IVa". Functional implications with respect to alternative respiration in *Arum* are discussed.

INTRODUCTION

Flowers of a group of monocotyledonous plants, mostly from the family Araceae, are able to regulate their flower temperature during blooming by active heat production (Seymour 2001). *Arum maculatum* is a typical European example for a plant using thermogenesis for pollination. Plants of this family deceit insects by volatilization of odoriferous compounds similar to that of feces or urine emitted by the appendix. This simulates the natural insect laying sites. Insects are attracted and trapped in the floral chamber of the protogynous inflorescence. Fertile male and female flowers are enclosed in this floral chamber at the base of the spathe, which is closed at the top by fibrous sterile male flowers to bar insects from escaping. When female flowers become receptive, insects are simultaneously allured and fall into the chamber (Gibernau et al. 2004). During the period of habitation in the floral chamber, insects may deposit pollen from other *Arum* plants on the receptive stigma. This phase mostly ends the next day when the pollen matures. During this time the sterile male flowers begin wilting, whereby the trapped flies are draped with pollen while escaping from the floral chamber. Thermogenesis seems to play different roles during this pollination process: A first

heating event appears to be responsible for the unfolding of the spathe, the second event for the release of the odors of the appendix and a third one for the maturation of pollen (Albre et al. 2003). In some species, heating often continues throughout the entire period of insect habitation and it is assumed that this may be related to the fact that insects require an elevated body temperature for activity. A warming floral environment may therefore be a significant energy reward for pollinators, enabling them to reduce the energy cost of their activity (Seymour et al 2003).

Thermogenesis in Araceae is based on the mitochondrial respiratory chain. Like in other eukaryotes, the respiratory electron transfer chain of plant mitochondria is composed of four protein complexes localized in the inner mitochondrial membrane, the NADH dehydrogenase (complex I), the succinate dehydrogenase (complex II), the cytochrome c reductase (complex III) and the cytochrome c oxidase (complex IV), and the two mobile electron transporters ubiquinone and cytochrome c. All these components cooperate to transfer electrons form NADH or $FADH_2$ to molecular oxygen and thereby generate a proton gradient across the inner mitochondrial membrane. By the act of the ATP synthase complex, which also is termed complex V, the proton gradient is used for the generation of ATP from ADP. Besides complexes I-V, the mitochondria of plants include quite a number of additional, so-called "alternative" oxidoreductases, e.g. rotenone-insensitive alternative NAD(P)H dehydrogenases and a terminal oxidase called "Alternative Oxidase" (AOX) (Vanlerberghe and McIntosh 1997, Juszczuk and Rychter 2003, Rasmusson et al. 2008). The latter competes with the complexes III and IV for electrons transferred form the "ubiquinone pool" of the inner mitochondrial membrane. However, in contrast to complexes III and IV, AOX does not translocate protons across the inner mitochondrial membrane, which is coupled to electron transfer. Instead the redox energy is released as heat, which in the case of Araceae is used for the active regulation of pollination.

The protein complexes of the respiratory chain were recently shown to interact in a defined manner forming the so-called respiratory supercomplexes (reviewed in Boekema and Braun 2007). The most stable are supercomplexes composed of $I+III_2$, III_2+IV and $I+III_2+IV$ (Dudkina et al. 2005, Heinemeyer et al. 2007, Schäfer et al. 2006). Interaction of the complexes is believed to be dynamically regulated. Since the $I+III_2$ supercomplex most likely directly channels electrons from complex I to complex III_2, formation of this supercomplex could restrict access of AOX to its substrate ubiquinol (Eubel et al. 2003). Therefore, formation of the $I+III_2$ supercomplex might indirectly regulate AOX activity.

Here we report an investigation on the supramolecular structure of the respiratory chain of thermogenic *Arum maculatum* appendix mitochondria. As reported for other higher plants, respiratory supercomplexes can be detected by mild solubilization of mitochondrial membranes in combination with blue native (BN) PAGE. The organization of the respiratory chain of *Arum maculatum* differs remarkably from the one of the model plant *Arabidopsis thaliana*. Functional implications are discussed.

Materials and Methods

Material

Appendices of *Arum maculatum* were collected in the "Berggarten Hannover" at developmental stages beta to delta as originally described in James and Beevers (1950).

Isolation of mitochondria

Mitochondria from *Arum maculatum* appendices were isolated as already described earlier (Proudlove et al. 1987). All steps were carried out at 4°C. *Arum maculatum* appendices were cut in small pieces of approximately 0.5 cm and homogenized in a Warring blender (3 x 20 sec full speed) in a grinding medium containing 0.3 M Mannitol, 0.2 mM EDTA, 20 mM MOPS, 0.2% (w/v) BSA, 2mM Pyruvic acid, 7 mM Cysteine, and a pH of 7.5. In a following step, the homogenate was additionally ground two times with a mortar and than filtered by the use of gauze. After this, the pH was re-adjusted to 7.5. Mitochondria were separated from other cell components by several steps of differential centrifugation and finally purified by Percoll gradient density ultracentrifugation as outlined in Werhahn et al. (2001) for *Arabidopsis thaliana*. The mitochondrial bands were washed several times in washing buffer containing 0.3 M Mannitol, 0.2 mM EDTA, 20 mM MOPS, 0.2% (w/v) BSA, 2 mM Pyruvic acid, a pH of 7.5 and either directly used for O_2 measurements or stored at -80°C at a concentration of 0.1g of mitochondria per ml washing buffer for further investigations.

O_2 Measurements

Oxygen consumption of the developmental stages β, γ and δ of *Arum maculatum* appendix mitochondria was measured in a Clark-type oxygen electrode with a reaction chamber of 2ml (Oxygraph, Hansatech, Norfolk, UK). Oxygen consumption of 1mg of mitochondria in a reaction buffer containing 0.3 M Mannitol, 10mM K_2HPO_4, 10mM KCl, 5mM MgCl and a pH of 7.2 was measured after addition of Succinate, ADP, KCN and SHAM. Oxygen consumption was calculated in nmol ΔO_2 min $^{-1}$ mg protein $^{-1}$ (Eubel et al. 2004).

Gel Electrophoresis Procedures

The purity of mitochondria preparations was tested on 2D blue native/SDS gels according to Wittig et al. (2006). 1D SDS PAGE was carried out as described by Schägger and von Jagow (1987). Solubilization of mitochondrial protein was performed using digitonin at a concentration of 5g/g mitochondrial protein (Eubel et al. 2003).

Staining procedures

All gels were either stained with coomassie colloidal (Neuhoff et al. 1985 and Neuhoff et al. 1990) or silver (Heukeshoven 1986). *In-gel* enzyme activity staining for mitochondrial respiratory complexes I, II and IV were carried out as described in Zerbetto et al. (1997).

Western Blotting

Proteins separated on acrylamide gels were blotted onto nitrocellulose membranes for antibody staining using the Trans Blot Cell from BioRad. Blotting was carried out as described in Kruft et al. (2001). Immune stainings were performed using the VectaStain ABC Kit.

RESULTS

Mitochondria were isolated from the developmental stages β, γ and δ from *Arum maculatum* appendices and from *Arabidopsis thaliana* suspension cell cultures as a control. To evaluate the intactness and purity of isolated mitochondria, oxygen consumption of organelle fractions from *Arum* and *Arabidopsis* were analyzed with a Clark-type oxygen electrode. Using succinate as a substrate, state II respiration was high in *Arum maculatum* (> 400 nmol O_2 / min / mg protein) and further increased significantly after ADP addition (700 nmol O_2 min^{-1} mg $protein^{-1}$), indicating good intactness of the isolated mitochondria (data not shown). Addition of KCN inhibited respiration by about 50%. In contrast, respiration of mitochondria purified from *Arabidopsis* suspension cell cultures exhibited a significantly lower state II and III respiration, which is in line with data reported in the literature (de Virville et al. 1998, Eubel et al. 2004, Lee et al. 2008). KCN addition nearly completely inhibited oxygen consumption, indicating that alternative respiration is very low. We conclude that mitochondrial fractions from both organisms are of good quality and suitable for further investigations on the Oxidative Phosphorylation (OXPHOS) system.

Characterization of the OXPHOS system from *Arum maculatum* appendix mitochondria

To characterize the composition of the OXPHOS complexes of *Arum maculatum*, appendix mitochondria of the developmental stages β, γ and δ were solubilized with 5 g/g digitonin and proteins were resolved on one dimensional blue native gels (1D BN) (Fig. 1). As a control, *Arabidopsis* mitochondria were resolved on the same gel. Overall, occurrence of OXPHOS complexes is similar in *Arum* and *Arabidopsis*. However, the band corresponding to mitochondrial complex I is completely absent in *Arum*. In fact, all complex I subunits seem to be associated within the 1500 kDa $I+III_2$ supercomplex, which previously was described by Eubel et al. 2003. To test this conclusion, an *in-gel* activity staining was carried out for complex I (Fig. 1). Indeed, complex I activity is clearly visible in the 1500 kDa range in *Arabidopsis* as well as in *Arum*. Furthermore, activity is observed in the low molecular mass range of the gel, which probably is due to one of the alternative NAD(P)H dehydrogenases. Complex II was detected by another *in-gel* activity stain (Fig. 1). It is of comparable abundance in *Arabidopsis* and *Arum*. However, for unknown reasons, it is much smaller in *Arum*. Finally, complex IV was detected on the 1D BN gel by another *in-gel* activity stain. It previously was reported for *Arabidopsis*, that this complex is present in a larger and smaller version termed complex IVa and complex IVb. The smaller version of this complex, which is much more abundant in *Arabidopsis*, lacks at least one subunit, which was identified to represent the Cox VIb protein (Eubel et al. 2003). *Arum* mitochondria also include the two versions of complex IV. However, in contrast to *Arabidopsis*, the larger complex IVa is clearly more abundant. Furthermore, the complex IV *in- gel* activity stain allows for the visualization of complex IV containing supercomplexes, which are absent in *Arabidopsis* but which were reported for potato (Eubel et al. 2004). In potato, complex IV can be associated

with dimeric complex III forming a III+IV supercomplex which migrates in the 700-800 kDa range. Additionally, complex I can be associated to the III+IV supercomplex forming a $I+III_2+IV$ supercomplex, the so-called "respirasome", which runs above the $I+III_2$ supercomplex in the 1700 kDa range. In accordance with previously published findings, *Arabidopsis* lacks complex IV containing supercomplexes. In contrast, the complex IV *in-gel* activity stain reveals weak signals in the regions of both, the III_2+IV and the $I+III_2+IV$ supercomplex in the expected gel regions. The complexes III_2 and V have similar sizes in *Arum* and *Arabidopsis*. In addition, abundances are comparable in the two organisms.

To further investigate the OXPHOS system in *Arum*, 2D BN/SDS PAGE was carried out to separate the subunits of the resolved protein complexes. Indeed, subunits of complex I are completely absent in the gel region normally covered by the monomeric complex. Instead, all complex I subunits co-migrate with the subunits of complex III and therefore form part of the $I+III_2$ supercomplex. Complex II has a very unusual subunit composition in all investigated dicotylodoneous plants (Eubel et al. 2003, Millar et al. 2004) because it is composed of eight distinct subunits, whereas complex II of all other investigated groups of organisms only includes four subunits. In *Arum*, the larger eight subunit complex is not visible on the 2D gels (Fig. 2). Instead, a four subunit complex is visible, which runs further to the right on the 2D gel. It currently can not be decided if the lacking subunits are absent in *Arum*, or if they are detached form the complex during electrophoresis. Complexes III_2 and V, which have similar molecular masses on 1D gels (Fig. 1), differ slightly in subunit composition between the two species. Therefore, identities of the subunits of the *Arum* complexes can not simply be deduced from their gel position in comparison to *Arabidopsis* but rather should be uncovered by mass spectrometry. In *Arabidopsis*, some complex V subunits not only are visible in the gel region corresponding to 550 kDa (F_0F_1 ATP synthase complex) on the 1D gel, but additionally in the 350 kDa range. This phenomenon is due to a partial dissection of the F_0F_1 complex into the F_1 and the F_0 part, the latter of which completely gets dissected and was described previously (Jänsch et al. 1996). In contrast, no F_1 subunits are visible in *Arum* on the 2D BN / SDS gels. This most likely reflects a high degree of intactness of the isolated organelles from this organism.

Carbonic anhydrase domain of complex I in *Arum* and *Arabidopsis*

Complex I of plant mitochondria includes some additional plant-specific subunits (Heazlewood et al. 2003). Most notably, a group of 3-5 structurally related 30 kDa proteins occur, which show high sequence similarity to γ-type carbonic anhydrases (Parisi et al. 2004, Perlaes et al. 2004, Perales et al. 2005, Sunderhaus et al. 2006, Peters et al. 2008). The carbonic anhydrases form part of a unique extra spherical domain attached to the membrane arm of complex I on its matrix-exposed side (Dudkina et al. 2005, Sunderhaus et al. 2006, Peters et al. 2008). The physiological role of this extra domain is unknown but hypothesized to be important in the context of an inner-cellular CO_2 transfer mechanism to supply the calvin cycle of the chloroplast with CO_2 liberated in mitochondria due to the decarboxlation of organic acids or glycine (Braun and Zabaleta 2007). So far, presence of the carbonic anhydrase subunits was reported for *Arabidopsis, Rice, Chlamydomonas* and *Zea maize* (Heazlewood et al. 2003, Cardol et al. 2004, Peters et al. 2008). Presence of the carbonic anhydrase subunits in *Arum* was addressed by Western blotting using 2D BN/SDS gels (Figure 3). A corresponding subunit clearly forms part of the $I+III_2$ supercomplex. It currently can not be decided whether the complex includes different forms of this protein as reported for *Arabidopsis*. In contrast, the immune signal is present at more than two positions on the control blot for *Arabidopsis*, which represents the $I+III_2$ supercomplex bound form, the

complex I bound form and some smaller forms which most likely represent subcomplexes of complex I (Perales et al. 2005). This in turn confirms the high degree of intactness of the isolated mitochondria from *Arum*.

Alternative oxidase in *Arum maculatum* and *Arabidopsis thaliana*

Alternative Oxidase does not form part of OXPHOS protein complexes or supercomplexes in *Arabidopsis* (Eubel et al. 2003) and is difficult to detect on coomassie-stained 2D BN/SDS gels. Therefore, the AOX protein was immunologically detected for *Arabidopsis* and *Arum* mitochondria using 1D SDS-PAGE and Western blotting (Figure 4). In correspondence with published experimental results, AOX represents a very abundant 30 kDa protein in *Arum*. In contrast, AOX was hardly detectable in *Arabidopsis* mitochondria isolated from suspension cell cultures. This confirms the low AOX activity detectable by O_2 consumption measurements. To test whether AOX might after all be associated with OXPHOS complexes in *Arum*, the enzyme was immunologically detected after protein separations by 2D BN/SDS PAGE (Figure 5). AOX clearly gives a signal in a gel region corresponding to the < 50 kDa range on the 1D BN gel and therefore seems not to be associated with any of the larger complexes.

DISCUSSION

This study reports a systematic investigation of the supramolecular structure and subunit composition of the OXPHOS system in *Arum* using mild protein solubilization with Digitonin and protein separation by BN-PAGE. The organization of the OXPHOS system in *Arum* clearly differs with respect to the one of the model plant *Arabidopsis*: (i) Singular complex I is absent (ii) the I+III_2 supercomplex is very abundant, (iii) the complex II has fewer subunits and (iv) complexes III_2 and V also differ with respect to subunit composition. Small amounts of III+IV and I+III_2+IV supercomplexes are detectable in *Arum* but not in *Arabidopsis*. In both organisms, AOX is not attached to any of the OXPHOS complexes or supercomplexes. To evaluate whether the organization of the OXPHOS system varies between the different developmental stages of appendices, mitochondria were isolated from β, γ and δ stages. However, there are no significant differences between the stages. This result partially could be due to difficulties in classifying the different stages of inflorescence development. However, differences at least should be visible between stages β and δ. Since this is not the case we conclude that the organization of the OXPHOS system during inflorescence development has to be considered as rather stable.

It was previously reported that alternative respiration by far exceeds “normal” respiration (cytochrome-pathway respiration involving the complexes III and IV) during thermogenesis in *Arum* (Wagner et al. 2008, Moore and Siedow 1991). In correspondence with these findings, AOX is clearly very highly expressed in all analyzed organellar fractions included in our investigations. However, at the same time, the “classical” respiratory protein complexes are of exceedingly high abundance and activity in *Arum* mitochondria. Indeed, activity of these complexes is rather comparable to the activity of the same complexes in *Arabidopsis*. Obviously, besides high AOX activity for thermogenesis, “normal” respiratory activity is also very important for ATP generation, which is needed to power various biochemical processes during inflorescence development. Large amounts of substrates must be imported into mitochondria during flowering of *Arum* to power the two highly active respiratory pathways.

Abundant research has been dedicated to discovering how AOX is regulated (reviewed in Siedow and Umbach 2000, Affourtit et al. 2002). Besides substrate activation by pyruvate, redox regulation is considered to be important for AOX activity. AOX forms a dimer via a covalent Cys-Cys bridge, which inactivates the protein. Furthermore, it recently was speculated that supercomplex formation of complexes I and III_2 might indirectly affect alternative respiration, because it could restrict access of AOX towards its substrate ubiquinol (Eubel et al. 2003). This would indicate that tissues exhibiting high alternative respiration should have a decreased abundance of the $I+III_2$ supercomplex. However, this clearly is not the case. *Arum* appendix mitochondria are highly active with respect to alternative respiration, but at the same time have a very high abundance of this supercomplex. In fact, momomeric complex I seems to be completely absent. We conclude that supercomplex formation most likely does not affect AOX activity. Thus far, it has not yet been proven that the $I+III_2$ supercomplex directly "channels" electrons via ubiquinol trapped within its assembly. Indeed, recent x-ray structural data for the peripheral arm of complex I (Sazanov and Hinchliffe 2006) and single particle EM data for the $I+III_2$ supercomplex (Dudkina et al. 2005) indicate that the ubiquinone reduction site and the ubiquinol oxidation site within the supercomplex are in proximity, but not in direct contact. Therefore, the physiological role of the $I+III_2$ supercomplex still remains elusive.

ACKNOWLEDGEMENTS

We thank the "Berggarten" in Hannover, Germany, for providing *Arum maculatum* plants. Furthermore, we wish to thank Tom Elton, University of Nebraska, USA, for providing the antibodies directed against the AOX. This research was supported by the Deutsche Forschungsgemeinschaft (grant Br 1829-7/3).

Literature cited

Affourtit C, Albury MS, Crichton PG, Moore AL (2002) Exploring the molecular nature of alternative oxidase regulation and catalysis. FEBS Lett 510, 121 – 126.

Albre J, Quilichini A, Gibernau M (2003) Pollination ecology of *Arum italicum* (Araceae). Bot. J. Linn. Soc. 141, 205 – 214.

Boekema EJ, Braun HP (2007) Supramolecular structure of the mitochondrial oxidative phosphorylation system. J. Biol. Chem. 282, 1 – 4.

Braun HP, Zabaleta E (2007) Carbonic anhydrase subunits of the mitochondrial NADH dehydrogenase complex (complex I) in plants. Physiol. Plant. 129, 114 – 122.

Cardol P, Vanrobaeys F, Devreese B, Van Beeumen J, Matagne RF, Remacle C (2004) Higher plant-like subunit composition of mitochondrial complex I from Chlamydomonas reinhardtii: 31 conserved components among eukaryotes. Biochim. Biophys. Acta 1658, 212 – 224.

De Virville JD, Alin MF, Aaron Y, Rémy R, Guillot-Salomon T, Cantrel C (1998) Changes in functional properties of mitochondria during growth cycle of *Arabidopsis thaliana* cell suspension cultures. Plant Physiol. Biochem. 36, 347-356.

Dudkina NV, Eubel H, Keegstra W, Boekema EJ, Braun HP (2005) Structure of a mitochondrial supercomplex formed by respiratory-chain complexes I and III. PNAS 102, 3225 – 3229.

Eubel H, Jänsch L, Braun HP (2003) New insights into the respiratory chain of plant mitochondria. Supercomplexes and a unique composition of complex II. Plant Physiol. 133, 274-286.

Eubel H, Heinemeyer J, Braun HP (2004) Identification and characterization of respirasomes in potato mitochondria. Plant Physiol. 134, 1450-1459.

Gibernau M, Macquart D, Przetak G (2004) Pollination in the genus *Arum* – a review. Aroideana 27, 148 – 166.

Heazlewood JL, Howell KA, Millar AH (2003) Mitochondrial complex I from *Arabidopsis* and rice: orthologs of mammalian and fungal components coupled with plant specific subunits. Biochim. Biophys. Acta 1604, 159 – 169.

Heinemeyer J, Braun HP, Boekema EJ, Kouril R (2007) A structural model of the cytochrome c reductase/oxidase supercomplex from yeast mitochondria. J. Biol. Chem. 282, 12240 – 12248.

Heukeshoven J, Dernick R in: Radula, B (Ed) Electrophoresis Forum ´86, Technische Universität München, 1986, 22 – 27.

Jänsch L, Kruft V, Schmitz UK, Braun HP (1996) New insights into the composition, molecular mass and stoichiometry of the protein complexes of plant mitochondria. Plant J. 9, 357 – 368.

Juszczuk IM, Rychter AM (2003) Alternative Oxidase in higher Plants. Acta. Biochim. Polonica 50, 1257 – 1271.

James WO and Beevers H (1950) The respiration of *Arum* spadix. A rapid respiration, resistant to cyanide. New Phytol. 49, 353 – 374.

Kruft V, Eubel H, Werhahn W, Jänsch L, Braun HP (2001) Proteomic approach to identify novel mitochondrial functions in *Arabidopsis thaliana*. Plant Physiol. 127, 1694-1710.

Lee CP, Eubel H, O´Toole N, Millar AH (2008) Heterogeneity of the mitochondrial proteome for photosynthetic and non-photosynthetic *Arabidopsis* metabolism. Mol. Cell Proteomics 7, 1297 - 1316.

Millar AH, Eubel H, Jänsch L, Kruft V, Heazlewood JL, Braun HP (2004) Mitochondrial cytochrome c oxidase and succinate dehydrogenase complexes contain plant specific subunits. Plant Mol. Biol. 56, 77 – 90.

Moore AL, Siedow JN (1991) The regulation and nature of the cyanide-resistent alternative oxidase of plant mitochondria. Biochim. Biophys. Acta 1059, 121 – 140.

Neuhoff V, Stamm R, Eibl H (1985) Clear background and highly sensitive protein staining with Coomassie Blue dyes in polyacrylamide gels: A systematic analysis. Electrophoresis 6, 427-448

Neuhoff V, Stamm R, Pardowitz I, Arold N, Ehrhardt W, Taube D (1990) Essential problems in quantification of proteins following colloidal staining with Coomassie Brilliant Blue dyes in polyacrylamide gels, and their solution. Electrophoresis 11, 101-117

Parisi G, Perales M, Fornasari MS, Colaneri A, Gonzalez-Schain N, Gomez-Casati D, Zimmermann S, Brennicke A, Araya A, Ferry JG, Echave J, Zabaleta E (2004) Gamma carbonic anhydrases in plant mitochondria. Plant Mol. Biol. 55, 192 – 207.

Perales M, Parisi G, Fornasari MS, Colaneri A, Villareal F, Gonzalez-Schain N, Echave J, Gomez-Casati D, Braun HP, Araya A, Zabaleta E (2004) Gamma carbonic anhydrase like complex interact with plant mitochondrial complex I. Plant Mol. Biol. 56, 947 – 957.

Perales M, Eubel H, Heinemeyer J, Colaneri A, Zabaleta E, Braun HP (2005) Disruption of a nuclear gene encoding a mitochondrial gamma-type carbonic anhydrase reduces complex I and supercomplex I+III_2 levels and alters mitochondrial physiology in *Arabidopsis*. J. Mol. Biol. 350, 263 – 277.

Peters K, Dudkina NV, Jänsch L, Braun HP, Boekema EJ (2008) A structural investigation of complex I and I+III2 supercomplex from *Zea mays* at 11 – 13 Å resolution: assignment of the carbonic anhydrase domain and evidence for structural heterogeneity within complex I. Biochim. Biophys. Acta 1777, 84 – 93.

Proudlove MO, Beechey RB, Moore AL (1987) Pyruvate transport by thermogenic-tissue mitochondria. Biochem J. 247, 441-447.

Rasmusson AG, Geisler DA, Møller IM (2008) The multiplicity of dehydrogenases in the electron transport chain of plant mitochondria. Mitochondrion 8, 47 – 60.

Sazanov LA, Hinchliffe P (2006) Structure of the hydrophilic domain of respiratory complex I from *Thermus thermophilus*. Science 311, 1430 – 1436.

Schäfer E, Seelert H, Reifschneider NH, Krause F, Dencher NA, Vonck J (2006) Architecture of active mammalian respiratory chain supercomplexes. J. Biol. Chem. 281, 15370 – 15375.

Schägger H, Jagow G (1987) Tricine-sodium dodecyl sulfate-polyacrylamide gel electrophoresis for the separation of proteins in the range from 1 to 100 kDa. Anal. Biochem. 166, 368-379.

Seymour RS (2001) Biophysics and Physiology of temperature regulation in thermogenic flowers. Bioscience Reports 21, 223 – 236.

Seymour RS, White CR, Gibernau M (2003) Heat reward for insect pollinators. Nature 426, 243 – 244.

Siedow JN, Umbach AL (2000) The mitochondrial cyanide resistant oxidase: structural conservation amid regulatory diversity. Biochim. Biophys. Acta 1459, 432 – 439.

Sunderhaus S, Dudkina NV, Jänsch L, Klodmann J, Heinemeyer J, Perales M, Zabaleta E, Boekema EJ, Braun H.-P. (2006) Carbonic anhydrase subunits form a matrix exposed domain attached to the membrane arm of mitochondrial complex I in plants. J. Biol. Chem. 281, 6482 – 6488.

Vanlerberghe GC and McIntosh L (1997) Alternative Oxidase: From gene to function. Annu. Rev. Plant Physiol. Plant Mol. Biol. 48, 703 – 734.

Wagner AM, Krab K, Wagner MJ, Moore AL (2008) Regulation of thermogenesis in flowering Araceae: The role of the alternative oxidase. Biochim. Biophys. Acta 1777, 993 – 1000.

Werhahn W, Niemeyer A, Jänsch L, Kruft V, Schmitz UK, Braun HP (2001) Purification and characterization of the preprotein translocase of the outer mitochondrial membrane from *Arabidopsis thaliana*: identification of multiple forms of TOM20. Plant Physiol. 125, 943-954.

Wittig I, Braun HP, Schägger H (2006) Blue native PAGE. Nat. Protoc. 1, 418 -428.

Zerbetto E, Verqani L, Dabbeni-Sala F (1997) Quantification of muscle mitochondria oxidative phosphorylation enzymes via histochemical staining of blue native polyacrylamide gels. Electrophoresis. 18, 2059-2064.

Figure 1:

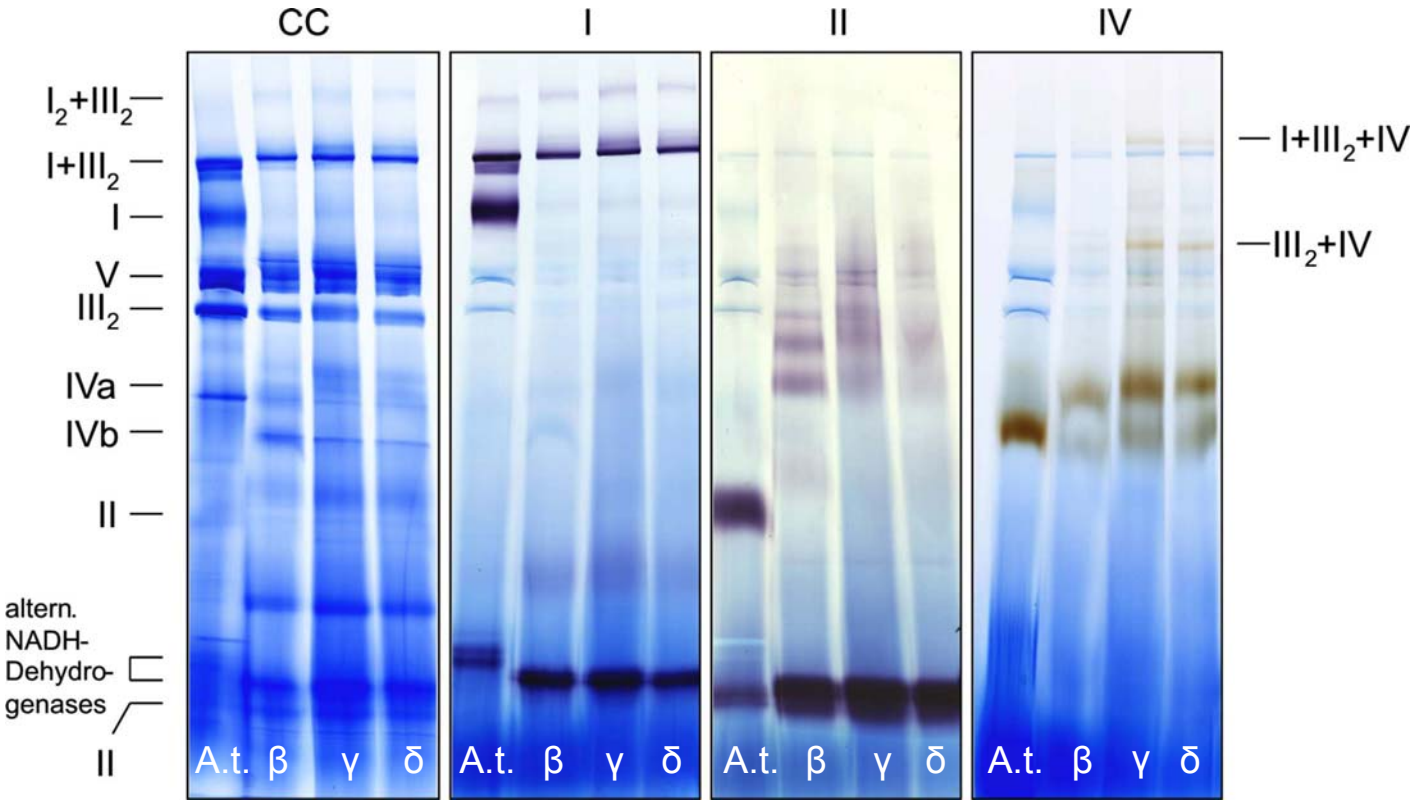

In-gel enzyme activity stainings of the respiratory protein complexes from *Arum maculatum*. Mitochondria were isolated from the developmental stages β, γ and δ. As a control, measurements were also carried out for isolated mitochondria from *Arabidopsis thaliana* (A.t.). Mitochondria were solubilized by 5g digitonin per g protein and separated by 1D BN-PAGE and either visualized by coomassie staining (CC) or by *in-gel* activity staining for NADH dehydrogenase (I), succinate dehydrogenase (II) and cytochrome c oxidase (IV). Identities of protein complexes are indicated on the left or right side of the gels: I – complex I; II – complex II; III_2 – dimeric complex III; IVa and IVb - large and small form of complex IV; V - ATP-synthase; $I+III_2$ - supercomplex containing complex I and III_2; III_2+IV - supercomplex composed of complex III_2 and complex IV; $I+III_2+IV$ - supercomplex composed of complex I, dimeric complex III and monomeric complex IV.

Figure 2:

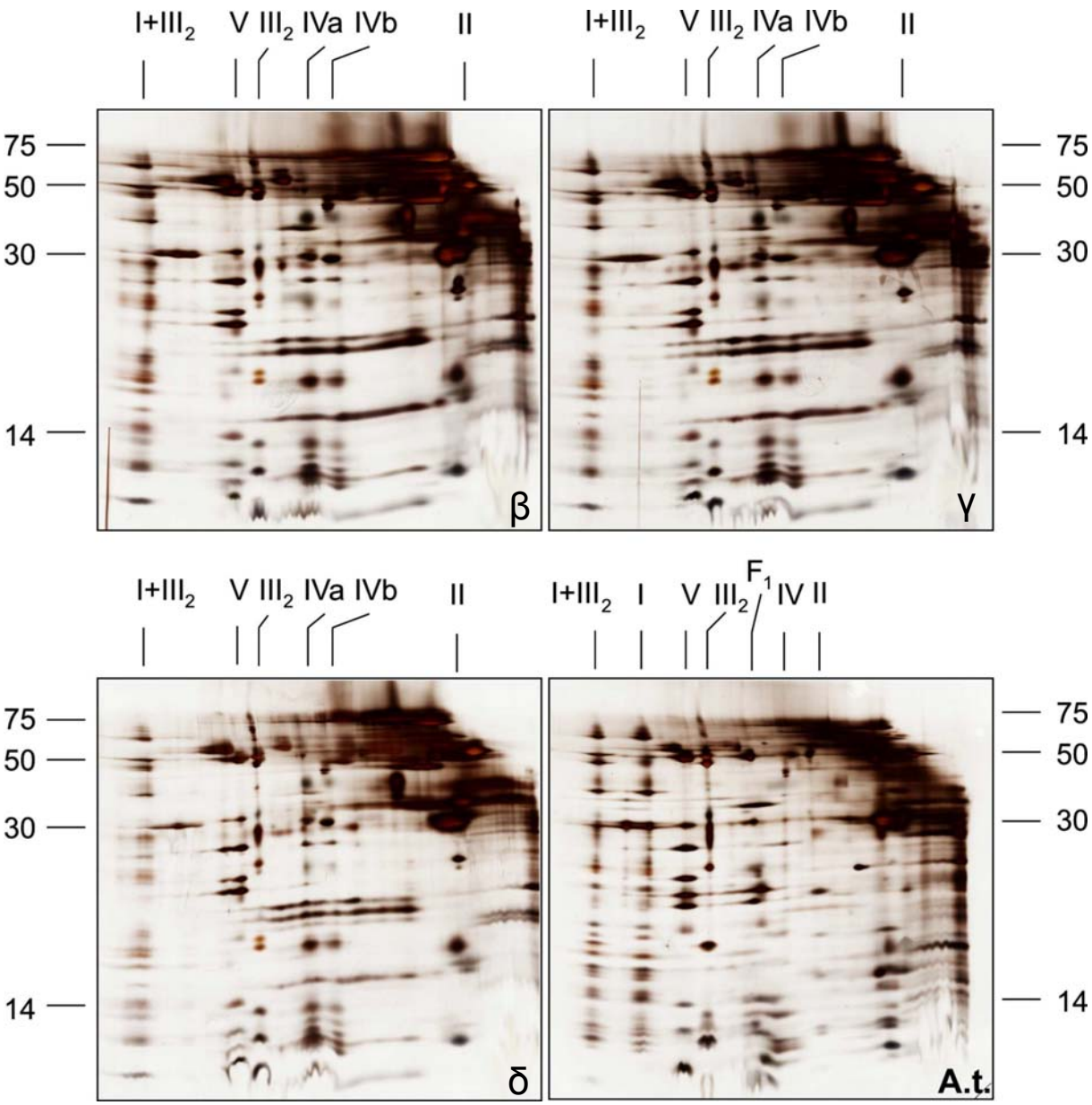

2D BN/SDS-PAGE of respiratory protein complexes from *Arum maculatum* developmental stages β, γ and δ as well as *Arabidopsis thaliana*. Mitochondria were solubilized by 5g digitonin per g protein. Proteins were visualized by silver staining. The identity of the protein complexes is given above the gels (for designations see Figure 1). Molecular masses of the standard proteins are given to the left or right of the gels.

Figure 3:

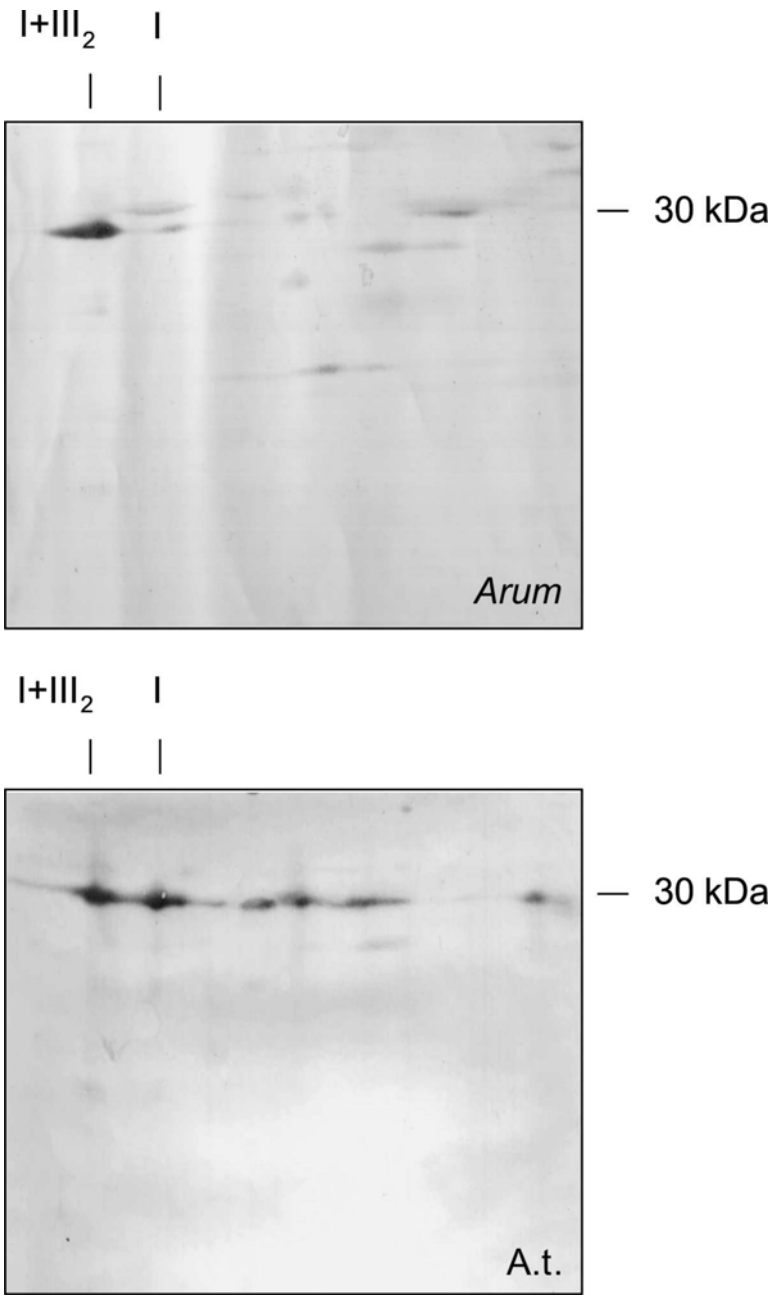

Immunological identification of carbonic anhydrases in mitochondrial fractions of *Arum maculatum* and *Arabidopsis thaliana* (A.t). Proteins were separated by 2D BN/SDS-PAGE and afterwards blotted onto nitrocellulose. The position of the $I+III_2$ supercomplex ($I+III_2$) and complex I (I) is given above the blots.

Figure 4:

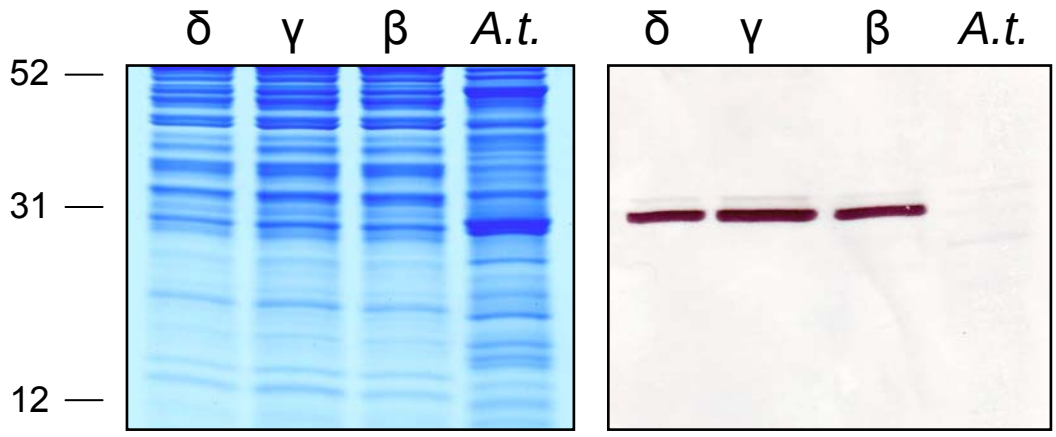

Immunological detection of alternative oxidase. Mitochondrial fractions of *Arum maculatum* appendices (developmental stages β, γ and δ) and *Arabidopsis thaliana* were resolved on 1D SDS-PAGE and either coomassie stained or blotted onto nitrocellulose and developed with antibodies directed against AOX. Molecular masses of the standard proteins are given to the left of the gel.

Figure 5:

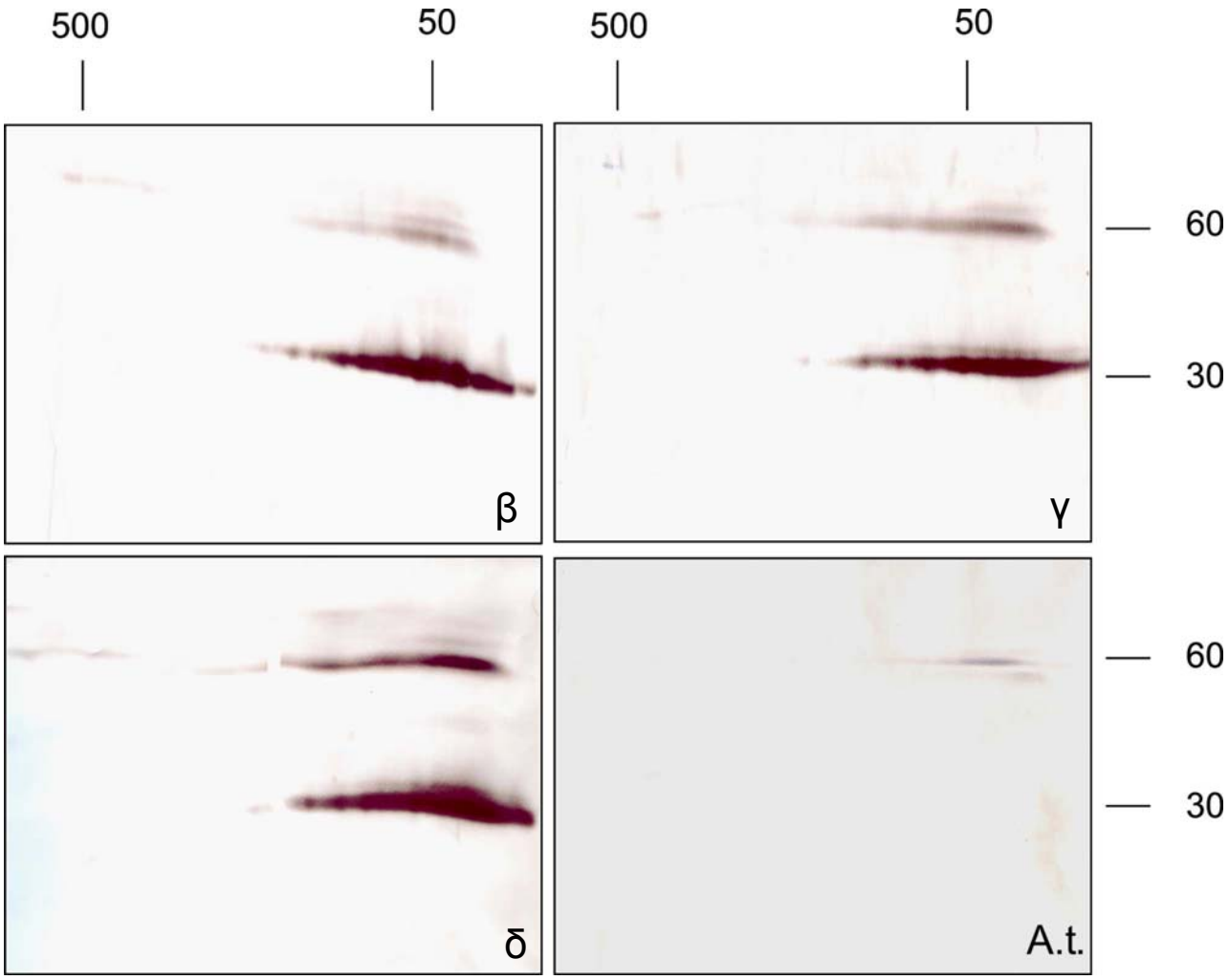

Immunological detection of alternative oxidase after resolution of mitochondrial fractions of *Arum maculatum* appendices (developmental stages β, γ and δ) and *Arabidopsis thaliana* by 2D BN/SDS-PAGE. Molecular masses of the standard proteins are given above the gel (native gel dimension) or to the right (SDS dimension).

Chapter 7

Supplementary Discussion and Outlook

SUPPLEMETARY DISCUSSION AND OUTLOOK

Special Functions of the OXPHOS System – Carbonic Anhydrase Subunits of Respiratory Complex I in *Arabidopsis thaliana*

The first indication of γCAs within plant mitochondrial complex I was suggested only 4 years ago (Parisi et al. 2004). Since that time, many indications confirmed these data. The localization within mitochondria was shown by *in vitro* import experiments (Parisi et al. 2004, Perales et al. 2004). The suborganellar localization was studied by 2D BN/SDS PAGE in combination with immuno blotting. Carbonate treatment of isolated mitochondrial membranes did not allow extraction of the protein, indicating a direct anchoring of the γCA within the IMM. All five *Arabidopsis* γCA/γCAL subunits were found to be associated with mitochondrial complex I (Haezlewood et al. 2003, Sunderhaus et al. 2006). The localization within complex I was addressed by 2D BN/BN-PAGE in combination with mass spectrometry. Four of the five γCAs could be identified in the membrane arm, none of them in the peripheral arm. The topological localization within complex I was furthermore investigated by protease protection experiments with isolated mitoplasts. Comparison of immuno blots with protease treated and untreated fractions revealed that γCAs are protected to a large extent, which indicates a matrix exposed localization. Interestingly, single particle EM pictures of mitochondrial complex I from *Arabidopsis*, *Polytomella* and *Zea maizes*, show a plant specific spherical extra domain at the matrix exposed side of the membrane arm. It seems, that the presence of γCAs within plant mitochondrial complex I correlates with the occurrence of an extra domain within the complex (Fig. 1). This extra-domain has a diameter of about 6nm, corresponding to a molecular mass of app. 75kDa. X-ray crystallography of CAM has revealed a trimeric structure of this enzyme, compatible to the diameter of the complex I extra-domain. (Iverson et al. 2000, Dudkina et al. 2005a, Sunderhaus et al. 2006, Peters et al. 2008).

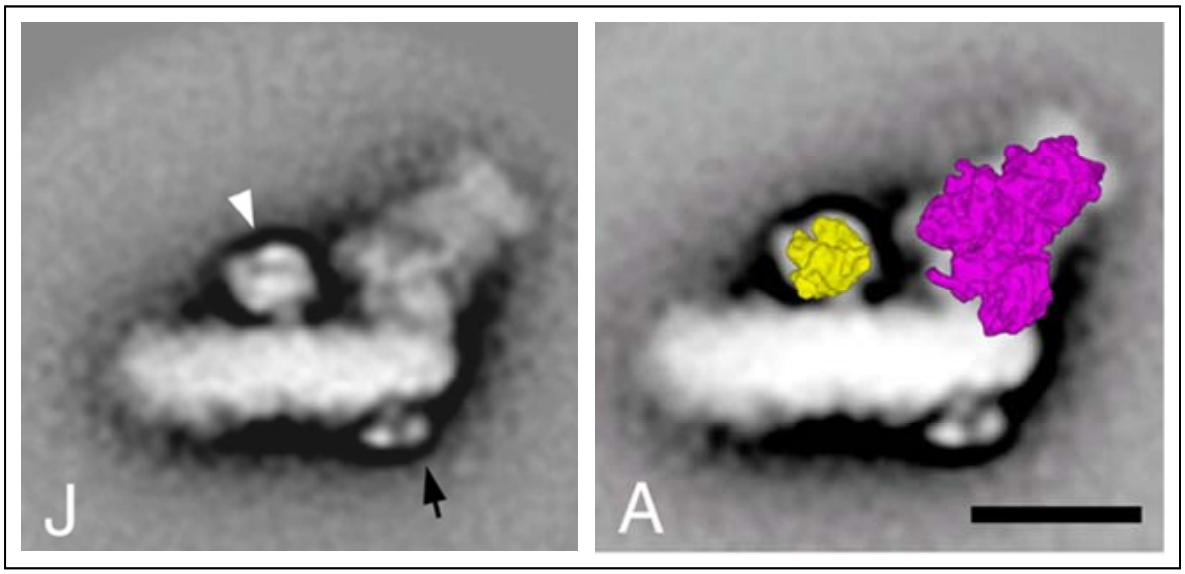

Figure 1. Fitting of 3D structures. (J) Complex I from maize. White arrowhead remarks the carbonic anhydrase domain, black arrowhead remarks another the plant specific extra domain. (A) Assignment of the Cam trimer and the the peripheral arm of complex I from *Thermus thermophilus* to complex I from maize (from Peters et al. 2008).

Currently, direct evidence of γCA activity in complex I is still lacking. *In-gel* enzyme assays using blue-native gels were carried out. These assays are based on monitoring a local pH shift within a gel at the location of a CA band in the presence of excess of CO_2 (Galvez et al. 2000 and references therein, Perales et al. 2005). Also, different enzyme assays with isolated complex I from *Arabidopsis thaliana* and over-expressed At1g47260 protein from *E. coli* were tested. These assays are carried out in barbiturate buffers and are based on a pH shift in the medium measured with a pH electrode (Hatch and Burnell 1990, Perales et al. 2005). No results could be obtained using any of these assays. Several reasons for the missing activity are conceivable. For instance, two functionally important residues, Glu 62 and Glu 84 of CAM, are missing in *Arabidopsis* γCAs. They are substituted by alternative amino acids, which probably adopt their role (Parisi et al. 2004). Additionally, a closer look at the EM analyses of complex I reveals a cavity within the membrane arm of complex I at the opposite side of the extra domain. Therefore it is speculated, that the γCAs of complex I are not only involved in CO_2 – HCO_3^- interconversion but at the same time are also involved in bicarbonate transport across the inner mitochondrial membrane. This transport could be proton driven. If complex I indeed would represent a proton driven bicarbonate translocase, inactivity of the γCA subunits could be explained due to the fact that a proton gradient across the inner mitochondrial membrane in vitro is absent. Enzyme assays as well as *in-gel* assays were carried out with isolated complex I

devoid of its natural lipid surrounding. Therefore, generation of a proton gradient is impossible, thus rendering the γCAs as inactive. Indirect evidence for the activity of complex I integrated γCA subunits comes from transcriptome analyses of *Arabidopsis*. Expression of the genes encoding for γCA1 or γCA2 is very constant under all conditions tested. However, both genes are considerably repressed if *Arabidopsis* is cultivated under elevated CO_2 conditions. This apparently suggests involvement of complex I/γCAs in plant carbon metabolism (Braun and Zabaleta 2007).

Furthermore, there is the fact that the *Arabidopsis* genome includes several genes encoding proteins of the α- and βCA families (Moroney et al. 2001). Targeting prediction analyses using the deduced protein sequences do not indicate the presence of αCAs within mitochondria, whereby only one of the six βCAs (At1g58180) is predicted to have a mitochondrial localization using several different targeting prediction software tools. However, this protein never was detected in mitochondrial fractions. Therefore it either has a different cellular localization or is of extremely low abundance. In consequence, the five γCA/γCAL proteins of complex I probably represent the only mitochondrial CAs in higher plants.

Advanced insights into the functional role of the plant complex I/γCA-complex can possibly be derived from cyanobacteria. Cyanobacteria have evolved a significant environmental adaption known as the CO_2-concentrating mechanism (CCM). The CCM functions to maximize the efficiency of C_i uptake and CO_2 fixation under conditions of limited CO_2 availability by actively accumulating C_i and then generating an elevated CO_2 level around the primary CO_2 fixing enzyme RubisCO. In contrast to plants, RubisCO is encapsulated within a proteinaceous polyhedral microcompartment in cyanobacteria, the carboxysome. By encapsulating RubisCO in a separate compartment and elevating CO_2 concentration within this compartment, cyanobacteria overcome the wasteful RubisCO oxygenase activity. The major components of the cyanobacterial CCM are therefore an active uptake system for both CO_2 and HCO_3^- as well as the existence of the carboxysome, where CO_2 can be generated in close proximity to RubisCO. In cyanobacteria there is an ensuing accumulation of HCO_3^- within the cytosol because of a cytosolic pH of approximately 7.8 – 8.2. This indicates, that HCO_3^- is held in a steady-state non-equilibrium favoring HCO_3^-. The cyanobacterial CAs are an integral part of the carboxysomal shell and have a structural as well as a catalytic role. It is proposed that HCO_3^- diffuses through the proteinaceous shell of the carboxysome, where the activity of

carbonic anhydrase inside the structure acts to catalyze the formation of CO_2 from HCO_3^- (Price et al. 2007).

Cyanobacteria contain up to five distinct transport systems for C_i uptake, including three HCO_3^- transporters and two CO_2 uptake systems. The three HCO_3^- transporters are (i) BCT1, an inducible high affinity transporter, (ii) SbtA, an inducible high affinity Na^+ dependent transporter and (iii) BicA, a low affinity Na^+ dependent transporter. SbtA and BicA may also be Na^+/HCO_3^- symporters. The CO_2 uptake systems are the NDH-1_3 complex and the NDH-1_4 complex. NDH-$1_{3/4}$ complexes are specialized types of the NDH-1 complex, which is the bacterial counterpart of complex I from eukaryotes. They include integral membrane proteins, ChpY/CupA and ChpX/CupB, directly catalyzing the conversion of CO_2 into HCO_3^-. The CO_2 hydration function of the NDH-$1_{3/4}$/Chp complexes is coupled with direct electron flow and proton translocation although they do not exhibit sequence homologies to any known member of the CA family (Battchikova et al. 2005, Herranen et al. 2004, Maeda et al. 2002, Zhang et al. 2005, Price et al. 2007). By analogy, the complex I integrated γCAs of plant mitochondria may also catalyze a proton driven interconversion of CO_2 and HCO_3^- similarly to their counterpart in cyanobacteria. This could be necessary, due to the fact that substantial amounts of CO_2 are released during catabolic reactions in the mitochondrial matrix. This aspect becomes more and more obvious especially under the aspect of photorespiration. Due to the oxygenation activity of RubisCO, plants have to handle a certain amount of 2-phosphoglycolat, a compound that cannot be utilized by the C_3 reductive photosynthetic carbon cycle. An additional cycle, the C_2 oxidative photosynthetic carbon cycle, salvages this carbon so that it is not lost to photosynthetic metabolism. The “waste product” 2-phosphoglycolat is recycled via a multi-step pathway through three cellular compartments: chloroplasts, peroxisomes and mitochondria. In a section of this pathway occurring in mitochondria, 2 molecules of glycine are oxidized to one molecule of serine, thereby releasing 1 molecule of CO_2 per molecule of serine into the mitochondrial matrix. Beyond photorespiration, CO_2 in mitochondria is also released during the citric acid cycle and fatty acid biosynthesis (3 molecules of CO_2 per pyruvate). Whereas there is now a surplus of CO_2 in mitochondria, there is an insufficiency of CO_2 in chloroplasts required for CO_2 fixation, especially under photorespiratory conditions. Therefore it is obvious that plants have an enormous interest in a mechanism, which provides mitochondrial CO_2 to chloroplasts. While CO_2 diffusion over membranes is slow, active bicarbonate transport can be much more efficient. Complex I together with γCAs most likely provides such a “bicarbonate transporter” via the IMM into the IMS and into the cytoplasm (Fig. 2).

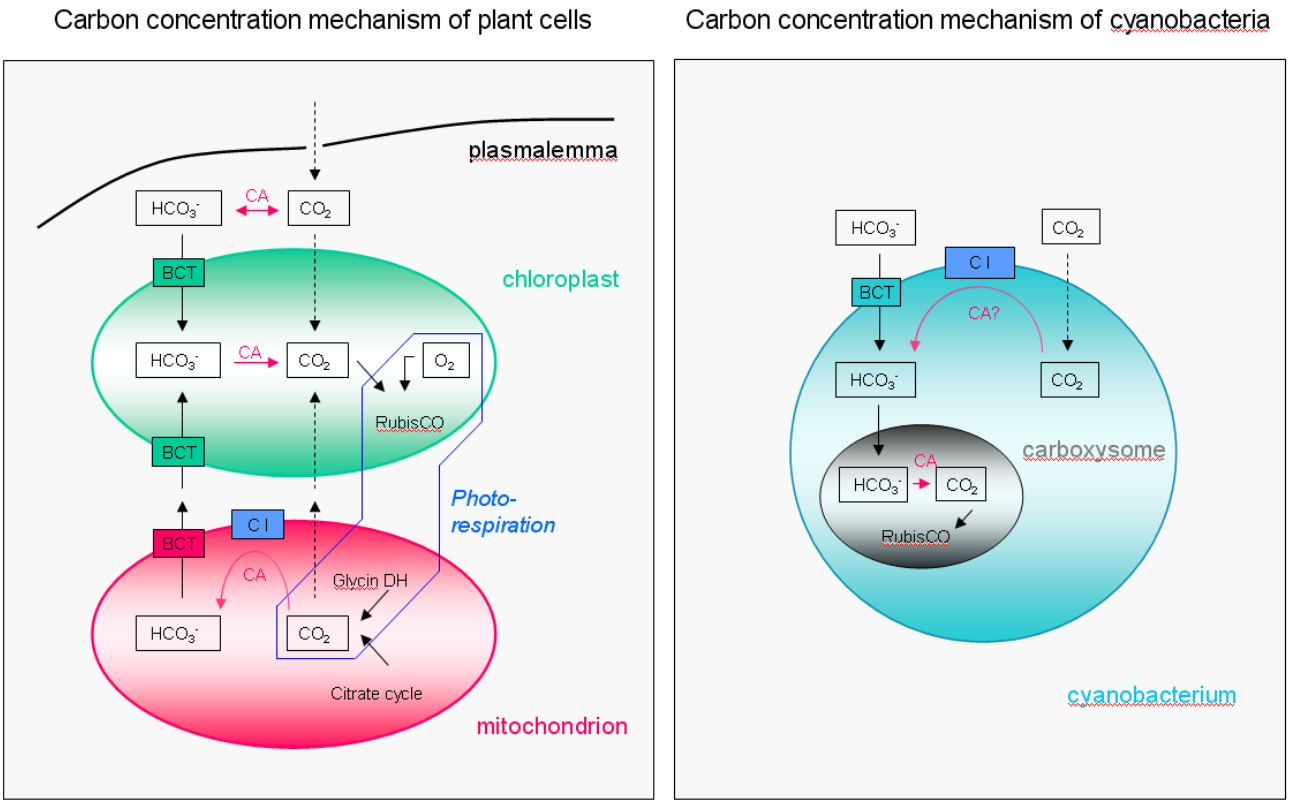

Figure 2. Model for the putative function of the complex I integrated CAs in plants. Solid lines represent active (fast) transport of bicarbonate, dashed lines represent diffusion of CO_2 (slow). Modified from Braun and Zabaleta (2007).

So far, many aspects of this proposed CO_2 recycling mechanism are unknown. Further experiments on physiological as well as on genetic levels are essential for gaining deeper insight into the "black box" complex I and its carbonic anhydrase subunits. Characterization of knock out mutants for one of the five carbonic anhydrases so far has not allowed for clarification of the physiological role of these proteins within complex I. Characterization of double and triple knock out mutants could provide further insights into the physiology of the complex I integrated carbonic anhydrase subunits and could help to elucidate one part of the higher plant CO_2 concentrating pathway. Also, new insights could be obtained from the investigation on cyanobacteria, which contain a protein homologous to γCAs termed CcmM (product of the ccmM gene). This protein forms part of the carboxysomal shell. Physiological and functional characterization of this protein might allow for new conclusions on the functional role of the mitochondrial γCA protein family in plants.

References

Battchikova N, Zhang P, Rudd S, Ogawa T, Aro EM (2005) Identification of NdhL and Ssl 1690 (NdhO) in NDH-1L and NDH-1M complexes of Synechocystis sp. PCC 6803. J. Biol. Chem. 280, 2587 – 2595.

Braun HP, Zabaleta E (2007) Carbonic anhydrase subunits of the mitochondrial NADH dehydrogenase complex (complex I) in plants. Physiol. Plant. 129, 114 – 122.

Dudkina NV, Eubel H, Keegstra W, Boekema EJ, Braun HP (2005a) Structure of a mitochondrial supercomplex formed by respiratory-chain complexes I and III. PNAS 102, 3225 – 3229.

Galvez S, Hirsch AM, Wycoff KL, Hunt S, Layzell DB, Kondorosi A, Crespi M (2000) Oxygen regulation of a nodule-located carbonic anhydrase in Alfalfa. Plant Physiol. 124, 1059 – 1069.

Hatch MD, Burnell JN (1990) Carbonic anhydrase activity in leaves and its role in the first step of C_4 photosynthesis. Plant Physiol. 93, 825 – 828.

Heazlewood JL, Howell KA, Millar AH (2003) Mitochondrial complex I from *Arabidopsis* and rice: orthologs of mammalian and fungal components coupled with plant specific subunits. Biochim. Biophys. Acta 1604, 159 – 169.

Herranen M, Battchikova N, Zhang P, Graf A, Sirpio S, Paakkarinen V, Aro EM (2004) Towards functional proteomics of membrane protein complexes in Synechocystis sp. PCC 6803. Plant Physiol. 134, 470 – 481.

Iverson TM, Alber BE, Kisker C, Ferry JG, Rees DC (2000) A closer look at the active site of gamma-class carbonic anhydrases: high resolution crystallographic studies of the carbonic anhydrase from *Methanosarcina* thermophila. Biochemistry 39, 9222 – 9231.

Maeda S, Badger MR, Price GD (2002) Novel gene products associated with NdhD3/D4-containing NDH-1 complexes are involved in photosynthetic CO_2 hydration in the cyanobacterium Synechococcus sp. PCC7942. Mol. Microbiol. 43, 425 – 435.

Moroney JV, Bartlett SG, Samuelsson G (2001) Carbonic anhydrases in plants and algae. Plant Cell Physiol. 24, 141 – 153.

Parisi G, Perales M, Fornasari MS, Colaneri A, Gonzalez-Schain N, Gomez-Casati D, Zimmermann S, Brennicke A, Araya A, Ferry JG, Echave J, Zabaleta E (2004) Gamma carbonic anhydrases in plant mitochondria. Plant Mol. Biol. 55, 192 – 207.

Perales M, Parisi G, Fornasari MS, Colaneri A, Villareal F, Gonzalez-Schain N, Echave J, Gomez-Casati D, Braun HP, Araya A, Zabaleta E (2004) Gamma carbonic anhydrase like complex interact with plant mitochondrial complex I. Plant Mol. Biol. 56, 947 – 957.

Perales M, Eubel H, Heinemeyer J, Colaneri A, Zabaleta E, Braun HP (2005) Disruption of a nuclear gene encoding a mitochondrial gamma-type carbonic anhydrase reduces complex I and supercomplex I+III2 levels and alters mitochondrial physiology in *Arabidopsis*. J. Mol. Biol. 350, 263 – 277.

Peters K, Dudkina NV, Jänsch L, Braun HP, Boekema EJ (2008) A structural investigation of complex I and I+III2 supercomplex from *Zea mays* at 11 – 13 Å resolution: assignment of carbonic anhydrase domain and evidence for structural heterogeneity within complex I. Biochim. Biophys. Acta 1777, 84 – 93.

Price GD, Badger MR, Woodger FJ, Long BM (2007) Advances in understanding the cyanobacterial CO_2-concentrating-mechanism (CMM): functional components, C_i transporter, diversity, genetic regulation and prospects for engineering into plants. J. Exp. Bot. 59, 1441 – 1461.

Sunderhaus S, Dudkina NV, Jänsch L, Klodmann J, Heinemeyer J, Perales M, Zabaleta E, Boekema EJ, Braun H.-P. (2006) Carbonic anhydrase subunits form a matrix exposed domain attached to the membrane arm of mitochondrial complex I in plants. J. Biol. Chem. 281, 6482 – 6488.

Zhang P, Battchikova N, Paakarinen V, Katoh H, Iwai M, Ikeuchi M, Pakrasi HB, Ogawa T, Aro EM (2005) Isolation, subunit composition and interaction of the NDH-1 complexes from Thermosynechococcus elongates BP-1. Biochem. J. 390, 513 – 520.

PUBLICATIONS 2004 – 2008

1. Eubel H, Heinemeyer J, Sunderhaus S, Braun HP (2004) Respiratory Chain Supercomplexes in the Plant Mitochondrial Membrane. Plant Physiol. Biochem. 42, 937 – 942.

2. Sunderhaus S, Dudkina NV, Jänsch L, Klodmann J, Heinemeyer J, Perales M, Zabaleta E, Boekema EJ, Braun HP (2006) Carbonic Anhydrase Subunits form a Matrix-Exposed Domain Attached to the Membrane Arm of Mitochondrial Complex I in Plants. J. Biol. Chem. 281, 6482 – 6488.

3. Dudkina NV, Heinemeyer J, Sunderhaus S, Boekema EJ, Braun HP (2006) Respiratory Chain Supercomplexes in the Plant Mitochondrial Membrane. Trends Plant Sci: 11, 232-40.

4. Dudkina NV, Sunderhaus S, Braun HP, Boekema EJ (2006) Characterization of Dimeric ATP Synthase and Cristae Membrane Ultrastructure from *Saccharomyces* and *Polytomella* Mitochondria. FEBS Lett. 580, 3427 – 3432.

5. Sunderhaus S, Eubel H, Braun HP (2007) Two-Dimensional Blue Native/Blue Native Polyacrylamide Gel Electrophoresis for the Characterization of Mitochondrial Protein Complexes and Supercomplexes. Meth. Mol. Biol. 372, 315 – 324.

6. Dudkina NV, Sunderhaus S, Boekema EJ, Braun HP (2008) The Higher Level of Organization of the Oxidative Phosphorylation System: Mitochondrial Supercomplexes. J. Bioenerg. Biomembr. 40, 419 – 924.

7. Braun HP, Sunderhaus S, Boekema EJ, Kouril R (2008) Purification of the cytochrome c reductase/cytochrome c oxidase supercomplex of yeast mitochondria. Meth. Enzymol., in press

8. Sunderhaus, S and Braun HP (2008) Supramolecular Structure of the OXPHOS System in Highly Thermogenic Tissue of *Arum maculatum*.
   to be submitted

CURRICULUM VITAE

Name	Stephanie Sunderhaus
Date of Birth	09.02.1979
Place of Birth	Mettingen
Citizenship	Citizen of Germany
Marital Status	unmarried

PRIMARY EDUCATION

1985 – 1988	primary school “Martinigrundschule” in Münster
1988 – 1989	primary school “Clemens-August-Schule” in Bocholt
1989 – 1998	secondary school “Euregio-Gymnasium” in Bocholt
1998	“Abitur”

PROFESSIONAL EDUCATION

1998 – 2000	practical training as a gardener in the “Gärtnerei Wissing, Senden”

ACADEMIC EDUCATION

2000 – 2004	Student at the “Leibniz University Hannover”, major: Horticulture
October 2004	Diploma-degree in Horticulture (Dipl. Ing. agr.)
	Thesis: “Untersuchungen zur supramolekularen Struktur der Atmungskette in Pflanzenmitochondrien” (“Investigation of the supra molecular structure of the respiratory chain of plant mitochondria.”)
	Grade: *Excellent*

2004 - 2008	PhD-Student at the Leibniz University Hannover, Department “Plant Molecular Biology” in the Plant Ptoteomics Group of Prof. Dr. Hans-Peter Braun.
November 2008	PhD in natural sciences (Dr. rer. nat.) Grade: „*magna cum laude*“
Since January 2009	Research Associate at Leibniz University of Hannover, Department “Plant Molecular Biology”, Germany.

DANKSAGUNG

Lieber Hans-Peter, ich möchte mich bei Dir ganz herzlich für Deine stete, nicht nur wissenschaftliche, sondern auch menschliche Unterstützung in den letzten vier Jahren bedanken. Ohne Deine Geduld und Deine ständige Mithilfe wäre diese Arbeit nicht entstanden. Deinem Engagement habe ich es zu verdanken, dass ich die vielen internationalen Konferenzen besuchen konnte. Durch Deine ganz persönliche Art hast Du eine tolle Arbeitsgruppe geschaffen.

Liebe Jenni, liebe Katrin, besonders euch beiden danke ich für eure Freundschaft und die schöne Zeit zusammen, vor allem auch außerhalb des Labors. Unser Japan-Ausflug war „echt abgefahren“ und vor allem unvergesslich.

Liebe Dagmar, bei Dir möchte ich mich für Deine unendliche Geduld, Mühe und immer verlässliche Hilfe im Labor bedanken. Auch die diversen „Therapiestunden“ auf der Weide waren meinem Wohlbefinden äußerst zuträglich. Ohne Dich wäre das Labor nur halb so viel wert.

Liebe Christina, lieber Holger, Frank, Hendrik, Joachim, Renke und Peter, vielen Dank für die schöne und lustige Zeit mit euch, ob im Urlaub auf dem Mt. Fuji oder im Labor.

Lieber Heinz, ohne Deinen unermüdlichen Einsatz wäre ich wohl heute nicht so selbständig, mutig und wortgewandt.

Liebe Mama, ohne Dich wäre ich hier nie angekommen. Danke, dass Du immer zu mir gehalten hast. Du bist die beste Mutter, die man sich wünschen kann!

Schätzchen, es ist schön, dass es Dich gibt. Ich freue mich auf unser Leben!